

NORTHWESTERN UNIVERSITY

Adopting Cochlear Place-Specific Stimulus Properties to Improve the Accuracy of Distortion
Product Otoacoustic Emission Measurements

A DISSERTATION

SUBMITTED TO THE GRADUATE SCHOOL
IN PARTIAL FULFILLMENT OF THE REQUIREMENTS

For the degree

DOCTOR OF PHILOSOPHY

Field of Communication Sciences and Disorders

By

Samantha Marie Stiepan

EVANSTON, ILLINOIS

December 2020

© Copyright by Samantha Stiepan 2020

All Rights Reserved

ABSTRACT

Adopting Cochlear Place-Specific Stimulus Properties to Improve the Accuracy of Distortion Product Otoacoustic Emissions Measurements

Samantha Marie Stiepan

The nonlinear attributes of cochlear function are fascinating. Responses are compressed with surprisingly little distortion, different stimuli interact in competitive ways, and tones are created either with or without acoustic stimulation. Moreover, because of their dynamism, these nonlinear phenomena have provided an invaluable means for noninvasively probing and understanding cochlear mechanisms using distortion product otoacoustic emissions (DPOAEs). DPOAEs are faint acoustic signals recorded using a sensitive microphone sealed in the ear canal. These DPOAEs originate as a byproduct of the active cochlear process and thus provide a window into the mechanisms underlying peripheral auditory function.

Because of the benefits associated with exploiting DPOAE measurements, DPOAEs have been incorporated in clinical settings, primarily for the purposes of screening for hearing loss. However, variability in measurement between tests and when compared to behavioral hearing sensitivity has resulted in DPOAEs being limited in their clinical use. Since the level of the DPOAE recorded in the ear canal depends on the frequency and level characteristics of the stimuli used to elicit it, the choice of stimulus parameters may influence the success with which DPOAEs can be used to assess cochlear function and predict auditory status.

DPOAEs are elicited when the nonlinear interaction between the two stimulus tones generates a distortion waveform at a frequency different from the stimulus tones. Changing the stimulus frequency relationship changes the number of distortion generators (i.e., outer hair cells), which changes the characteristics of the distortion produced that eventually travels back to the ear canal. Because the spatial properties of the traveling waves are determined by local cochlear mechanics, which change from base to apex, the frequency and level characteristics between the stimulus tones need to be adjusted as a function of frequency to maintain optimal interaction between them.

Therefore, the timely and accurate detection of cochlear pathology remains suboptimal as current protocols: 1) do not consider the changing local cochlear mechanical properties when using fixed stimulus parameters, and 2) do not assess the entire length of the cochlea through the base, where high frequencies are encoded and where environmental and age-related cochlear decline first manifests. The purpose of this work was to develop a measurement protocol guided by cochlear mechanical properties to derive physiologically motivated and locally appropriate stimulus parameters up to the highest frequencies of human hearing.

This dissertation explored and quantified DPOAE responses across a wide range of stimulus parameter settings in young and middle-aged adults with either audiometrically normal hearing sensitivity or sensorineural hearing loss. We hypothesized that DPOAE stimulus parameters that are optimized to the region around the cochlear place of stimulation would evoke emissions that accurately reflect cochlear health and, therefore, would be closely related to behavioral thresholds. DPOAE responses were then used to explore more complex ideas and theoretical frameworks regarding human DPOAE generation and propagation. Overall, stimulus frequency ratio and levels that were adjusted in a frequency-specific manner maximized DPOAE

generation and improved test performance for measuring normal cochlear function and screening for hearing loss.

ACKNOWLEDGEMENTS

This work would not be possible without the contributions and support of many important individuals, to whom I owe the deepest gratitude. First, I would like to thank my advisor and mentor, Dr. Sumitrajit Dhar, who provided invaluable support, intellectual engagement, and a healthy dose of encouragement throughout my time in his lab. I am also indebted to the other members of my dissertation committee: Dr. Jonathan Siegel, Dr. Pamela Souza, and Dr. Shawn Goodman. Many of the technical, theoretical, and practical aspects of this work were shaped by discussions both individually and in the group with Drs. Siegel, Souza, and Goodman. My committee members were a reliable source of constructive criticism, support, and guidance and furthered my enthusiasm for the auditory system with each passing year.

I am grateful to many other Northwestern faculty members who fostered my intellectual growth while in the Ph.D. program, especially fellow members of the Cochlea Journal Club, and in particular Dr. Mario Ruggero, Dr. Mary Ann Cheatham, Dr. Elizabeth Norton, Dr. Jason Sanchez, and Dr. Tina Grieco-Calub. A special thanks to Dr. Julia Lee for her invaluable knowledge of statistical methods and reporting. Another special thanks goes out to Dr. Chun Liang Chan for his ingenious database organization and navigation skills. There are also individuals outside of Northwestern that were essential to the development of this project, including Dr. Karolina Charaziak, who provided the code and technical support necessary to create the frequency swept paradigm.

Of course, thanks are also due to the organizations that supported this work financially: the National Institutes of Health (NIH/NIDCD grant F32 DC016773) and the Northwestern's School of Communication.

I am also very thankful to a large group of friends, peers, colleagues, and mentors associated with the Dhar lab and the Department of Communication Sciences and Disorders at Northwestern University. A heartfelt thanks goes out to Dr. Uzma Wilson, Dr. Courtney Glavin, Dr. Alexandra Brockner, Dr. Mary Meskan, Dr. Niall Klyn, Dr. Sriram Boothalingham, and Dr. Kristina Ward.

Lastly, I am eternally grateful for the support, patience, and love offered by my family. To my father, Steve Stiepan, who always made sure that I was humble and driven in my endeavors. To my mother, Michelle Stiepan, who has been unwavering in her faith in me and taught me that hearing loss is not a barrier but a challenge to be overcome. To my sisters and my first friends, DeeDee and Nicki Stiepan, who have always been there to instill confidence in my chosen endeavors while providing a needed laugh.

LIST OF ABBREVIATIONS

ARHL –	age-related hearing loss
BM –	basilar membrane
CF –	characteristic frequency
CF _{dp} –	characteristic frequency place of the 2f ₁ -f ₂ distortion product
DPOAE –	distortion product otoacoustic emission
EMT –	electromechanical transduction
EPL –	emission pressure level
f ₁ –	frequency of first stimulus tone
f ₂ –	frequency of second stimulus tone
f ₂ /f ₁ –	stimulus frequency ratio
f _{dp} –	frequency of distortion product
iFFT –	inverse fast Fourier transform
FPL –	forward pressure level
FPP –	false positive percentage
ICC –	intra-class correlation coefficient
IHC –	inner hair cell
L ₁ –	first primary stimulus level
L ₂ –	second primary stimulus level
LSF –	least-squares fit

MET –	mechano-electrical transduction
OAE –	otoacoustic emission
OHC –	outer hair cell
ROC –	receiver operating characteristic
SFOAE –	stimulus frequency otoacoustic emission
SOAE –	spontaneous otoacoustic emission
SPL –	sound pressure level
SNHL –	sensorineural hearing loss
TEOAE –	transient-evoked otoacoustic emission
TPP –	true positive percentage

DEDICATION

-- FOR GRANDMA DEE --

This dissertation is dedicated to one of the strongest women I've known, my grandmother, Delores Eggert. Thank you for your love, support, friendship, and guidance.

TABLE OF CONTENTS

ABSTRACT	3
ACKNOWLEDGEMENTS	6
LIST OF ABBREVIATIONS	8
DEDICATION	10
TABLE OF CONTENTS	11
LIST OF TABLES	16
LIST OF FIGURES	17
CHAPTER 1: Introduction.....	19
1.1. Overview	19
1.2. Anatomy and physiology of the peripheral auditory system.....	21
1.2.1. The outer ear.....	21
1.2.2. The middle ear	21
1.2.3. The inner ear.....	22
1.3. The cochlea.....	22
1.4. The traveling wave	24
1.4.1. The tonotopic map	24
1.4.2. Hair cell transduction.....	25
1.5. Cochlear amplification	27
1.5.1. Amplification occurs at the peak of the traveling wave	28

1.5.2. Mechanisms of amplification	12
1.5.3. Nonlinear responses of the cochlear partition	28
1.6. Motions in the Organ of Corti	29
1.6.1. Basilar membrane	30
1.6.2. Nonuniform vibrations across organ of Corti structures	30
1.7. Otoacoustic emissions	31
1.7.1. Classification of OAEs	32
1.7.2. Distortion product otoacoustic emissions.....	33
1.7.2.1. DPOAEs and OHC dysfunction	34
1.7.3. Characterizing auditory function.....	35
1.7.3.1. DPOAEs and hearing pathology.....	38
1.7.3.2. DPOAE applications in clinical settings	39
1.8. Rationale.....	40
1.8.1. Importance of early identification	41
1.8.2. Age-related hearing loss	42
1.8.3. Establishing appropriate DPOAE stimulus parameters.....	42
1.8.3.1. Early investigations of DPOAE stimulus parameters.....	45
1.8.3.2. Local cochlear mechanics.....	46
1.8.3.3. Limitations of previous investigations	46
1.8.4. Recent calibration and procedural innovations	49
1.8.5. Purpose of dissertation.....	51
CHAPTER 2: Optimizing DPOAE Recordings in Normal-Hearing Ears by Adopting Cochlear	
Place-Specific Stimuli	52

	13
2.1. Introduction	53
2.2. Materials and Methods	57
2.2.1. Participants	57
2.2.2. Instrumentation, Calibration & Signal Processing	57
2.2.3. Protocol.....	60
2.2.4. Analysis	62
2.3. Results	63
2.3.1. Reliability	66
2.3.2. DPOAE amplitude across all stimulus conditions.....	71
2.3.3. Calculating optimal primary frequency ratio.....	79
2.4. Discussion.....	82
2.4.1 Previous investigations of the DPOAE stimulus space.....	82
2.4.2. DPOAE measurement reliability	85
2.4.3. Interactions between primary frequencies and levels.....	86
2.4.4. Optimal DPOAE stimulus parameters.....	88
2.4.5. Future Directions	88
2.4.6. Conclusions	91
 CHAPTER 3: Utilizing Cochlear Place-Specific Properties in Distortion Product Otoacoustic	
Emission Stimuli for the Identification of Hearing Loss.....	92
3.1. Introduction	92
3.2. Materials and Methods	95
3.2.1. Participants	95
3.2.2. Instrumentation, Calibration & Signal Processing	96

3.2.3. Protocol.....	14
3.2.3. Protocol.....	98
3.2.4. Analysis	100
3.3. Results	101
3.3.1. Receiver operating characteristic curves	105
3.3.2. Creating a DPOAE screening protocol.....	110
3.4. Discussion.....	113
3.4.1. Place-specific stimulus parameters are best for screening for hearing loss	113
3.4.2. Clinical Implications.....	117
3.4.3. Other applications of place-specific stimulus parameters	120
3.4.4. Conclusions	121
CHAPTER 4: Discussion.....	123
4.1. Overview	123
4.2. Chapter summaries	125
4.2.1. Chapter 2.....	125
4.2.2. Chapter 3.....	126
4.3. Implications	128
4.3.1. Aligning DPOAE measurements with known cochlear mechanics	128
4.3.1.1. Local cochlear mechanical properties need to be considered when setting DPOAE stimulus parameters.....	128
4.3.1.2. Mechanisms of DPOAE generation	130
4.3.1.3. Maximizing DPOAE generation	131
4.3.2. Importance of evaluating high frequencies	133
4.3.3. Changing the way we screen for hearing loss	135

	15
4.3.3.1. Hearing screenings in adults are underutilized.....	135
4.4.3.2. Benefits of early identification	137
4.4.3.3. Improving outcomes by increasing the access and accuracy of hearing screenings	138
4.4. Limitations.....	139
4.5. Future work.....	141
4.5.1 Generalizability	141
4.5.1.1 Aging	142
4.5.1.2 Ototoxic medications.....	144
4.5.1.3. Acoustic trauma.....	147
4.5.2. DPOAE input/output functions	149
4.5.3. Separating DPOAE source components.....	151
4.5.4. Individualized optimal stimuli for DPOAE recordings.....	153
4.6. Conclusions	154
REFERENCES	156

LIST OF TABLES

Table 1. Interrater reliability using intra-class correlation coefficient (ICC)	68
Table 2. DPOAE stimulus conditions evaluated.....	100
Table 3. Optimized DPOAE test protocol for screening for hearing loss	112

LIST OF FIGURES

Figure 1. The cochlear amplifier	27
Figure 2. DPOAE generation.....	35
Figure 3. DPOAE fine structure visible in a normal hearing participant	38
Figure 4. Aging and auditory decline	45
Figure 5. The strength of the nonlinear distortion generated depends on the overlap region created by the stimulus tones.....	47
Figure 6. The f_2/f_1 relationship of the stimulus tones needs to be adjusted as a function of frequency to maintain optimal distortion generation in the overlap region	48
Figure 7. Previous studies showing optimal DPOAE stimulus frequency ratio as a function of frequency	50
Figure 8. Simultaneous, concurrent frequency sweeps for DPOAE measurement.....	51
Figure 9. Average behavioral hearing thresholds from audiometrically normal-hearing participants.....	61
Figure 10. DPOAE fine structure from three participants.....	66
Figure 11. Average test-retest DPOAE level differences.....	67
Figure 12. Bland–Altman plots comparing the difference in DPOAE level between the first and last test session.....	70
Figure 13. Median DPOAE level as a function of stimulus frequency ratio.....	72
Figure 14. Example participant with strong high frequency DPOAE responses	74
Figure 15. DP-grams for four different normal-hearing participants	76

	18
Figure 16. Median DP-grams for normal-hearing participants	79
Figure 17. Optimal DPOAE stimulus frequency ratios for normal-hearing ears	82
Figure 18. Behavioral hearing thresholds for normal-hearing (A) and hearing-impaired (B) groups	102
Figure 19. DP-grams for one participant with normal-hearing (A) and three with SNHL (B-D)	104
Figure 20. Receiver operating characteristic curves at 2 kHz.	106
Figure 21. Receiver operating characteristic curves at 12.5 kHz	107
Figure 22. Area under the ROC curve (A_{ROC}) as a function of f_2/f_1	110
Figure 23. Optimized DPOAE measurement protocol for screening for hearing loss	113
Figure 24. Bandpass shape seen when DPOAE levels are plotted as a function of stimulus frequency ratio	132
Figure 25. Median DPOAE level as a function of f_2 frequency for three different age groups .	144
Figure 26. DPOAE input/output functions for 18 different f_2 frequencies.....	151

CHAPTER 1

Introduction

1.1. Overview

Human hearing is a remarkable and vital trait. It enables us to stay connected to the outside world allowing us to socialize, work, and communicate while also keeping us safe by warning of potential danger. A substantial and vulnerable part of this auditory processing takes place in the peripheral stage of the hearing pathway – in the sensory organ of hearing, the cochlea. It is here where acoustic signals are transcribed and transduced into electrical signals sent to the auditory cortex. Therefore, to fully understand audition it is necessary to understand the intricacies of cochlear processing. However, the cochlea is not accessible for direct observation and measurement in humans due to its location deep within the temporal bone. Fortunately, the examination of cochlear function can be done noninvasively and efficiently by presenting acoustic signals into the ear canal and recording the acoustic responses that return back from the inner ear. These acoustic consequences of the essential mechanical processes responsible for our remarkable hearing are known as otoacoustic emissions (OAEs). These faint sounds are a byproduct of an active cochlear process that is responsible for the acute sensitivity, frequency selectivity, and wide dynamic range that is characteristic of mammalian hearing. Therefore, many changes in active cochlear function that result in degraded sound perception are also expected to be reflected in changes in OAE characteristics.

With increasing understanding of the early onset and prevalence of hearing loss in adult populations, the demand for developing objective and accurate tools for assessing hearing

function is undeniable. Without a deep understanding of normal function as well as the physiological underpinnings and perceptual consequences of auditory decline, individualized intervention strategies cannot be realized. Accurate assessment of specific auditory function can aid in a patient preventing hearing loss, receiving appropriate rehabilitation, or regaining lost function, allowing for improved quality of life in the acoustically complex listening environments of the world.

The global aim of this research is to directly examine the relationship between various methods of evoking OAEs in individuals with normal and impaired hearing sensitivity, setting the groundwork for developing a new and objective test of auditory function for use in both clinical and laboratory settings. A secondary motivation of the work included in this dissertation is to better understand the potential utility of OAE measurements up to the highest frequencies of human hearing. This dissertation characterizes OAEs evoked by two tones, i.e., distortion product (DP) OAEs, across a wide range of stimulus settings in young individuals with either audiometrically normal hearing or sensorineural hearing loss (SNHL). DPOAE responses are then used to explore more complex ideas surrounding the theoretical framework regarding human DPOAE generation and propagation.

The remainder of this chapter will provide a general background for the dissertation as a whole. Each aforementioned topic will be examined in two studies, described separately in Chapters 2 and 3, containing detailed Introduction, Method, Results, and Discussion sections pertinent to the study reported in each chapter. Lastly, the findings of the studies will be summarized and discussed in the final chapter (Chapter 4).

1.2. Anatomy and physiology of the peripheral auditory system

The mammalian peripheral auditory system consists of three major sections: the outer, the middle, and the inner ear. Each section is structurally unique and functionally distinct ultimately allowing sound in our environment to be transformed and carried into the central auditory pathway for processing.

1.2.1. The outer ear

The outer ear consists of a partially cartilaginous flange called the pinna, the external auditory meatus or ear canal, and the tympanic membrane or eardrum. The basic role of the outer ear is to collect impinging sound waves and to channel them toward the tympanic membrane, the start to the middle ear. The pinna, which includes a resonant cavity called the concha, modifies the incoming sound, particularly at high frequencies, which is important for our ability to localize. The geometry of the pinna and ear canal shape the sound arriving at the tympanic membrane, typically adding a broadly tuned peak around 2.5 kHz of 15-20 dB (Wiener & Ross, 1946).

1.2.2. The middle ear

The middle ear, consisting of the tympanic membrane, middle ear cavity, and ossicles, is responsible for transforming sound energy into mechanical motion while overcoming the impedance mismatch between the ear canal (air-filled space) and the cochlea (fluid-filled space).

The middle ear impedance transformer consists of a force transformer (lever mechanism formed by the malleus and long process of the incus) and a pressure transformer (large ratio of the tympanic membrane area to stapes footplate area along with the tympanic membrane's curvature). The middle ear also contains muscles that will contract in response to loud inputs, effectively decreasing transmission into the inner ear. The contraction increases the stiffness of

the middle ear transformer, limiting the transmission of sounds at low frequencies. This reduction may have a role in protecting the cochlea from noise damage and reduce low-frequency masking effects for complex stimuli (Pickles, 2012).

The main function of the middle ear is to transform sound energy into mechanical motion that is delivered to the inner ear. The energy of the acoustic pressure waves in the ear canal is translated into mechanical vibration by the tympanic membrane and carried through the ossicular chain. Vibrations transmitted through the ossicular chain end at the oval window, the input port of the inner ear.

1.2.3. The inner ear

In vertebrates, the inner ear consists of the cochlea, responsible for sound detection, and the vestibular system, dedicated to balance. In mammals, the inner ear is housed in the bony labyrinth, a hollow cavity, deep in the otic capsule of the temporal bone. The piston action of the stapes footplate in and out of the oval window, reciprocated at the round window, creates a pressure differential above and below the cochlear partition (described in more detail below). This pressure difference creates and propagates mechanical waves in the cochlear fluid and membranes which are eventually converted into action potentials by cochlear hair cells allowing transmission of the signal to the brain.

1.3. The cochlea

The cochlea within the inner ear is an exquisite structure that converts sound-induced mechanical motion to electrical signals that excite afferent auditory nerve fibers. The structures that make up the cochlea are hidden in the bony labyrinth, a fairly inaccessible part of the skull. The cochlea itself is a coiled, fluid-filled tube that is split into three chambers (scalae) by the osseous spiral lamina and by two membranes that stretch along the cochlear canal, the basilar

membrane (BM) and Reissner's membrane. The outer two chambers, the upper being the scala vestibuli and the lower being the scala tympani, contain perilymph and the middle chamber, or scala media, contains endolymph. The scala vestibuli and the scala tympani are merged together at the apical end of the cochlea via a narrow opening called the helicotrema.

The human cochlea contains a sensory epithelium, the organ of Corti, that spirals for ~ 35 mm from the high-frequency base to the low frequency apical tip within the scala media. The organ of Corti, sitting on the elastic BM, comprises a highly organized structure consisting of sensory cells and supporting cells. Mammalian hearing relies on two types of sensory cells: inner hair cells (IHCs) that convert the mechanical stimulus into neural signals communicable to the brain, and outer hair cells (OHCs) which mechanically modulate the stimulus through active feedback. Stimulation of a hair cell is mediated by displacements of its mechanosensitive hair bundle which protrudes from the apical surface of the cell into a narrow fluid-filled space between the reticular lamina and tectorial membrane. There is a single row of ~3,500 IHCs and three rows of ~12,000 OHCs that are positioned on top of the BM and surrounded by various supporting cells. In a cross-section of the organ of Corti, the sensory IHCs are located at a medial position and the OHCs are separated radially from the IHCs by pillar supporting cells. There are tight junctions between the apex of the hair cells and the surrounding supporting cells forming a barrier between the endolymph and the perilymph called the reticular lamina. The reticular lamina is a thin, stiff lamina that extends from the OHCs to the supporting Hensen's cells. OHC stereocilia insert into the overlying tectorial membrane while the IHC stereocilia freely float in the endolymphatic fluid space just below the tectorial membrane. During acoustic stimulation, the tectorial membrane will interact with the IHCs via viscous forces from the subtectorial fluid and with the OHCs via a direct connection to the tallest stereocilia.

Mechanically, the cochlea can be modeled as a series of radial sections ranging from the base to the apex. The resonant frequency of each section is based on the mass, stiffness, and damping of the cochlear partition, all of which change gradually and systematically across the cochlear length. The BM at the base of the cochlea has the lowest mass and highest stiffness causing it to vibrate maximally in response to high-frequency sounds. In contrast, the BM at the apex has the highest mass and lowest stiffness and thus vibrates maximally in response to low-frequency stimulation.

1.4. The traveling wave

1.4.1. The tonotopic map

Vibrations of the stapes footplate in and out of the oval window cause a displacement of the perilymphatic fluids in the scala vestibuli, initiating the cochlear traveling wave. The displacement of this essentially incompressible fluid is compensated by an outward movement of the round window at the base of the scala tympani. The pressure difference that results between the two scalae initiates a mechanical wave that propagates along the length of the spiraling cochlear canal. This transverse traveling wave propagates apically, growing in amplitude until it peaks at a location determined by the frequency of stimulation followed by a rapid decay more apically. This hydromechanical disturbance (i.e., the traveling wave) along the cochlear partition, produces a rudimentary spectral analysis in the cochlea. The passive mechanical properties of the cochlear partition, including the mass and stiffness of the organ of Corti and the BM, are important in determining the exact properties of the traveling wave. The peak of the traveling wave varies according to the tonotopic map defined by these basal-to-apical gradients of mass and stiffness, producing the frequency-to-place mapping (i.e., tonotopicity) of the cochlear partition. This tonotopic map along the cochlear length responds characteristically with high

frequency sounds creating maximal displacement near the cochlear base, which has a narrow, thick, and stiff BM, and low frequencies creating maximal displacement near the apex, which has a wider, thinner, and more compliant BM.

Each longitudinal position along the cochlear partition has a “best frequency” which produces the greatest vibration amplitude of transverse partition motion for a given stimulus tone. At levels near threshold in a living cochlea, this is referred to as the characteristic frequency (CF). As the traveling wave moves across the cochlear length, partition vibration is maximal at the point where the frequency of the incoming pressure wave matches the CF of that cochlear place. There is minimal propagation of mechanical energy to cochlear regions apical to the CF place for stimulation at a specific frequency. CFs are exponentially mapped such that an octave difference between two CF places corresponds to the same distance along the cochlear partition.

1.4.2. Hair cell transduction

Ultimately, the traveling wave creates the mechanical forces necessary to deflect the hair cell stereocilia, instigating the mechano-electrical transduction (MET) process necessary to relay the auditory signal to the central auditory system. Though the entire organ of Corti vibrates in response to the traveling wave propagation, the differing radial positions of the insertion points of the basilar and tectorial membranes onto the osseous spiral lamina cause a transverse shearing movement in the sub-tectorial space between the reticular lamina and the tectorial membrane.

This shearing directly deflects OHC stereocilia and indirectly deflects IHC stereocilia by the fluid movement in the sub-tectorial space. The hair bundles of OHCs connect the reticular lamina, in which the apical surfaces of the cells are embedded, to the tectorial membrane that lies in parallel above it. They are therefore stimulated by the sound-evoked shearing between the

reticular lamina and tectorial membrane which occurs in the radial direction, perpendicular to the rows of hair cells. In contrast, hair bundles of IHCs are anchored only in the reticular lamina and are stimulated by radial fluid flow between the reticular lamina and tectorial membrane. This fluid flow can comprise a shear flow, as elicited by shearing between the reticular lamina and tectorial membrane, as well as a net flow, as could result from squeezing of the narrow space between the two structures (Guinan, 2012; Bell & Fletcher, 2004).

Deflected hair bundle stereocilia initiate the MET process by opening channels present at the stereocilliary tips of IHCs and OHCs. MET is a term that specifically refers to the flow of ions through these transduction channels as a result of stereocilia deflection. Deflection of the bundle one way opens the channels and deflection of the bundle the other way closes the channels (Hudspeth, 1989). Because of the positive endolymphatic potential (approximately +80 mV) and the high cation (K^+ and Ca^{+2}) concentrations in the endolymph, opening the transduction channels causes an influx of current, depolarizing the hair cell. While the normal resting potential of a hair cell is around -60 mV, during stimulation the receptor potential can vary by up to several millivolts with high-intensity sound stimuli (Preyer et al., 1994; Sellick et al., 1983).

Mechanical amplification, provided by the OHCs, is then achieved when an electrical event (the current flow or a voltage difference) is converted into a mechanical event. This is called electromechanical transduction (EMT) or the active process. The mechanical event generates a force that increases BM vibration. The increase in BM vibration further deflects the hair cell stereocilia, increasing the modulated current that flows through the transduction channels which in turn increases the power added by the active process – this is the process of cochlear amplification (Figure 1).

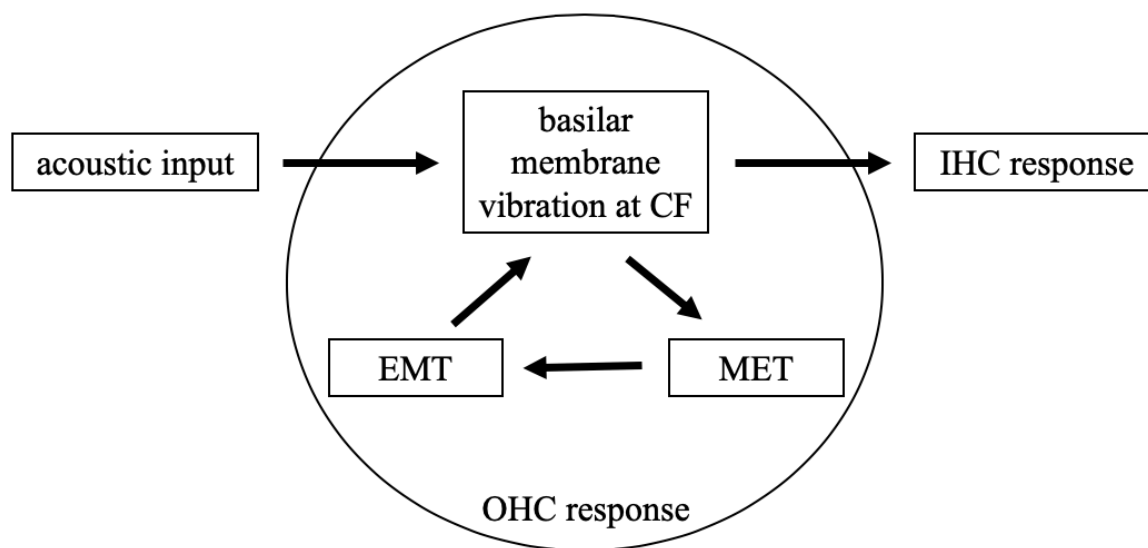


Figure 1. The cochlear amplifier

Summary of the positive feedback process that enhances BM vibration. MET transduction modulates the flow of ions through ion channels in the stereocilia as a result of stereociliary deflection. EMT converts an electrical event into a mechanical event. [Adapted from Withnell et al. (2002)]

1.5. Cochlear amplification

Early experimental measurements of BM vibrations within human cadavers indicated that BM responses were insensitive, broadly tuned, and linear (Békésy, 1960). Furthermore, these measurements demonstrated that increasing sound pressure level (SPL) linearly increased BM motion by the same degree. Yet, years before these passive properties were reported by Békésy, the existence of an active element within the cochlea was proposed by Thomas Gold (Gold, 1948). Gold's work was the first to consider that the ear cannot simply act passively but rather must be an active detector. He suggested that a form of electromechanical feedback could overcome the viscous damping that must be imposed by the fluids surrounding the cochlear structures allowing for the high sensitivity and frequency selectivity observed psychophysically. Decades later, this active cochlear mechanism that was first proposed by Gold was later

demonstrated by William Rhode in the squirrel monkey in 1971 (Rhode, 1971). Ever since, the cochlear active process has been a focus of intense research with numerous scientific reports aimed at characterizing the biophysical, biochemical, and molecular properties of the cochlear amplifier.

1.5.1. Amplification occurs at the peak of the traveling wave

The cochlear amplifier is characteristic of a healthy, normally functioning mammalian auditory system. It is a level-dependent, physiologically vulnerable process within the cochlea that amplifies cochlear partition vibration. Meaning, the cochlear amplifier does not act to amplify sounds equally at all frequencies. Inherent in the operation of the cochlear amplifier is a motor or active process that imparts mechanical energy into the cochlear partition.

Evidence has accumulated to implicate the OHCs as the origin of this cellular mechanical amplification (Dallos, 1992; Yates et al., 1992). During the active process, current influx triggers processes within the OHC to generate force and amplify the partition vibration at the peak of the traveling wave. Therefore, this a frequency-specific, positive feedback loop that is tuned to generate maximal force only at the CF (Olsen, 2004). Eliminating the power to drive OHC motility by removing the endocochlear potential (Ruggero & Rich, 1991; Mills & Schmidt, 2004), removing OHC stimulation by removing the tectorial membrane (Legan et al., 2000), or inactivating the OHC motor protein prestin (Dallos et al., 2008) are all known to reduce both the gain and the sharpness of frequency tuning in the BM vibratory response. These data indicate that OHCs are needed for both amplification and sharp frequency tuning.

1.5.2. Mechanisms of amplification

The explanation underlying the positive feedback that is selectively added to the traveling wave in order to create this active process has been described by two main mechanisms: 1) a

force generation by somatic motility contributions, and 2) a mechanical force generated by hair bundle motility contributions. A voltage-dependent somatic electromotility (Brownell, 1990) results from the activity of the motor protein prestin which is densely expressed in the lateral walls of the OHC (Brownell et al., 1985; Zheng et al., 2000). In particular, OHCs respond to acoustic stimulation through static contraction and sometimes elongation with changes in receptor potential. Moreover, the static length change is largest when the frequency of the stimulation matches the CF of the cochlear location of the OHC (Brundin et al., 1989; Brundin & Russell, 1994). The hair bundles of OHCs can also generate mechanical force (Kennedy et al., 2003, 2005) via hair-bundle motility driven by calcium currents of the OHCs. Although there is sound evidence that both mechanisms may contribute to active modulation of the sound-evoked motion of the cochlear partition (see Ashmore, 2008 for review), there are still many important questions that remain to be answered before the basis of the cochlear amplifier is fully understood.

1.5.3. Nonlinear responses of the cochlear partition

Regardless of the precise mechanisms, the consequences of this active, cycle-by-cycle, force production that is mediated by the OHCs gives rise to a host of nonlinear phenomena in a living cochlea. This includes a sensitive response to weak stimuli (i.e., improved hearing sensitivity), sharpened frequency tuning (i.e., improved frequency selectivity), and a compressive nonlinear response over a large range of input levels (i.e., improved dynamic range) (Patuzzi, 1996; Robles & Ruggero, 2001). Additionally, the existence of spontaneous otoacoustic emissions (SOAE), sounds of cochlear origin that are radiated back into the ear canal, is taken as a signature of the feedback process and used to infer the presence of amplification in a variety of vertebrates (Hudspeth, 1997). Lastly, nonlinearities are also evident when more than one

stimulus tone is present. Depending on the frequency and level relationship, the presence of two tones can cause one tone to reduce or suppress the other (i.e., two-tone suppression) or they can produce vibratory energy at frequencies not included in the stimuli (i.e., distortion products). In fact, the active processes underlying cochlear amplification are thought to be the source of OAE generation.

1.6. Motions in the Organ of Corti

1.6.1. Basilar membrane

Cochlear amplification has been evidenced in the vibratory amplitude of BM motion that increases in a compressive nonlinear manner that is largest for lower input levels (Davis, 1983; Rhode, 1971). Furthermore, measurements of BM motion in living cochlea show a much wider range of peak motion near the CF place, dramatically improving sensitivity and sharpness of tuning (Rhode, 1971; Cooper & Rhode, 1992a,b). Positive feedback occurs locally along the length of the cochlea, to amplify vibrations on the BM on a cycle-by-cycle basis.

These precise BM response characteristics are then conveyed to auditory nerve fibers via synaptic transmission from the IHCs (Narayan et al., 1998; Ruggero et al., 1990; Ruggero et al., 1992). Specifically, the frequency-specific responses of the BM vibration and auditory nerve firing rate closely approximate each other, especially near the threshold of hearing (Narayan et al., 1998). Thus, the concept that auditory nerve tuning mimics BM vibrations has been ingrained as a fundamental property of mammalian hearing (Davis, 1958). Although, this notion has been challenged for auditory nerve suprathreshold stimulation that are efferent inhibited (Stankovic & Guinan, 1999, 2000) and for lower-frequency cochlear regions (Guinan et al., 2012).

1.6.2. Nonuniform vibrations across organ of Corti structures

Although the entire organ of Corti vibrates in response to sound pressure waves, recent studies that were able to measure motion near the BM, reticular lamina, tectorial membrane, and hair cells have shown that organ of Corti motion is more complex (Cooper et al, 2018; Lee et al., 2016; Ren et al., 2016; Warren et al., 2016; Recio-Spinoso et al., 2017; Lee et al., 2015; Dong et al., 2018). In fact, different microstructures within the organ of Corti are displaced differently.

Recent innovations in optical recording techniques that allow for visual inspection of intact, live animal cochlea, have opened up a whole new understanding of cochlear micromechanics. With the use of high-speed optical coherence tomography, intra-cochlear vibrations are found to not be uniform across structural elements of the organ of Corti. Numerous studies have now demonstrated that different structures within the cochlear partition move to differing degrees, in differing directions, with different phases and different frequency-dependencies (Chen et al., 2011; Ramamoorthy et al., 2014; Gao et al., 2014; Lee et al., 2015; Lee et al., 2016; Cooper et al., 2018; Dewey et al. 2019).

One of the most significant findings in this area is that the largest intra-cochlear motion does not come from BM displacement, the cochlear structure that has been the focus of important experimental and theoretical work for over 50 years. Tissue located closer to the OHCs of the organ of Corti, including the reticular lamina and tectorial membrane, have been shown to vibrate with much larger amplitudes and at different phases (Chen et al., 2011; Ramamoorthy et al., 2014; Gao et al., 2014; Lee et al., 2015; Lee et al., 2016; Cooper et al., 2018) than the BM. Measurements viewed through the transparent round window membrane (Lee et al., 2015; Lee et al., 2016; Cooper et al., 2018) in the basal turn of the cochlea and the bony wall of the apical

cochlea reveal reticular lamina motion that is more broadly tuned, more extensively nonlinear, and up to ten times larger than BM motion (Lee et al., 2015; Lee et al., 2016).

When looking at the cells and tissues of the organ of Corti as a whole, the greatest vibrations have been measured at the level of the OHC. Cooper et al. (2018) found sound-evoked motion to be funneled into a “hotspot region” whose epicenter lies where the basal poles of the OHCs and the heads of the adjoining Deiters’ cells couple. Functional considerations of the larger vibrations in the hotspot region could reveal a greater relevance to hearing than the smaller and more peripheral vibrations of the BM as the hotspot is closer to the transduction sites of the OHC stereocilia. OHC/Deiter cell hotspots were reduced in physiologically compromised cochleae and disappeared from healthy cochleae soon after death, indicating the need for cochlear amplifier function in order for the hotspot to exist.

1.7. Otoacoustic emissions

The concept that a generator source of mechanical energy exists in the mammalian cochlea was further validated in 1978 when David Kemp discovered that sounds, now known as OAEs, can be produced by the inner ear. The discovery of OAEs (Kemp, 1978) – which were measured initially in humans – has not only changed previous thinking about cochlear sound processing but has also produced a totally new tool for assessing auditory function.

For reasons still not well-understood, active cochlear processes result in waves that propagate in reverse (i.e., toward the base). These waves drive the stapes, setting the ossicular chain and eardrum in motion, and are often large enough to produce detectable sound pressures in the ear canal (i.e., OAEs). Whether this reverse propagation is essentially a backward traveling wave or a compression wave through the fluids in the cochlea is a matter of scientific debate (Olson, 1998; Robles & Ruggero, 2001; Nobili et al., 2003; Ren, 2004; Ruggero, 2004; Siegel et

al., 2005). OAEs themselves are the by-product of the nonlinear sound amplification process in the cochlea (Davis, 1983; Dallos, 1992) and hence can serve as a measure for evaluating cochlear integrity and understanding cochlear mechanisms.

1.7.1. Classification of OAEs

Historically, OAEs have been classified based on the type of the evoking stimulus: transient-evoked (TE) OAEs evoked with clicks or tone-bursts, stimulus- frequency (SF) OAEs evoked with a single pure tone, and distortion product (DP) OAEs evoked with two tones of differing frequencies (f_1 and f_2). SOAEs are unique in that they are OAEs measured as acoustic signals in the ear canal that are not evoked by an external stimulus. Fairly recently, it has become more useful to understand OAEs in terms of the mechanisms that may be responsible for their generation rather than classifying them according to the type of evoking stimulus.

1.7.1.1. Mechanism-based taxonomy

Shera and Guinan (1999) proposed a mechanism-based taxonomy where OAEs are grouped based on their hypothetical mechanism of generation: coherent linear reflection or nonlinear distortion. In the coherent reflection mechanism, the forward traveling wave is scattered off hypothesized random inhomogeneities in cochlear micromechanics, but the coherent reflection occurs only for irregularities within the peak region of the traveling wave. The phase of the net reflected wave rotates with the stimulus frequency as the scattering occurs from preexisting irregularities fixed in space. This framework is very similar to so called “place-fixed” emissions originally proposed by Kemp (1978). The distortion type emissions are generated via spatial perturbation caused by the stimulus traveling wave itself due to nonlinear properties of the cochlea. In other words, the forward traveling wave induces mechanical distortions giving rise to a backward traveling wave. In this view the emission sources “travel”

with the stimulus excitation pattern, i.e., they are “wave-fixed”, thus the OAE phase does not change with stimulus frequency in a scale invariant cochlea. Meaning, the signal accumulates the same phase regardless of where it peaks along the BM (Kemp, 1978,1979; Shera and Guinan, 1999; Knight & Kemp, 2001).

The taxonomy described by Shera and Guinan (1999) has been used to further classify the different types of OAEs that can be measured in the ear canal. Since cochlear mechanical amplification is thought to be achieved by a positive feedback process, it is not surprising that OAEs can exist without an evoking stimulus – since positive feedback processes are prone to instability (hence SOAEs). SOAEs are viewed as amplitude stabilized standing waves arising via multiple internal reflections within the cochlea (Shera, 2003). TEOAEs and SFOAEs evoked with low-level stimuli are considered reflection-type emissions, while at higher stimulation levels contributions from nonlinear sources could be present (e.g., Yates & Withnell, 1999; Talmadge et al., 2000; Withnell et al., 2000; Goodman et al., 2003; Withnell et al., 2008). DPOAE, which are the most commonly used OAE test in clinical settings and the focus of this dissertation, are unique and complex in their generation.

1.7.2. Distortion product otoacoustic emissions

When two acoustic pure tones (f_1 and f_2), close in frequency ($f_2 > f_1$), are simultaneously presented to the cochlea, intermodulation distortion occurs at frequencies not present due to the interaction of the stimulus tones. These distortion products are produced due to the frequency-selective, compressive nonlinearity of OHCs and can be measured as acoustic signals in the ear canal, namely, DPOAEs (Kemp, 1978; Brownell et al. 1985; Kemp et al., 1986). In fact, the presence of a distortion emission itself is a manifestation of nonlinearity because it represents energy not present in the input stimulus. The simultaneous presentation of two primaries elicits

many distortion products at arithmetic frequencies of the stimulus tones, but the largest DPOAE in humans occurs at a frequency equal to $2f_1 - f_2$. For this reason, the most prominent and widely studied DPOAE in humans occur at the frequency $2f_1 - f_2$, also known as the cubic distortion product.

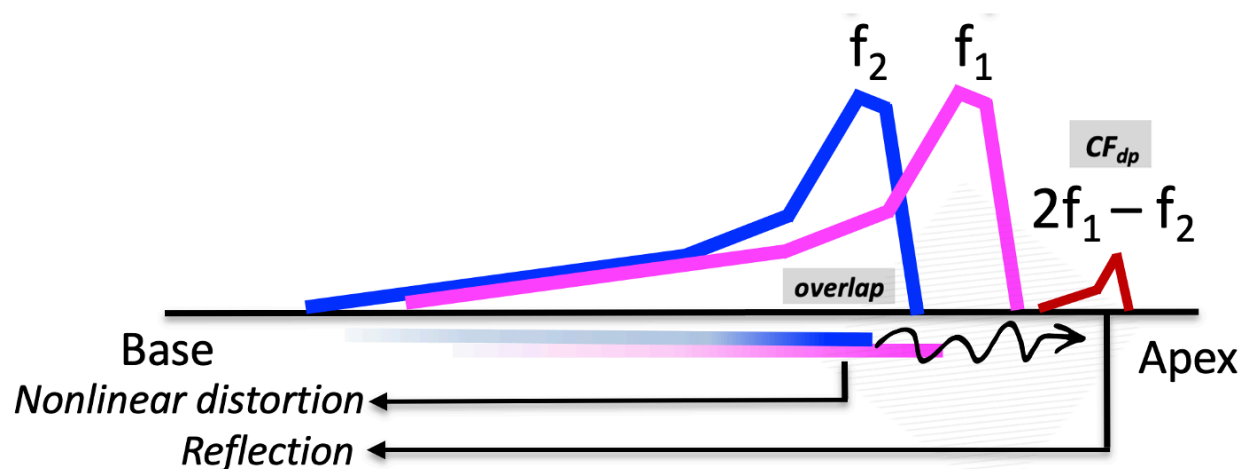


Figure 2. DPOAE generation

DPOAE generation has two mechanistic components: a, typically, dominant nonlinear distortion component generated around the overlap region of the two stimulus tones (near the f_2 peak) and a, typically, smaller reflection component at the characteristic place (CF_{dp}) of the distortion product.

1.7.2.1. DPOAEs and OHC dysfunction

DPOAEs generated by low-level stimuli have been shown to be physiologically vulnerable to the same factors that affect or destroy hair cells, as seen in animal studies (Kim, 1980; Kim et al., 1980; Lonsbury-Martin et al., 1987; Brown et al., 1989). Brown et al. (1989) reported that OHC damage, confirmed by histological examination, corresponded to reduced DPOAE levels, supporting the involvement of OHCs in the generation of DPOAEs. BM tuning properties also depend on the status of hair cells (Khanna & Leonard, 1986; Ruggero & Rich, 1991), as does the sensitivity and frequency selectivity observed in the tips of neural tuning curves (Liberman & Dodds, 1984).

Recent measurements on mutant mice that lack the gene coding for stereocilin have raised a surprising issue regarding the part played by MET channels in the generation of distortion waveform (Verpy et al., 2008). Stereocilin, a protein, is associated with horizontal top connectors that join adjacent stereocilia within and between rows, and with the links that attach the tallest stereocilia to the tectorial membrane (Verpy et al., 2011). In the absence of stereocilin, horizontal top connectors do not develop, and the tips of OHC stereocilia are less clearly aligned. Cochlear sensitivity is found to be normal as illustrated by auditory brainstem evoked and compound action potential thresholds. MET currents derived from round-window measurements of cochlear microphonics are normal as well, indicating the presence of a full supply of normally functioning MET channels. Yet, DPOAEs and waveform distortion in the electrical responses of OHCs are abolished in response to stimuli below 90 dB SPL. Whereas in wild-type mice they are evident in the 20- to 90-dB SPL interval. Thus, waveform distortion can vanish even though OHC MET channels provide normal amplification and filtering. This leads to the deduction that the top connectors and, possibly, the contact of the stereocilia bundle to the tectorial membrane contribute to distortion production.

1.7.2.2. DPOAE generation

DPOAE generation has two mechanistic components: a typically dominant nonlinear distortion component generated around the overlap region of the two primary tones, which is near the f_2 place, and a typically smaller reflection component at the characteristic frequency place of the distortion product (CF_{dp}) (Figure 2). The distortion component is generated by nonlinearities linked to cochlear OHC transduction (Hudspeth & Corey, 1977) in the overlap region where the two traveling waves, evoked by the stimulus tones, maximally overlap. It has been called the generator, distortion, overlap, or nonlinear component. The extent of the overlap

region that contributes to the distortion component generated is controversial. Recent evidence suggests in some species and for certain stimulus conditions there could be contributions from sources much basal to the overlap region (Martin et al., 2011; Charaziak & Siegel, 2015; Lewis & Goodman, 2015). The phase of the distortion component is nearly constant across frequency because the emission generation mechanism is tied to the traveling wave. That is, when frequency-scaled stimuli are presented to the ear, the number of wavelengths to the peak of the traveling wave is nearly constant.

Once the distortion component is generated, some of the energy travels toward the base and, eventually, out to the ear canal and some travels apically and acts similarly to an external tone at the distortion product frequency traveling to its characteristic place on the cochlear partition. Once the energy reaches its characteristic place, it is partially reflected near the $2f_1-f_2$ frequency place (i.e., the CF_{dp}). This linear reflection component is thought to stem from coherent reflection near the peak of the resulting amplified traveling wave and changes phase more rapidly with frequency. Like the distortion component, the reflection component then travels toward the base of the cochlea, through the middle ear, to the ear canal where the vector sum of the distortion and reflection components together are recorded as one composite DPOAE.

When in phase, the components interfere constructively and when out of phase, they interfere destructively. Since the two components differ in phase as a function of the stimulus frequencies, the resulting emission recorded shows maxima and minima in the amplitude of the composite DPOAE visible when small frequency increments are used (e.g., in a frequency swept paradigm). This resulting pattern of peaks and valleys is called DPOAE fine structure (Figure 3). The changes in DPOAE amplitude due to fine structure can be significant, > 20 dB (Gaskill & Brown, 1990; He & Schmiedt, 1993; Heitmann et al., 1996; Shera & Guinan, 1999; Talmadge et

al., 1999). If DPOAEs are collected with widely spaced frequency separation, like in a discrete frequency testing paradigm used clinically, one would not know for certain if the DPOAE level represents a maxima, minima, or in-between, leading to an increase in the variability in group norms (reviewed in Mauermann & Kollmeier, 2004).

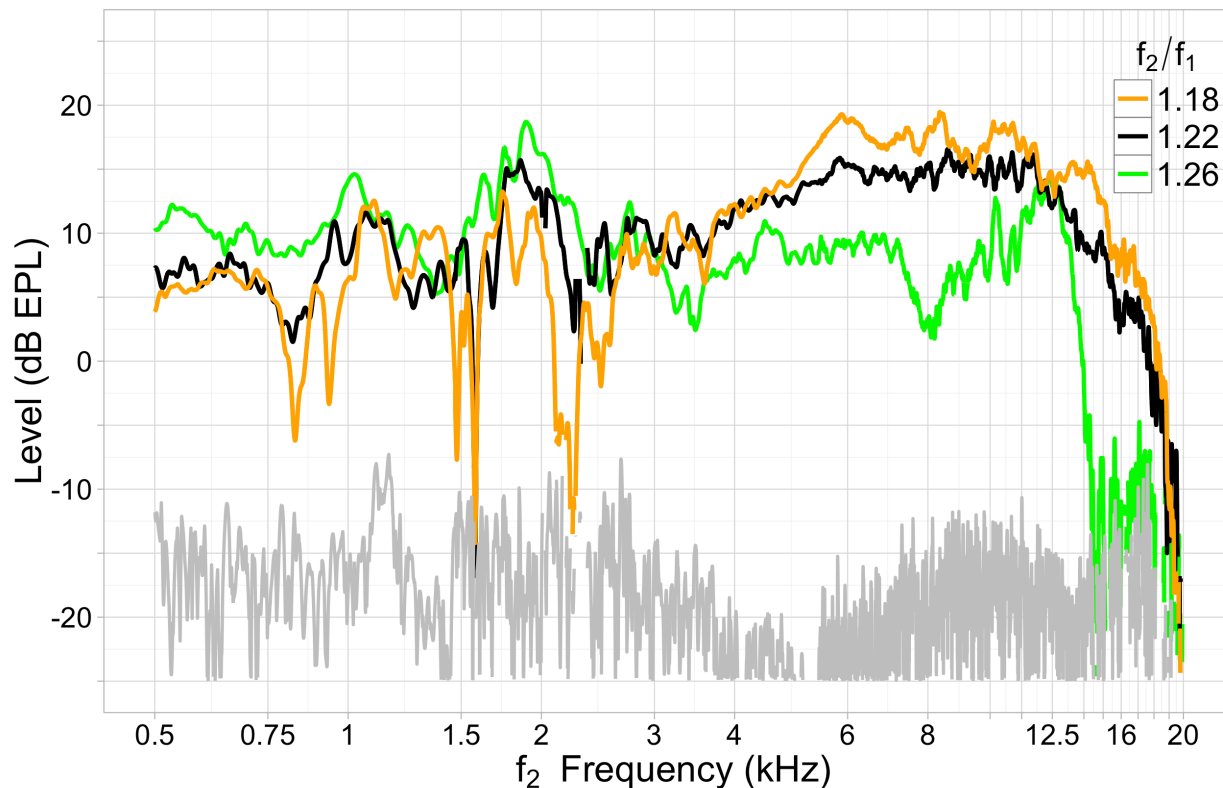


Figure 3. DPOAE fine structure visible in a normal hearing participant

Average DPOAE level and noise floor (gray line) as a function of f_2 frequency for participant 010_SSDP obtained using three concurrent frequency sweeps presented simultaneously. DPOAE level is reported for three ratio conditions when stimulus primaries were presented at a 65 & 55 dB FPL. When in phase, the components interfere constructively and when out of phase, they interfere destructively. Since the two components differ in phase as a function of the primary frequencies, this results in maxima and minima in the amplitude of the composite DPOAE when it is measured using small frequency increments. This resulting pattern of peaks and valleys is called DPOAE fine structure.

1.7.3. Characterizing auditory function

Because DPOAEs provide this unique window into cochlear function, it is no surprise that these measurements have been of great research and clinical interest. Certain advantages of

OAEs were recognized almost immediately following their discovery. Abnormalities in OAE measurements are often associated with common causes of hearing loss such as middle ear dysfunction or cochlear dysfunction. Furthermore, as a non-invasive, window into cochlear function, OAEs can be used in research settings to directly compare human and animal model data.

1.7.3.1. DPOAEs and hearing pathology

The objective and noninvasive assessment of OHC function using DPOAEs is desirable for their practical application. OHCs are reported to be negatively affected by sound overexposure (e.g., Engdahl & Kemp, 1996), ototoxic drugs (e.g., Katbamna et al., 1999), infections (e.g., meningitis, mumps, materno-fetal infection), and anoxia (e.g., birth trauma), or in relation to a known, genetically caused SNHL. Many of these SNHLs resulting from OHC damage or dysfunction have shown DPOAEs to be frequency specific and positively correlated with cochlear status in the region of the f_1 and f_2 overlap (Kim et al., 1980; Schmiedt, 1986; Lonsbury-Martin et al., 1987; Martin et al., 1987; Widerhold et al., 1986).

When investigating auditory function and hearing pathology, animal studies provide a unique advantage as they allow direct comparison of OAEs with electrophysiological measures of cochlear function, as well as the underlying histopathology (e.g., Martin et al., 1998). For example, in guinea pigs chronically treated with aminoglycoside gentamicin, Brown et al. (1989) demonstrated that in frequency regions where there was substantial OHC pathology, DPOAEs elicited by stimulus tones below 60 to 70 dB SPL were greatly reduced. However, those produced by higher level stimuli were unaffected, highlighting the importance of appropriate stimulus parameters for detecting dysfunction.

Exposure to damaging levels of noise can also affect DPOAEs evoked by both low- and high-level stimuli (Howard et al., 2002). Sound exposures in human ears producing a temporary behavioral threshold elevation have also shown reduced DPOAEs in a frequency-specific manner (Sutton et al., 1994). In the recovery, postexposure DPOAE levels, in general, follow a time course similar to that of corresponding behavioral thresholds. Irreversible reductions in DPOAE levels resulting from chronic noise overexposure have been described in chinchillas (e.g., Harding et al., 2002), rabbits (e.g., Franklin et al., 1991), and mice (e.g., Jimenez et al., 1999). These have corresponded with frequencies of permanent behavioral threshold shifts (Franklin et al., 1991) and frequency regions associated with histologically observed damage to the organ of Corti (Vázquez et al., 2004).

In human and animal models, DPOAEs are shown to be reduced with increasing age. In the latter decades of life, functional declines reflected in behavioral hearing thresholds have, historically, been the marker of age-related hearing loss (ARHL), the most common form of adult-onset hearing loss. ARHL is known to have OHC decline outpace IHCs by >2:1 (Liberman & Liberman, 2019), highlighting the importance of evaluating OHC function in order to fully characterize the cochlear effects of aging. In fact, experimental findings in mice with ARHL have indicated that both moderate- and high-level DPOAE stimuli accurately follow the progressive degeneration of high-frequency OHCs (Jimenez et al., 1999).

1.7.3.2. DPOAE applications in clinical settings

In clinical applications, the measurement of DPOAEs has provided a unique tool for evaluating cochlear sound processing in normal and impaired human ears. Common clinical uses for DPOAEs include screening for presence of hearing loss, differential diagnosis, and serial monitoring of cochlear damage due to ototoxic agents (noise or medications). Today, OAEs are

most often used routinely for newborn hearing screening and as part of a test battery for diagnosing hearing loss. Along with other non-behavioral tests, like tympanometry and auditory brain stem responses, DPOAEs can objectively differentiate between middle-ear, cochlear, and neural disorders. Additionally, because many damaging agents initially target OHCs, monitoring DPOAEs are ideal for assessing ototoxicity (Roland, 2004; Reavis et al., 2008, 2011; Dille et al., 2010) especially since physiological change can be detected before a perceptual difference is noticed by the patient (Katbamna et al., 1999; Ress et al., 1999). This supports the use of monitoring using DPOAEs as they may allow for earlier detection of cochlear damage.

Although DPOAEs are measured in clinical settings, there are limitations to their use. DPOAE testing has been used for diagnostic purposes; however, they are currently used most in clinical settings for simply differentiating between normal-hearing and hearing-impaired ears. DPOAE tests have been found to be most accurate for screening at audiometric frequencies from 2 to 6 kHz. Yet, even at this seemingly basic task of detecting dysfunction, clinical DPOAE measurements are not absolute in that some ears with normal hearing are misdiagnosed as hearing-impaired while some ears with hearing loss are incorrectly diagnosed as normal-hearing (e.g., Gorga et al., 1993a, 1997; Kim et al., 1996). Moreover, measurements are even worse for frequencies between 0.75 and 1.5 kHz and at the highest test frequency of 8 kHz.

1.8. Rationale

Hearing loss is the most common sensory deficit worldwide. It is the third most common chronic physical condition among Americans, with as many as 3 in 10 adults having a measurable hearing loss (Agrawal et al., 2008; Cruickshanks et al., 2003); yet, only 1 in 10 adults will actually self-report a hearing loss (Kochkin, 2009). Of those limited individuals who

actually seek hearing health care treatment (e.g., hearing aids), the average person will wait 6 to 9 years after his or her hearing loss is identified (Kochkin, 2010; Simpson et al, 2019).

1.8.1. Importance of early identification

One way to close this 6- to 9-year gap can come from early identification and monitoring of hearing loss progression. There are several benefits to monitoring for hearing loss: (1) monitoring can allow a patient time to accept his or her hearing loss before it becomes severe enough to warrant treatment; (2) monitoring for dysfunction from noise overexposure or ototoxic medications has major implications for hearing conservation purposes; (3) when future drug, stem cell, or genetic therapy options become available, measures that test the entire cochlea could be utilized for monitoring the preservation or restoration of hearing.

Early identification of treatable hearing loss has major implications as untreated hearing loss has been linked to depression, anxiety, fatigue, and cognitive decline (Bess et al, 1989; Mulrow et al, 1990; LaForge et al., 1992; Carabellese et al., 1993; Appollonio et al., 1996; Heine et al., 2002; Dalton et al; 2003; Gates et al., 2005; Kochkin, 2010). Additionally, the socioeconomic consequences of hearing loss have been associated with low educational attainment and economic hardship (Emmett & Francis, 2014). Fortunately, many of these negative consequences are avoidable if early and appropriate intervention is established following the early identification of the dysfunction. In fact, individuals with treatable hearing loss that opt to use hearing aids are more likely to report better physical, emotional, mental, and social well-being than those who do not opt for hearing aids (Agrawal et al., 2008).

1.8.2. Age-related hearing loss

When thinking about the numerous types of hearing losses that exist, the most common form of adult-onset hearing loss is age-related which starts early and progresses slowly through

the lifespan. In several studies, thresholds were found to increase (Harris & Myers, 1971; Osterhammel & Osterhammel, 1979; Dreschler et al., 1985; Green et al., 1987; Stelmachowicz et al., 1989; Frank, 1990; Hallmo et al., 1994; Sakamoto et al., 1998; Ahmed et al., 2001; Lee et al., 2012; Stiepan et al., 2019) and DPOAE levels were found to decrease (Dorn et al., 1998; Poling et al., 2014; Stiepan et al., 2019) with age and with increasing test frequency. Recently, Stiepan et al. (2019) showed age-related behavioral threshold, DPOAE, and SFOAE changes in a large group of young and middle-aged adults (Figure 4). Threshold declines from the youngest age group (of 10-21 years) to the oldest age group (of 55-68 years) were seen first in the highest frequencies and then progressed gradually to lower frequencies. Interestingly, a noticeable shift in hearing could be seen as early as the fourth decade of life. However, there are limitations to behavioral threshold testing such as the time it takes to execute and the requirement of active participation.

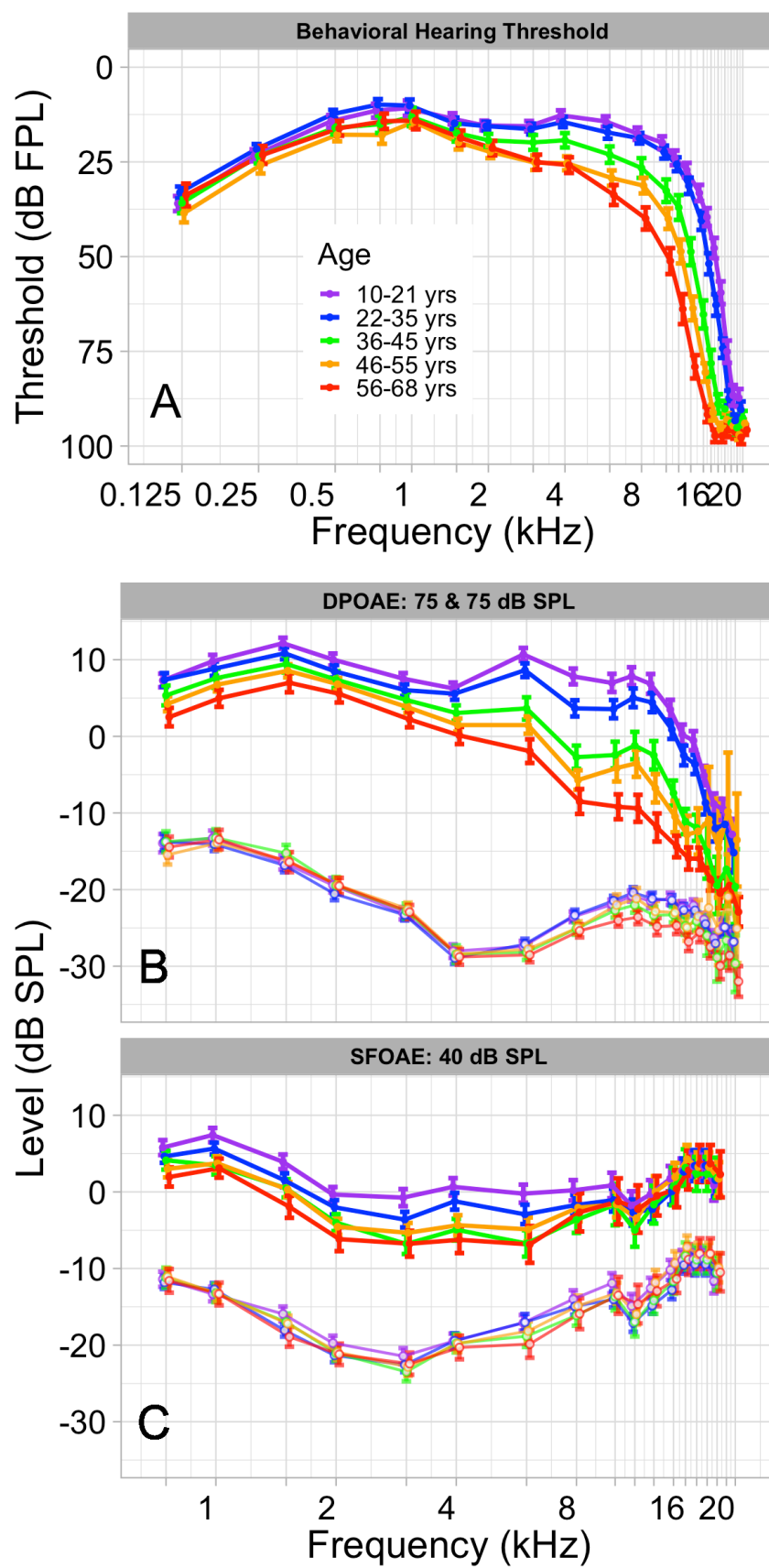


Figure 4. Aging and auditory decline

Average hearing thresholds (A) and OAE levels and noise floor levels (B-C) for different age groups as a function of frequency. Error bars indicate the 95% confidence interval. Note the different frequency ranges in the threshold and OAE panels. (Reproduced from Figure 1 of Stiepan et al. (2019), with permission).

Since OHC damage or dysfunction is associated with aging in the cochlea, DPOAEs are an ideal alternative to behavioral threshold testing. DPOAEs themselves are the by-product of the nonlinear sound amplification process in the cochlea and hence can serve as a measure for evaluating cochlear OHC integrity. Furthermore, DPOAE plotted as a function of frequency shows age-related decline in the same high frequencies as behavioral thresholds (Figure 4). Additionally, DPOAEs are an ideal choice after behavioral threshold testing as they are already a familiar tool in clinical settings. The objective, efficient, and noninvasive nature of DPOAEs have made them a clinical tool utilized for both screening and diagnostic purposes.

1.8.3. Establishing appropriate DPOAE stimulus parameters

In clinical settings, DPOAE levels across frequency that fall above the noise floor are evaluated as normal or abnormal when compared to an established normative range. The level of the DPOAE recorded in the ear canal depends on the frequency and level characteristics of the stimuli used to elicit it. Thus, the choice of stimulus parameters may influence the success with which DPOAEs can be used to assess cochlear function and predict auditory status. It may be more important to focus on maximizing DPOAE level rather than other DPOAE measures, such as signal-to-noise ratio (SNR), on the assumption that DPOAE level is correlated with cochlear function. Additionally, while DPOAE phase may be important for basic research applications (e.g., Shera & Guinan, 1999), current clinical applications of DPOAE measures depend on DPOAE level (with an SNR cut-off requirement), but largely ignore phase measurements.

1.8.3.1. Early investigations of DPOAE stimulus parameters

A number of early investigations examined the influence of stimulus parameters on the DPOAE (e.g., Harris et al., 1989; Brown & Gaskill, 1990; Gaskill & Brown, 1990; Hauser & Probst, 1991; Whitehead et al., 1995 a,b), resulting in recommendations for stimulus conditions likely to yield robust emissions in human ears. A primary-frequency ratio of 1.22 has been recommended as optimal (Harris et al., 1989; Gaskill & Brown, 1990; Brown et al., 1994), although variability in the frequency ratio producing the largest DPOAE across stimulus frequency has been reported (Harris et al., 1989).

A pioneering study by Harris et al. (1989) showed how optimal frequency ratio as a function of DPOAE frequency and as a function of stimulus level influenced DPOAE measurements in 10 ears (of 5 participants). Average performance revealed how the largest DPOAE amplitudes occurred at narrower ratios in response to higher frequency and lower level stimulus primaries, while wider ratios were needed to generate maximum DPOAE amplitude for low frequency and higher-level stimulus primaries. These findings are reasonable if we consider what we know about mammalian cochlear mechanics.

1.8.3.2. Local cochlear mechanics

The mechanical properties of the cochlea, driven by a combination of passive and active properties, change systematically across its length. The passive mechanical properties, which determine gross tuning characteristics, are responsible for the tonotopic map defined from base to apex. The active cochlear process, which allows for the positive feedback loop that amplifies the traveling wave at its peak, is responsible for sharper tuning from apex to the base. As a result of these mechanical gradients, stimulus tones of different frequencies cause maximum displacement at specific positions along the cochlear length.

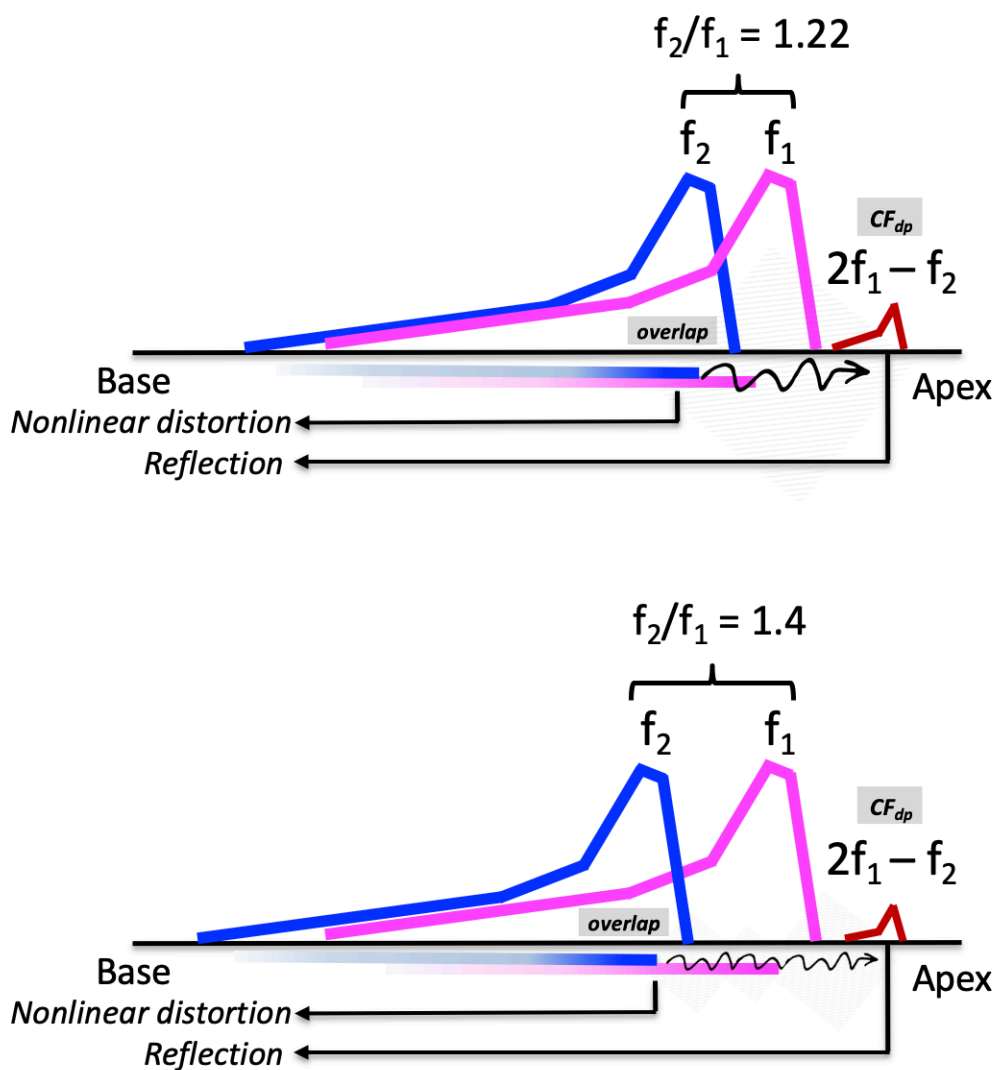


Figure 5. The strength of the nonlinear distortion generated depends on the overlap region created by the stimulus tones

In DPOAE stimulation, the nonlinear interaction between the two stimulus tones generates a distortion component in the overlap region of the f_1 and f_2 tones (indicated by the orange circle). Changing the f_2/f_1 relationship changes the overlap region, changing the characteristics of the distortion component.

DPOAE generation is hypothesized to be maximized at that cochlear place when the mechanical interaction between the two stimulus tones is optimal with minimal mutual suppression or phase interference between them (Figure 5). In DPOAE stimulation, the nonlinear interaction between the two stimulus tones generates a distortion component in the overlap region of f_1 and f_2 tones. Changing the f_2/f_1 relationship changes the number of generators

(i.e., OHCs) in the overlap region, thus, changing the characteristics of the distortion component and the DPOAE that travels back to the ear canal (Figure 5). Because the spatial properties of the traveling waves are determined by local cochlear mechanics, which change from base to apex, the frequency and level characteristics between the stimulus tones, which will affect the distortion generation, need to be adjusted as a function of frequency to maintain optimal interaction between them (Figure 6). Therefore, with the systematically varying mechanical properties along the cochlear partition, optimal stimulus frequency ratios would also change with frequency and stimulus level.

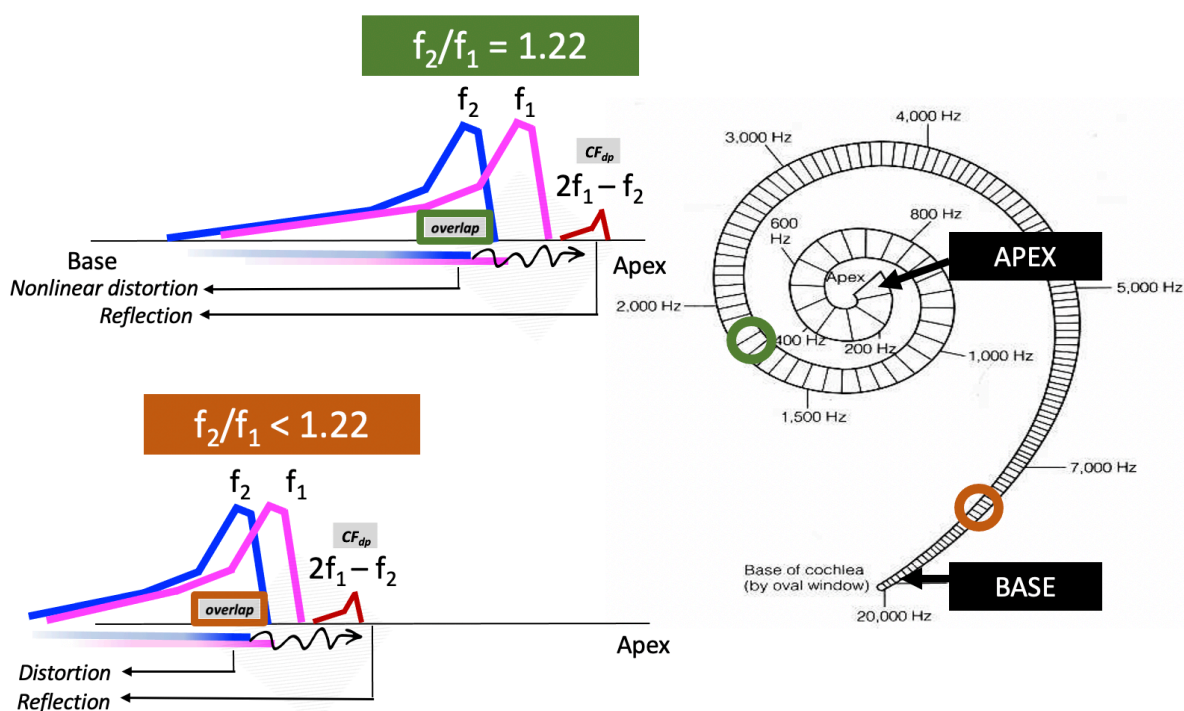


Figure 6. The f_2/f_1 relationship of the stimulus tones needs to be adjusted as a function of frequency to maintain optimal distortion generation in the overlap region

The place-specific mechanical properties of the cochlea change across its length. Because the spatial properties of the traveling waves are determined by these local cochlear mechanics, which change from base to apex, the frequency and level characteristics of the stimulus tones need to be adjusted as a function of frequency to maintain optimal interaction (i.e., an optimal overlap) between them.

1.8.3.3. Limitations of previous investigations

Even though Harris et al. (1989) found stimulus frequency ratios to be f_2 frequency and stimulus level dependent, at the conclusion of the study the message that resonated was that, “Despite the frequency and level dependence of the f_2/f_1 ratio effect on DPOAEs, a ratio of 1.22 elicited the largest DPOAE between 1 and 4 kHz.” From this and other early studies investigating the DPOAE stimulus parametric space, clinical protocols have maintained using a DPOAE protocol with fixed stimulus parameters. Clinical protocols use a single stimulus frequency ratio (Harris et al., 1989) and level combination (Gaskill & Brown, 1990; Stover et al., 1996; Whitehead et al., 1995a,b) that represents the midpoint or average of performance over multiple test frequencies. Using this fixed stimulus setting, considerable effort then focused on how well both the level of the DPOAE and the separation of the DPOAE level from the noise floor (i.e., SNR) can be used to determine if a DPOAE is normal or abnormal (i.e., indicative of hearing loss) (e.g., Gorga et al. 1997, 2005). These gold standard studies established the normative ranges for measuring DPOAEs at discrete, clinically utilized frequencies (ranging from 0.5 to 8 kHz), using a fixed stimulus frequency ratio of 1.22 and stimulus level of 65- and 55-dB SPL.

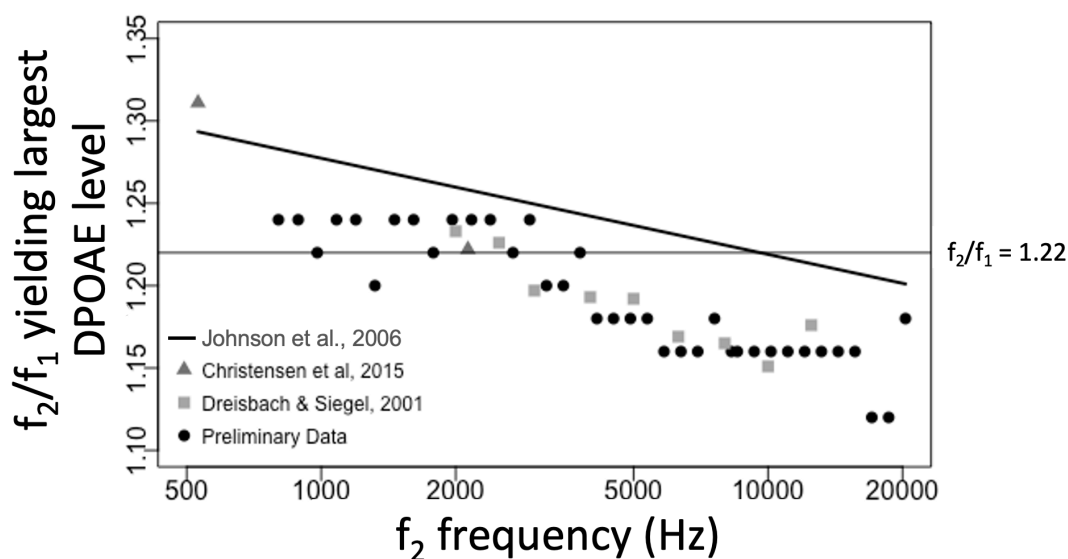


Figure 7. Previous studies showing optimal DPOAE stimulus frequency ratio as a function of frequency

The accuracy of the best fit function extrapolated from Johnson et al. (2006) compared to findings from other groups that have reported frequency ratio yielding the largest DPOAE (including preliminary data collected for this dissertation). The Johnson et al. (2006) model made to predict optimal ratio does not accurately reflect actual test performance from other groups testing normal-hearing adults. This difference in the model could be related to a limited sample size used or inaccurate assumptions of systematic changes in the cochlea which are especially noticeable when high frequencies are evaluated.

More recently, frequency specific stimulus parameters have been investigated, like in Johnson et al. (2006) when optimal stimulus parameters were evaluated at 1, 2, 4, and 8 kHz in 20 normal hearing individuals. From the individual optimal f_2/f_1 conditions, a frequency-specific best fit to the stimulus conditions producing the maximum DPOAE were derived. Although, using a fit like this is a desirable way to summarize and extrapolate beyond the raw data, it also assumes that the linear fit represents that the data changed in a certain systematic way that could hold for other frequencies and samples. The accuracy of this fit across frequency compared to findings from other groups that have reported frequency ratio yielding the largest DPOAE is displayed in Figure 7. The Johnson et al. (2006) model predicting optimal ratio (i.e., a function fit to the individual data producing maximum DPOAE levels), does not accurately reflect actual test performance from other groups testing normal-hearing adults. This difference in the model

could be related to a limited sample size used or inaccurate assumptions of systematic changes in the cochlea which are especially noticeable when high frequencies are evaluated.

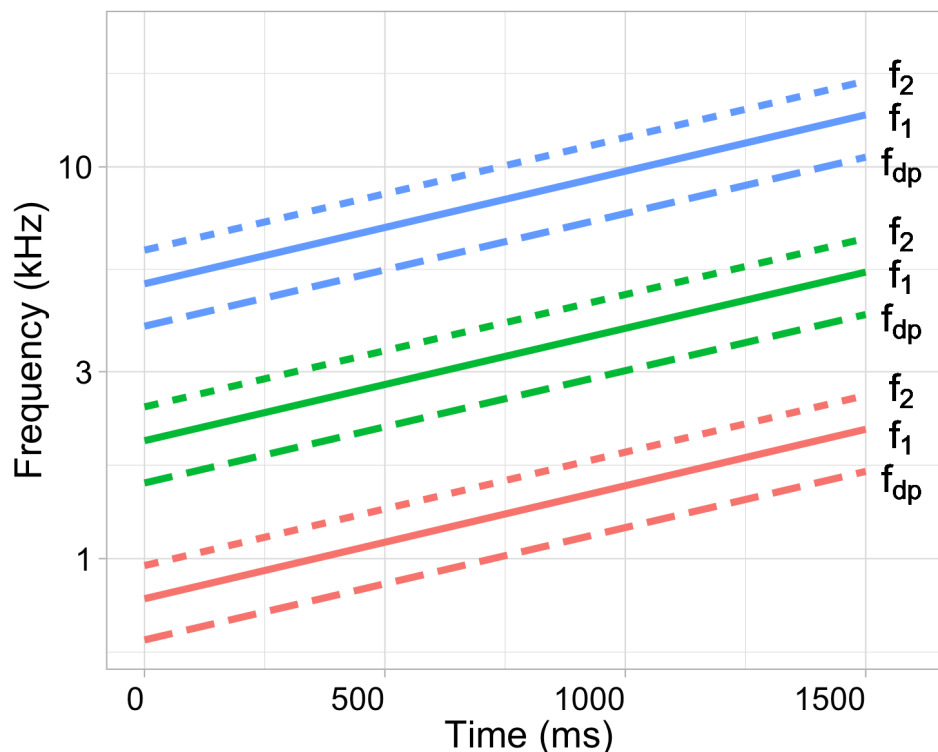


Figure 8. Simultaneous, concurrent frequency sweeps for DPOAE measurement

Schematic of stimulus frequency (f_1 and f_2) and DPOAE frequency (f_{dp}) behavior over time when presenting three concurrent frequency sweeps simultaneously. Each of the three concurrent sweeps is represented by line color. Primary frequencies are indicated by line type.

1.8.4. Recent calibration and procedural innovations

Since the Johnson et al. (2006) study, further advancements to DPOAE measurement systems and protocols have been made that allow for more accurate and extensive data collection. This includes the ability to accurately measure frequencies above 8 kHz, which is especially important for identifying early signs of ARHL. Additionally, new advancements now allow for more accurate calibration of the stimulus presented and emission recorded during OAE measurement—reducing test variability. This variability, which occurs due, in part, to standing

wave effects when a probe is sealed in the ear canal, can be ameliorated by using forward pressure level (FPL) and emission pressure level (EPL) corrections. Lastly, DPOAE test protocols can now be executed faster (Figure 8) using swept frequency stimulation techniques that allow for recordings with higher frequency resolution (Figure 3)

1.8.5. Purpose of dissertation

Yet still, a critical question remains. Should fixed stimulus parameters be used when testing up to the highest frequencies of human hearing when the passive and active properties of the cochlea are known to change across its length? We contend that the varying mechanical properties along the cochlear partition are not accounted for in current DPOAE test protocols where stimulus properties remain invariant with frequency. This is a critical weakness in current DPOAE test protocols.

For this dissertation, we hypothesized that DPOAE stimulus parameters that are optimized for the cochlear place of stimulation would evoke large emission levels that accurately reflect cochlear health and, thus, be closely related to behavioral hearing when OHC mechanisms are affected. We explored the DPOAE stimulus parametric space in humans in order to identify the most appropriate stimulus frequency ratio and level combinations for measuring DPOAEs up to 20 kHz. DPOAEs were recorded using a range of stimulus frequency ratios and levels that are known to produce large DPOAE levels and SNRs in audiometrically normal-hearing, young adults. In a second study, we used clinical decision theory to identify optimal stimulus conditions that improved the accuracy of differentiating between normal-hearing and hearing-impaired ears. These optimizations are likely to aid in the early and accurate detection of cochlear decline in human ears by improving DPOAE test performance.

CHAPTER 2

Optimizing DPOAE Recordings in Normal-Hearing Ears by Adopting Cochlear Place-Specific Stimuli

2.1. Introduction

DPOAEs provide a unique window into evaluating OHC integrity and function as they are a by-product of the active and nonlinear cochlear amplification process (Davis, 1983; Dallos, 1992; Zheng et al., 2000; Dallos et al., 2008). By appropriately exploiting DPOAEs recorded in the ear canal, we can better understand the fundamental active physiology of the human cochlea that leads to the sharp frequency selectivity, wide dynamic range, and acute sensitivity characteristic of mammalian hearing. Because cochlear function can be assessed in an objective, efficient, and noninvasive way, DPOAEs should be positioned as an indispensable tool in both research and clinical settings. Yet, DPOAEs are limited in use, particularly in clinical settings. Specifically, most clinical applications of DPOAEs are limited to screening for hearing loss only. Perhaps DPOAEs are not used for more precise clinical purposes because current measurement protocols are not aligned with the known variation in cochlear mechanics that change from base to apex. This could explain the variability traditionally seen in emission amplitudes within and across individuals which limits their clinical use in applications that demand precision. A measurement protocol that accounts for the differences in cochlear mechanics as a function of cochlear length could then position DPOAEs as a more accurate and widely used clinical tool. In this study, we explored stimulus characteristics that align DPOAE stimuli with place-specific

cochlear properties in order to accurately quantify cochlear function up to the highest frequencies of human hearing.

Most DPOAE measurement protocols use stimulus tones that are fixed in level (L_1 & L_2) and frequency ratio (f_2/f_1) when measuring across f_2 frequency. This is in conflict with the systematic variation in local anatomical and physiological properties of the cochlea. The use of these suboptimal stimulus combinations could compromise both the recording of robust DPOAEs in normal ears and their sensitivity in ears with cochlear dysfunction. Furthermore, these fixed stimulus parameters likely contribute to the variability seen in DPOAE characteristics across normal-hearing ears.

The physical characteristics as well as active mechanical properties change as a function of place along the cochlear length. It is these passive (e.g., mass, stiffness, and damping) and active (e.g., OHC-driven amplification) local cochlear mechanics that determine the spatial properties of the traveling wave. Modifying the stimulus frequency ratio characteristics to suit known cochlear partition vibration patterns is expected to create optimal interaction between the stimulus tones leading to the largest emission response at a given cochlear place in normal ears.

It is hypothesized that DPOAE generation is maximized at a specific cochlear place when the mechanical interaction between two stimulus tones is optimal with minimal mutual suppression or phase interference between them. The mechanical properties of the cochlear partition change from apex to base resulting in tuning becoming sharper as a function of increasing frequency and decreasing stimulus level. These findings are consistent with the tuning profile of BM mechanical responses and is comparable with neural and psychophysical data from several studies (Kiang et al., 1967; Dallos & Cheatham, 1976; Moore, 1978; Moore et al., 1984; Robles & Ruggero, 2001). Therefore, it is expected that stimulus frequency ratio and/or

levels need to be adjusted as a function of frequency to adapt to local cochlear mechanics in order to generate the maximum distortion amplitude. Specifically, at a constant L_1 & L_2 combination, the f_2/f_1 producing the maximum DPOAE level should be narrower for high frequencies compared to low frequencies. Similarly, for a fixed f_2/f_1 , higher L_1 & L_2 combinations would be optimal at high frequencies compared to low frequencies. This is consistent with the idea that excitation patterns for the eliciting two primaries are more spatially separated at high frequencies than at low frequencies, requiring a decrease in the primary frequency ratio or an increase in the primary levels in order to create the optimal mechanical overlap between the vibration patterns of the stimulus tones for generating distortion.

When a range of stimulus frequency ratios are evaluated, DPOAE levels measured as a function of varying stimulus frequency ratio depict a bandpass shape such that the DPOAE amplitude is highest at an optimal ratio value and is reduced at ratios higher and lower (Harris et al., 1988; Brown et al., 1992; O'Mahoney & Kemp, 1995; Abdala, 1996; Stover et al., 1999). At higher ratios, the DPOAE recorded is reduced because the vibrations due to the stimulus tones are spatially separated on the BM with minimal or no overlap to generate distortion. On the opposite side, the ratio becomes too narrow such that the spatial overlap becomes so large that other nonlinear phenomena such as two-tone suppression (Shera et al., 2007) and destructive phase interference (Sisto et al., 2018) appear to contribute to reductions in DPOAE amplitude.

Evidence supporting increased distortion generation when place-specific stimulus frequency ratios are employed have been reported in both psychophysical and OAE experiments. Previously, a prominent argument that psychophysical combination tones were generated in the cochlea, rather than the middle ear, was based on evidence of a steep drop in the combination tone levels as the ratio of the stimulus frequencies was increased (Zwicker, 1981). It was

theorized that this trend resulted from decreased overlap of the excitation patterns of the stimuli. The level of DPOAE itself has also been shown to vary depending on the frequency ratio of the stimuli. This trend has been shown in studies using rabbits (Lonsbury-Martin et al., 1987; Whitehead et al., 1990,1992), guinea pigs (Brown and Gaskill, 1990), and humans (Wilson, 1980; Harris et al., 1989; Gaskill and Brown, 1990; Abdala, 1996; Stover et al., 1999).

A number of previous investigations have examined the influence of stimulus parameters on DPOAE levels in human ears (e.g., Harris et al., 1989; Brown & Gaskill, 1990; Hauser & Probst, 1991; Brown et al., 1994; Whitehead et al., 1995a,b; Kummer et al., 1998, 2000; Dreisbach & Siegel, 2001; Johnson et al. 2006, Sisto et al., 2018), resulting in recommendations for stimulus parameters likely to yield large emissions. Even in the earliest study by Harris et al. (1989), evidence that the f_2/f_1 yielding the largest DPOAE was seen to be frequency- and level-specific. Yet, when data were averaged across all f_2 frequencies and all stimulus levels, the f_2/f_1 stimulus frequency ratio that yielded the largest DPOAEs was 1.22. It was this finding that eventually led to the standardization of an f_2/f_1 of 1.22 for all DPOAE measurements (Gorga et al., 1997). To this day, this fixed stimulus parameter remains the gold standard frequency ratio used in DPOAE measurements conducted in clinical and most research settings. However, any casual examination of previous reports makes clear that a ratio of 1.22 does not always elicit the largest DPOAE response from all participants, at all stimulus levels, and especially at all stimulation frequencies.

With the advent of advanced calibration and measurement techniques, OAEs can now be measured faster, more accurately, with finer frequency resolution, and up to the highest frequencies of human hearing. Significant advances in stimulus calibration (e.g., Souza et al., 2014) and emission level correction (Charaziak & Shera, 2016), which eliminate errors due to

resonances in the ear canal, now allow these measurements to be completed reliably.

Additionally, measurement techniques using frequency swept stimuli enable more stimulus conditions to be evaluated in a practical time frame, more efficiently, and using finer frequency resolution (Long et al., 2008; Kalluri & Shera, 2013). Using these advancements, the purpose of this study was to quantify DPOAE levels across a large stimulus parametric space in young, audiometrically normal-hearing human ears. The goal was to identify stimulus combinations that would allow the recording of the largest and most stable DPOAE levels in young, normal-hearing ears. This information could then be used to design clinical protocols that would improve the efficacy of hearing screening using DPOAEs.

2.2. Materials and Methods

2.2.1. Participants

Data are reported from a randomly selected ear of 30 participants (17 female) between the ages of 18 and 30 years (mean 21 years). Participants reported no history of ear surgery, fluctuating hearing loss, Meniere's disease, labyrinthitis, auditory neuropathy, brain injury, ototoxic medications, dementia, or extensive noise exposure. All participants had normal outer ear and middle ear function as determined using otoscopy and tympanometry. The racial and ethnic distribution of the participants was proportional to the population of Evanston, Illinois. Participants provided written, informed consent and were compensated monetarily. All procedures were conducted in accordance with the guidelines of the Institutional Review Board at Northwestern University.

2.2.2. Instrumentation, Calibration & Signal Processing

Signals were generated and recorded using custom software written in MATLAB (2015R) (The MathWorks Inc., Natick, MA), running on an Apple Macintosh computer. DPOAE

measurements, Thévenin calibration of the probe, ear canal acoustic impedance and reflectance, and forward pressure calculations from the pressure response measured in individual ear canal were performed using custom-designed software (ARLas, Shawn Goodman). Behavioral threshold tracking used custom-designed software which automatically controlled stimulus levels delivered (Lee et al., 2012). Signal generation and recording were done using an RME Fireface 400 for analog-to-digital (96 kHz sample rate, 24-bits) and digital-to-analog conversion. Generated signals were sent through an Etymotic Research ER10X probe (Etymotic Research, Inc., Elk Grove Village, IL). During DPOAE measurements, signals from the test ear were recorded using the ER10X microphone and preamplifier combination, digitized, and stored for post hoc analysis. All testing was conducted in a sound treated audiometric booth that met the ambient noise standard (ANSI S3.1–1999).

Stimuli were calibrated using a procedure that allowed the derivation of acoustic quantities that were not affected by standing waves in the ear canal (described in Souza et al., 2014). Thévenin source pressure and impedance calibration of the probe was performed prior to each participant's arrival. In-situ calibration was performed in the subject's ear canal at the beginning of each test session with the same probe and wideband chirp stimulus as was used for source calibration. Recorded DPOAEs were corrected to EPL and stored along with the associated SPL recordings. EPL corrected DPOAEs are equivalent to the DPOAE measured in an anechoic ear canal, resulting in no standing wave effects for the DPOAE traveling through the ear canal (Charaziak & Shera, 2016).

The presence of an air leak was suspected, and the probe was repositioned in the ear canal, when absorbance at low frequencies (A_{low}) was 0.2 (-7 dB) or higher based on criteria recommended by Groon et al. (2015). A_{low} was calculated by averaging over a frequency range

of 0.1 to 0.2 kHz. The recording and analysis software alerted the experimenter when an air leak was suspected prompting the experimenter to remove and reset the probe in the participant's ear canal.

Stimulus generation and DPOAE acquisition were controlled using an algorithm that swept a tone upward in frequency at a rate of 1 octave/second (each primary tone was played through a separate speaker). Stimulus tones that are swept in frequency allow for rapid OAE measurements with high frequency resolution (e.g., Long et al., 2008; Kalluri & Shera, 2013). In a single swept-tone procedure, the full range of tested frequencies were presented over ~ 5.6 seconds having f_2 {start, stop} frequencies of {0.48, 20.78} kHz. Whenever possible, to expedite data collection, three separate frequency sweeps were presented concurrently (Abdala et al., 2015), each lasting ~ 1.88 seconds. During concurrent swept-tone measurements, the full range of tested frequencies was divided into three overlapping segments having f_2 {start, stop} frequencies of {0.48, 1.776}, {1.646, 6.075}, and {5.63, 20.78} kHz, respectively, resulting in ~ 0.1 octave overlap between the sweeps. In pilot experiments, no significant differences were found between DPOAEs recorded using three concurrent sweeps, a single sweep covering the entire frequency range at the same rate, or discrete primary tones. Thus, using the swept-tone method allowed for recording of DPOAEs from a multitude of stimulus combinations for each participant. Data collection was stopped after 32 repetitions. Phase-rotation averaging was employed to cancel out the f_1 and f_2 primaries from the measured response (Whitehead et al., 1996). This was accomplished using three stimulus segments with different stimulus-tone starting phases that were interleaved such that the f_1 and f_2 tones canceled when the responses were averaged while leaving the DPOAE at $2f_1-f_2$ unaffected.

2.2.3. Protocol

A detailed case history was taken and tympanometry was conducted using a GSI Tymptstar Middle Ear Analyzer (Grason-Stadler Inc., Eden Prairie, MN) on the first visit. Before, in-ear calibration, otoscopy was performed to ensure clear ear canals and a visibly intact eardrum. Within a visit, the experimental procedures were administered over a ~2 hour session. In order to complete the multitude of DPOAE test conditions, on average, a participant came in for five visits total.

Pure-tone hearing thresholds were obtained at 19 standard audiometric frequencies from 0.5 to 20 kHz using a modified Békésy audiometry technique. Signals were pulsed tones, 250 ms in duration with 25 ms rise and fall times, presented twice per second. The adaptive threshold task required the participant to press a computer mouse button to indicate that the pulsed tone was heard. In the first reversal, the participant would press the button when the pulsed tone was heard and release when it was not heard. The second reversal followed when the button was pressed while the presentation level was increasing. A step size of 6 dB was used for the first two reversals followed by a step size of 2 dB for the remainder of the threshold estimation process. Midpoints between reversals were calculated for each ascending run (going from below to above audibility). After six ascending runs, the tracking procedure would converge on the threshold once the standard error of the mean was less than or equal to 1. Threshold estimation started at 1 kHz, proceeding to the highest frequency, repeating the measurement at 1 kHz, and then proceeding downward to the lowest test frequency. Further description of the adaptive threshold task can be found in Lee et al. (2012). Figure 7 shows average behavioral hearing thresholds plotted as a function of frequency across participants. Inclusionary criteria, established using data

from Lee et al. (2012), required behavioral thresholds to fall within the normative range for each frequency tested (indicated by the gray shading in Figure 9).

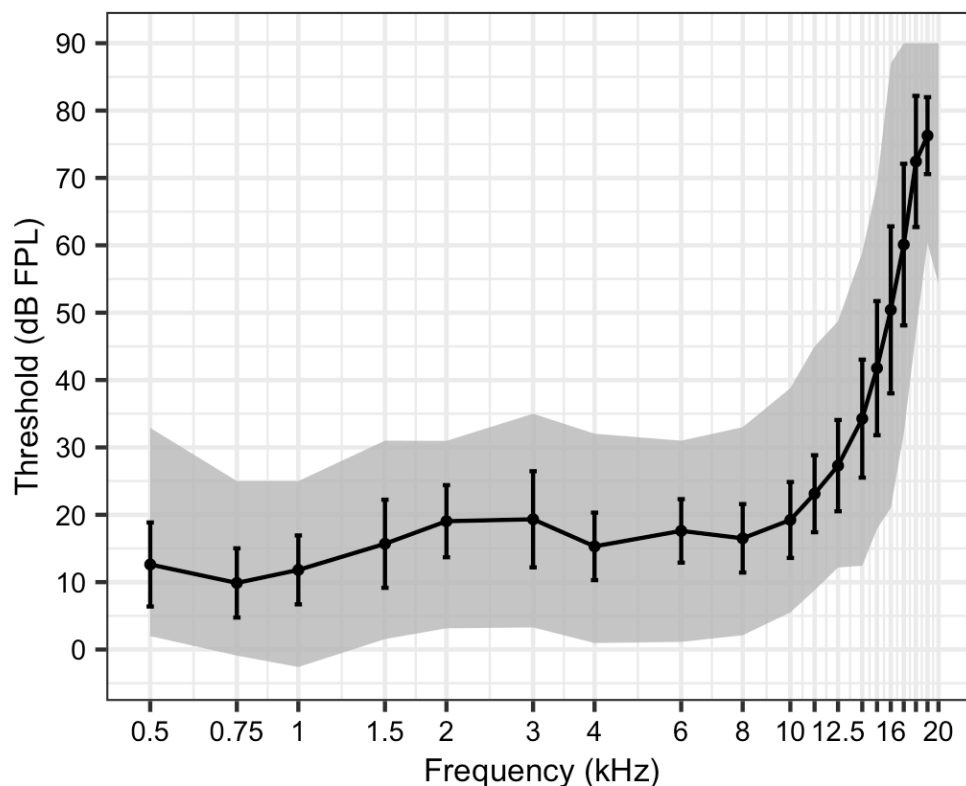


Figure 9. Average behavioral hearing thresholds from audiometrically normal-hearing participants

Average behavioral hearing thresholds using a modified Békésy tracking technique from 30 ears. Error bars indicate ± 1 SD. All thresholds fell within the gray shaded area which indicates the 5th to 95th percentile range of thresholds for young, audiometrically normal-hearing ears between 17 and 21 years of age (Lee et al., 2012).

DPOAEs were evoked by pairs of stimulus tones (f_1 and f_2) and recorded at the frequency of the cubic distortion ($2f_1 - f_2$). Recordings from 90 total stimulus conditions were obtained over five stimulus levels (L_1 & L_2 in dB FPL: 45 & 20, 50 & 30, 55 & 40, 65 & 55, and 75 & 75) and 18 stimulus frequency ratios (ranging from 1.06 to 1.4 in 0.02 steps). Composite DPOAE levels were plotted as a function of f_2 frequency; therefore, noise floor levels were estimated on-band at the f_2 frequency. Before commencing the study, coupler measurements revealed system distortion that influenced DPOAE recordings when concurrent stimulus pairs were presented at

75 & 75 dB FPL. To circumvent this measurement artifact, DPOAE measurements made at 75 & 75 dB FPL were obtained using the single sweep procedure. Further coupler measurements revealed stimulus contamination when measuring at f_2 frequencies above 16 kHz using frequency ratios of 1.06, 1.08, and 1.10. Therefore, measurements made using these conditions at f_2 frequencies > 16 kHz were removed from further analysis.

2.2.4. Analysis

Composite DPOAE level and phase were derived using a least-squares fitting (LSF) procedure described by Long & Talmadge (1997). In the LSF technique, the DPOAE time waveform was segmented into moving analysis windows that shifted in 0.01 octave steps. Models for the stimuli and DPOAEs were created. The amplitude and phase within each analysis window was estimated by minimizing the sum of the squared residuals between the model and the data to achieve the best fit. Following the LSF procedure, DPOAE level and corresponding noise floors were averaged into one-third-octave frequency bands centered at octave and inter-octave audiometric test frequencies from 0.5 and 19 kHz.

Test-retest reliability (i.e., the consistency of a measurement over time) was established by repeating the same DPOAE measurement (65 & 55 dB FPL, $f_2/f_1 = 1.22$) at each test visit (five visits in total). The average test-retest difference was calculated after finding the median DPOAE measured and subtracting it from each of the remaining four DPOAE measurements made at that frequency. Intra-class correlation coefficients (ICC) were computed as they are a widely used reliability index and take into account a variety of statistical assumptions such as normality and stable variance. Generally speaking, the ICC determines the reliability of ratings by comparing the variability of different ratings of the same individuals to the total variation across all ratings and all individuals. Therefore, ICC refers to correlations within a class of data

(i.e., correlations within repeated measurements of DPOAE level). Reliability was further assessed using Bland-Altman analysis to describe the agreement between the first and last visit in order to determine if there was a learning effect. Statistical limits were also calculated by using the mean and the standard deviation of the differences between two measurements.

Lastly, ranking was used to calculate the “optimal” f_2/f_1 that produced the maximum DPOAE level at each f_2 frequency for each of the five stimulus presentation levels. In statistics, ranking is the data transformation in which numerical or ordinal values are replaced by their rank when the data are sorted (in this case from largest to smallest). For example, if DPOAE levels are measured at 3.4, 5.1, 2.6, 7.3 dB EPL across different stimulus frequency ratio conditions, the ranks of these data items would be 3, 2, 4 and 1 respectively. For this study, DPOAE data at a given f_2 for a specific stimulus level was separated by frequency ratio for ranking. The f_2/f_1 condition that produced the highest DPOAE level was ranked best informing the optimal frequency ratio for that individual. Each participant’s highest ranked frequency ratio was tabulated to determine the frequency ratio that most often produced the highest DPOAE levels across participants at that f_2 frequency. Plotting and statistical analysis were all performed in R (version 4.0.2).

2.3. Results

The level of the $2f_1-f_2$ DPOAE was measured across 18 primary frequency ratio values for each of five stimulus level combinations (75 & 75, 65 & 55, 55 & 40, 50 & 30, 45 & 20 dB FPL), resulting in 90 conditions in total. DPOAE recordings were obtained with stimuli swept continuously in frequency that allowed registration of DPOAE levels with fine frequency resolution (Figure 10). From these plots, the complexity of the fine structure minima and maxima can be visualized and the potential downfall of presenting widely spaced, discrete stimulus pairs

can be appreciated. To circumvent the ramifications of DPOAE recordings falling within a deep fine structure minimum, DPOAEs will be reported as averages across one-third-octave bands of f_2 frequencies. Across participants, DPOAE level was found to vary as a function of stimulus frequency ratio, level, and f_2 frequency. Overall, findings showed: 1) At a given stimulus level combination, as f_2 frequency increased, the f_2/f_1 producing the largest DPOAE amplitude decreased, and 2) at a given f_2 frequency, as primary levels increased, the f_2/f_1 producing the largest DPOAE amplitude increased.

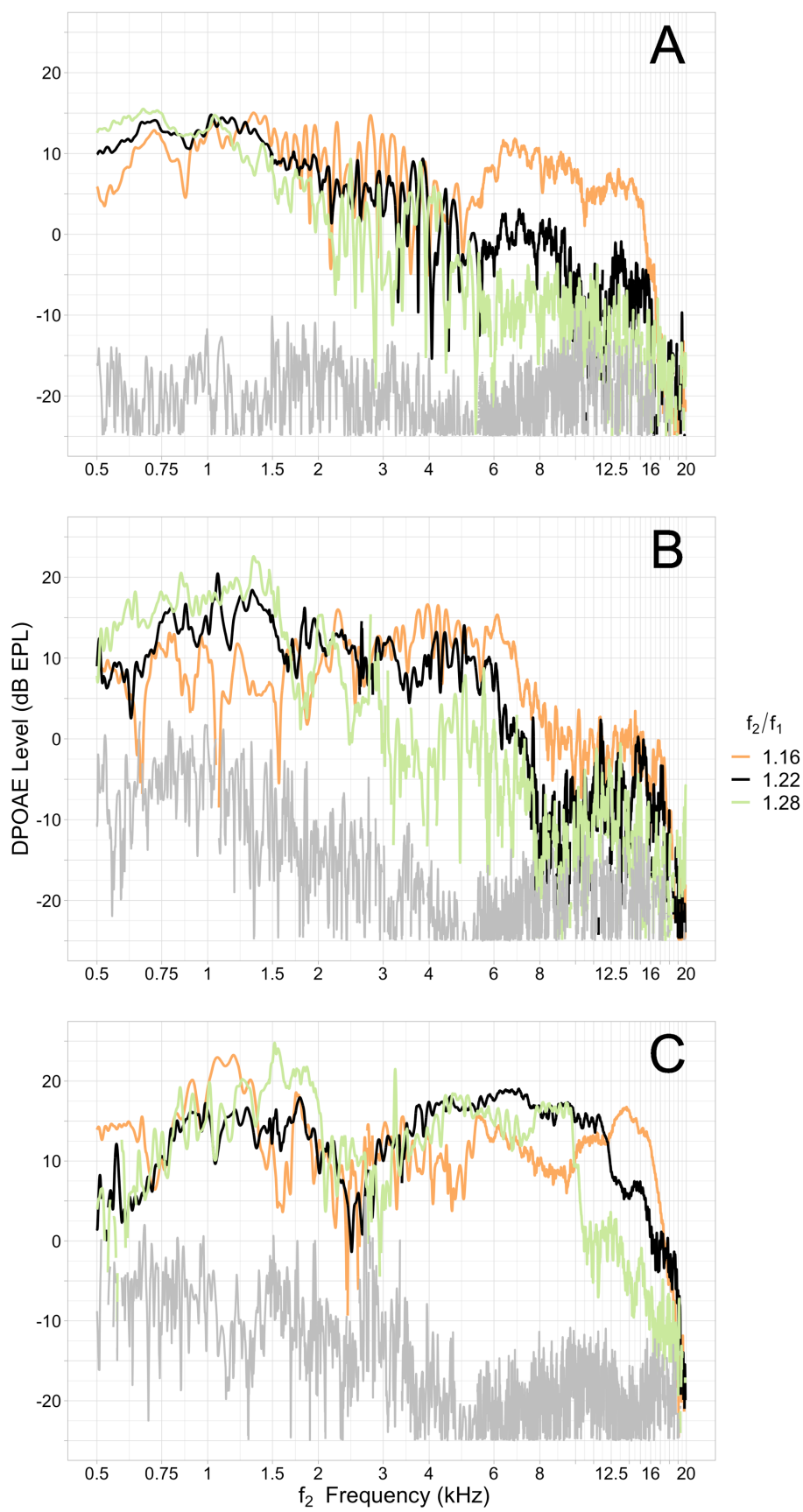


Figure 10. DPOAE fine structure from three participants

Examples here show DPOAE fine structure from three randomly selected participants (A: participant 021_SSDP, B: participant 017_SSDP, and C: participant 013_SSDP). Data from panel A are from stimuli presented at 65 & 55 dB FPL and panel B and C from stimuli presented at 75 & 75 dB FPL. Further analyses were conducted on DPOAE levels averaged over one-third octave bands to avoid local maxima or minima.

2.3.1. Reliability

To establish the reliability of measurements, DPOAEs were measured at 65 & 55 dB FPL with a 1.22 frequency ratio at each test session (five test sessions in total). The test-retest reliability was determined by calculating the test-retest differences across test sessions and participants. To do this, the median DPOAE level for a given participant across test sessions was identified and used in calculating the test-retest difference for the other four test sessions. Finally, the average difference was calculated across participants and plotted in Figure 11. The average test-retest difference was found to be within 0.5 dB across all test frequencies with the variability remaining low. The greatest variability was seen at the lowest frequencies, which was likely a result of noise floor effects being more confounding at those frequencies.

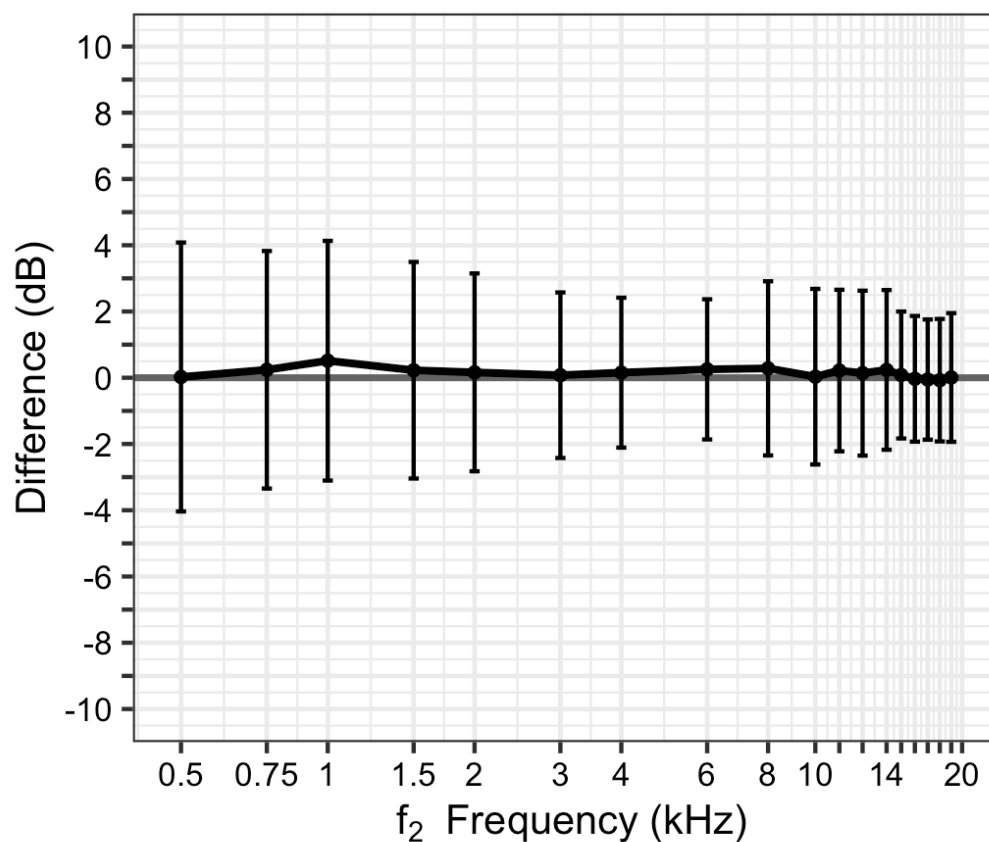


Figure 11. Average test-retest DPOAE level differences

Average test-retest differences for DPOAE levels measured for stimuli presented at 65 & 55 dB FPL with a 1.22 frequency ratio. Error bars indicate +/- 1 SD.

ICC was used to quantify the variation in data measured from each participant across the five trials. ICC estimates and their 95% confident intervals were calculated using the psych package in R based on a mean-rating (k=5), absolute agreement, 2-way mixed-effects model (**Error! Not a valid bookmark self-reference. 1**). The 95% confidence interval of the ICC estimate was used as the basis to evaluate the level of reliability. ICC values less than 0.5 are indicative of poor reliability, values between 0.5 and 0.75 indicate moderate reliability, values between 0.75 and 0.9 indicate good reliability, and values greater than 0.90 indicate excellent

reliability (Koo & Li, 2016). The level of reliability was “excellent” for $0.75 < f_2 < 16$ kHz, “good” to “excellent” for 0.5 and 17 kHz, and “moderate” to “good” for 18 kHz.

Table 1. Interrater reliability using intra-class correlation coefficient (ICC)

Results here describe the intra-rater reliability using an average fixed raters ICC calculation. ICC confidence interval values less than 0.5 are indicative of poor reliability, values between 0.5 and 0.75 indicate moderate reliability, values between 0.75 and 0.9 indicate good reliability, and values greater than 0.90 indicate excellent reliability (Koo & Li, 2016).

f_2 (kHz)	ICC	95% Confidence Interval	
		Lower Bound	Upper Bound
0.5	0.9	0.84	0.94
0.75	0.94	0.9	0.96
1	0.93	0.9	0.96
1.5	0.94	0.9	0.96
2	0.95	0.93	0.97
3	0.96	0.94	0.98
4	0.97	0.96	0.99
6	0.97	0.95	0.98
8	0.97	0.95	0.98
10	0.97	0.96	0.98
11.2	0.98	0.97	0.99
12.5	0.98	0.97	0.99
14	0.97	0.95	0.98
15	0.97	0.96	0.98
16	0.95	0.93	0.97
17	0.91	0.85	0.94
18	0.81	0.7	0.89

Reliability was also assessed using the Bland-Altman method which takes measurements from two tests and analyzes the accuracy of the results by comparing the average of the results against their difference (Bland & Altman, 1986). The Bland–Altman plots for DPOAE level data from the first and last test session are displayed in Figure 12. *Bland–Altman plots comparing the difference in DPOAE level between the first and last test session.* Superimposed on each plot are three horizontal reference lines. The center dashed line is plotted at the mean of the differences

between the first and last test. The upper and lower dashed lines are plotted at the boundaries of the 95% confidence interval about the mean (i.e., the mean difference ± 1.96 SD). If test measures were repeatable, one would expect the mean test differences to be zero and 95% of the differences to be less than ± 1.96 SD. Mean test differences or bias (i.e., between the first and last test) for DPOAE level were largest at low frequencies and had a tendency to be smaller with increasing frequency. Mean test differences were smallest at the highest frequencies. This was likely due to DPOAEs falling into the noise floor making the difference reflective of internal noise floor differences and not DPOAE differences. No systematic bias was observed between sessions in the Bland-Altman plots.

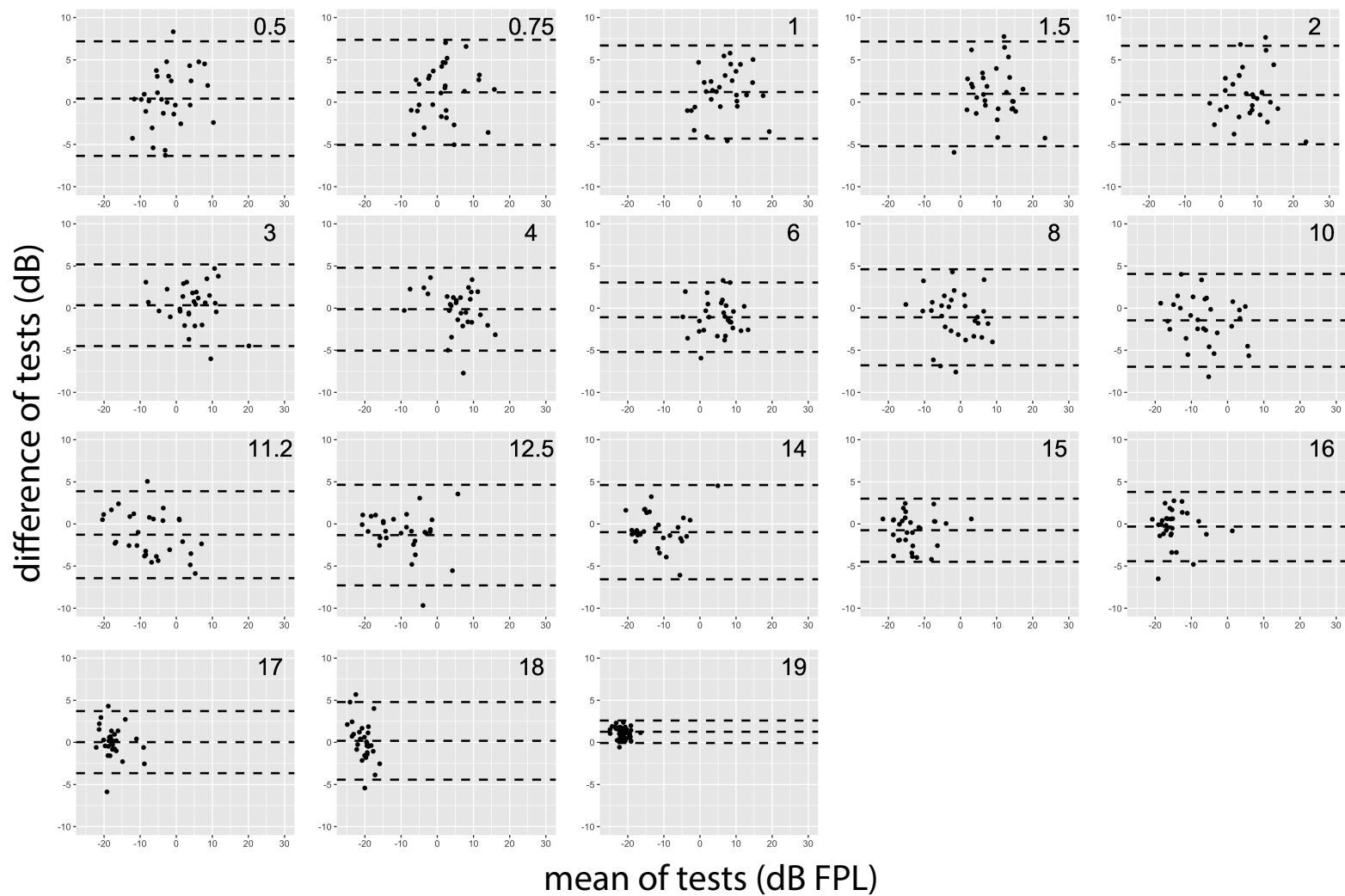


Figure 12. Bland–Altman plots comparing the difference in DPOAE level between the first and last test session

Reliability assessed using the Bland–Altman method. DPOAE level differences are plotted as a function of the mean of the first and last tests sessions. The center dashed line is plotted at the mean of the differences and the upper and lower dashed lines are plotted at the boundaries of the 95% CI about mean. Each panel represents a different f_2 frequency in kHz (as indicated by the label in the upper right corner).

2.3.2. DPOAE amplitude across all stimulus conditions

The absolute DPOAE level varied by stimulus frequency ratio, stimulus level, f_2 frequency, and participant. Yet, a principal outcome reflected in the detailed structure of both average and individual frequency ratio functions was a nonmonotonic change in DPOAE amplitude as a function of f_2/f_1 . Despite the presence of amplitude nonmonotonicities, there was clearly a region of f_1 and f_2 separation that generated the maximum DPOAE response. This bandpass property was evident when DPOAE amplitude was plotted as a function of f_2/f_1 showing a peak in the DPOAE response at a specific f_2/f_1 with general declines in DPOAE levels at f_2/f_1 values above and below the local peak (Figure 13). Median DPOAE levels are plotted separately for each stimulus level combination allowing for the relationship to be seen between stimulus frequency ratio, level, and f_2 frequency.

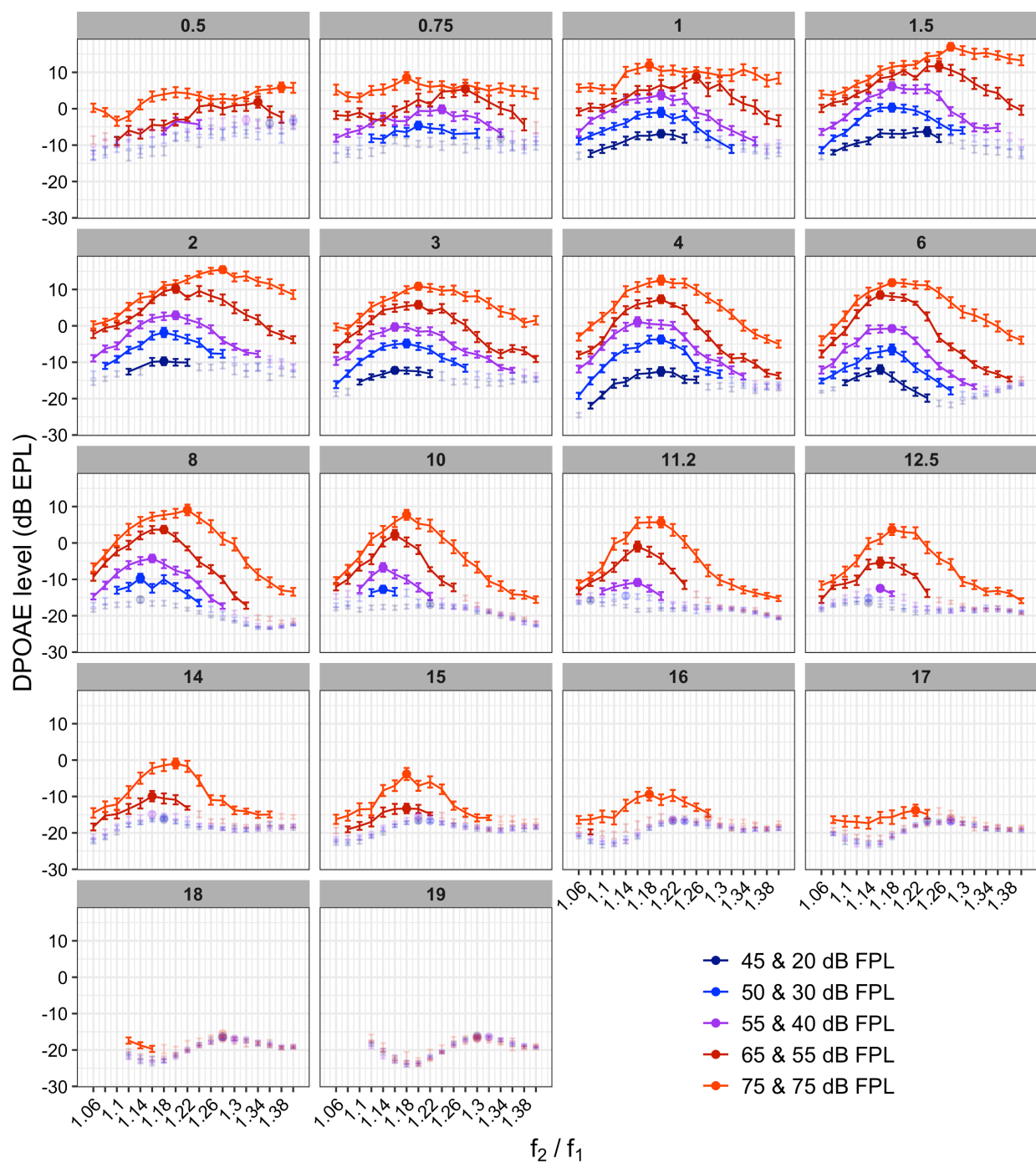


Figure 13. Median DPOAE level as a function of stimulus frequency ratio

Median DPOAE level as a function of stimulus frequency ratio. Panels represent the separate f_2 frequencies (kHz), labelled in each panel title, while line color represents the separate stimulus level combinations. The solid circle shows the f_2/f_1 condition with the largest DPOAE median level for a given stimulus level combination. Data that did not pass a 3 dB SNR criterion are shown with increased line transparency. Error bars indicate ± 1 SE.

Looking collectively at these bandpass-like curves, it is apparent that the f_2/f_1 condition where the peak occurred varied in a systematic way across stimulus conditions. This bandpass shape was found to narrow as f_2 frequency increased and primary levels decreased, both trends consistent with the sharpening of mechanical tuning of the cochlea, although other factors such as changes in suppression and phase interference cannot be ruled out. The maximum DPOAE amplitude at the lowest frequencies was elicited by stimulus pairs with the widest frequency separations. Then, as frequency increased, the maximum DPOAE was produced using gradually narrowing frequency ratios. Furthermore, for DPOAE responses at all f_2 frequencies, high level stimulus tones produced maximum amplitude responses when frequency ratios were set wider than at lower levels. These trends for the group data are apparent in Figure 13 by tracking peak DPOAE levels (indicated by the solid circle on each curve) and how they change with stimulus level (indicated by line color) and f_2 frequency (indicated by panel).

Although DPOAE SNRs are not directly reported in Figure 13, regions with lightened or more transparent symbol and line colors indicate where SNRs were less than 3 dB. The reader should weigh data with adequate SNR to a greater degree. These regions with reduced SNRs occurred at the f_2/f_1 extremes, particularly when stimulus levels were reduced or when f_2 frequencies increased. This highlights where DPOAE measurements require careful selection of stimulus frequency ratios as they are critical to the success of recording measurable DPOAEs.

At the highest f_2 frequencies in Figure 13, the majority of DPOAEs did not pass a 3 dB SNR criterion, resulting in the plotted data depicted using transparent lines and symbols. In addition, the separate L_1 & L_2 curves appear indistinguishable as the traces overlap, indicating that the intended DPOAE response likely fell below the noise floor leaving a measurement of noise floor levels instead. Even though DPOAE levels above the noise floor were difficult to

record in a majority of the participants, some exhibited relatively high DPOAE levels even at these high measurement frequencies. Figure 14 depicts an example of an individual with such measurable high frequency DPOAEs allowing for the identification of the best stimulus frequency ratio (solid circle). Therefore, even though the majority of normal-hearing individuals in this study did not have measurable DPOAEs above the noise floor at the extreme high frequencies, DPOAE responses could be measured in ears that showed exceptional cochlear sensitivity when appropriate stimulus conditions were used (i.e., narrow in frequency ratio and high in stimulus level).

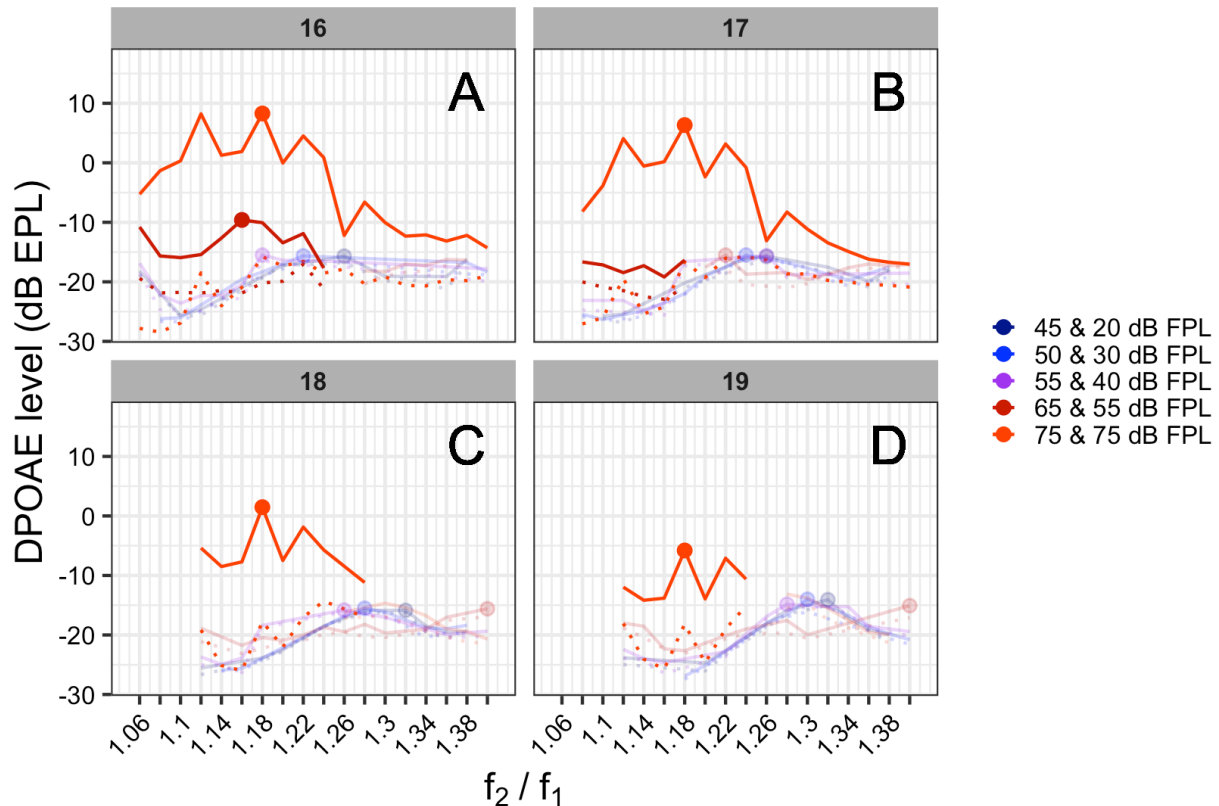


Figure 14. Example participant with strong high frequency DPOAE responses

DPOAE level (solid line) and noise floor level (dotted line) plotted as a function of stimulus frequency ratio for participant 010_SSDP at the four highest f_2 frequencies evaluated (A: 16 kHz, B: 17 kHz, C: 18 kHz, and D: 19 kHz). This is an example of a participant with measurable high frequency DPOAEs, allowing for the identification of the best stimulus frequency ratio (solid circle).

DPOAE amplitudes displayed as a function of f_2 frequency (i.e., a DP-gram) shows how emission levels change when the stimulus frequency ratio and level remain fixed across test frequency. The DP-grams shown in Figure 15 allow for comparison across four audiometrically normal-hearing individuals chosen at random. By plotting in this manner, one can see shared response patterns as well as the individual differences. For example, the behavior of the individual DPOAE recordings show how emission levels that fall above the noise floor can vary by as much as 30 dB based on the frequency ratio used at a given f_2 frequency. Another similarity includes how the frequency ratio that gave the largest DPOAE response was widest in the low frequencies and narrowest in the high frequencies. Although the f_2/f_1 pattern of behavior was similar across participants, there were differences in the exact f_2/f_1 that produced the largest DPOAE at a given frequency. Additionally, differences between participants can be seen in the absolute level of the DPOAE or noise floor at a given frequency. For example, participant 007_SSDP had, overall, greater DPOAE levels compared to the others while participant 031_SSDP had noise floors that were greater and more variable than the others. This highlights how the same DPOAE test parameters can produce findings that vary across normal-hearing participants.

Although this investigation was not designed to study aging and gender differences, individual DPOAE measures seem to mirror generalized trends. DPOAE amplitudes were found to decrease with age (compare panel A with C and B with D in Figure 15) and be relatively lower for males compared with females (compare panel A with B and C with D in Figure 15).

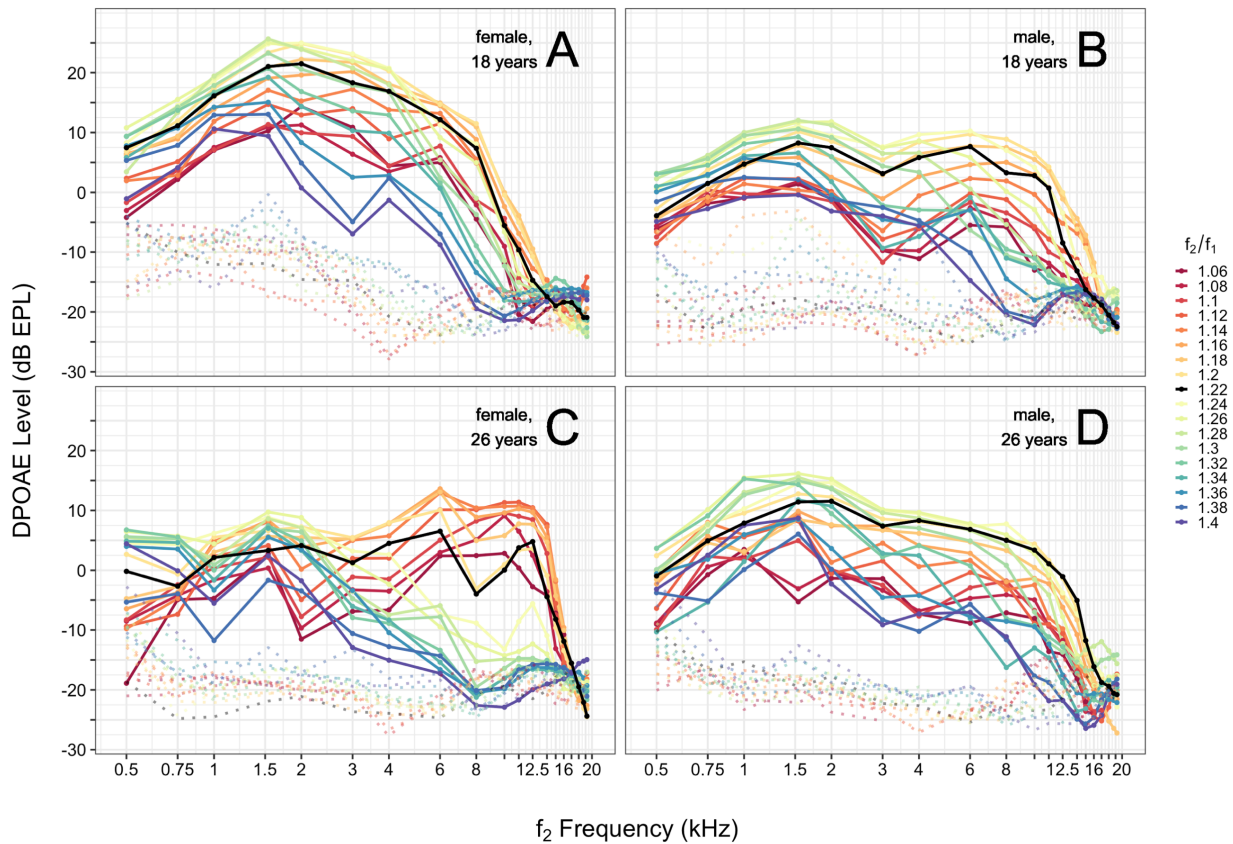


Figure 15. DP-grams for four different normal-hearing participants

DPOAE levels averaged over third-octave frequency bands from four individual participants when primaries were presented at 65 & 55 dB FPL (A: participant 007_SSDP, B: participant 023_SSDP, C: participant 010_SSDP, and D: participant 036_SSDP). Each f_2/f_1 ratio condition is indicated by line color. DPOAEs are represented by solid lines and noise floor are represented by dotted lines.

Results across all 30 ears continued to reveal these same patterns when median DP-grams were plotted for each stimulus frequency ratio and level combination (Figure 16). Depending on the f_2 frequency tested, different frequency ratios were associated with greater DPOAE amplitudes. At low frequencies, wider ratios produced the largest DPOAE responses. While narrower stimulus frequency ratios produced the largest DPOAEs at higher test frequencies. Higher level primary tones also produced maximum amplitude responses when ratios were set wider than at lower levels.

While large DPOAE amplitudes and SNRs could be seen across frequencies tested, DPOAE levels were maximized in the 1.5 – 6 kHz region, with amplitudes dropping gradually at either frequency extreme. The drop in amplitude at f_2 frequencies > 6 kHz occurred in conjunction with decreasing hearing sensitivity that was also visible in the audiogram (Figure 9). The greatest effect of frequency ratio, as indicated by the frequency region with the greatest range in median DPOAE level, was found between 6 and 10 kHz for the three highest stimulus levels and 4 kHz for the two lowest stimulus levels. This indicates that DPOAE levels were most affected by frequency ratio at these f_2 frequencies.

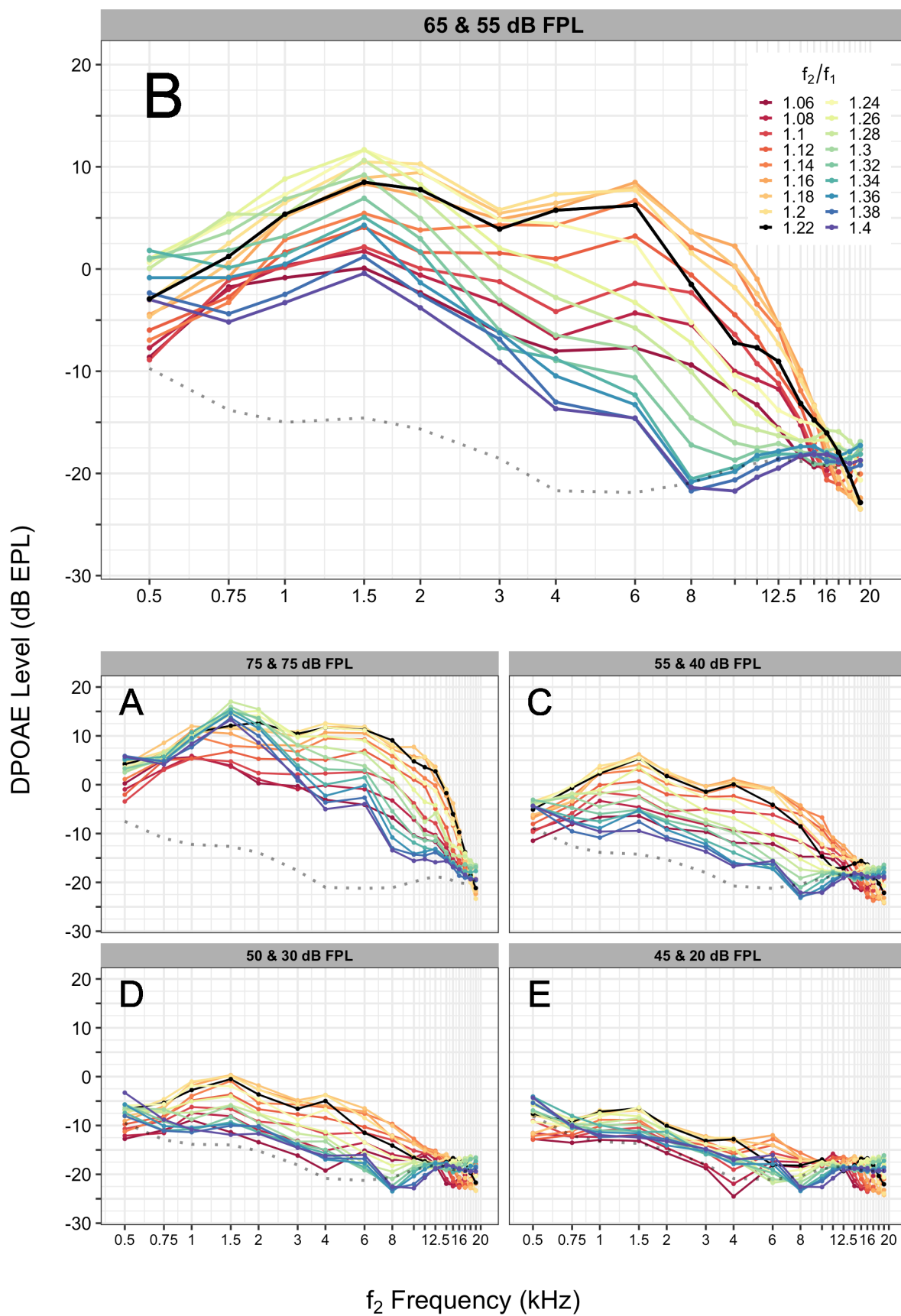


Figure 16. Median DP-grams for normal-hearing participants

Median DPOAE level and noise floor as a function of f_2 frequency for each f_2/f_1 ratio condition (indicated by line color). DPOAE levels are averaged across third-octave frequency bands. Each panel represents a different L_1 & L_2 stimulus level combination (A: 75 & 75 dB FPL, B: 65 & 55 dB FPL, C: 55 & 40 dB FPL, D: 50 & 30 dB FPL, and E: 45 & 20 dB FPL). For ease of viewing, noise floor levels (dotted line) represent the median for that f_2 frequency across f_2/f_1 conditions.

Measured noise floor levels were also an interesting finding in this study. DPOAE noise floor measurements are an independent estimate of physiological noise. Common sources of noise, as recorded in the ear canal, are related to circulation, respiration, and general muscle activity (Shaw, 1974). As expected, noise floor levels were found to be higher in low frequency regions across individuals (Figure 16) likely originating from physiological noise within the individual. What was particularly interesting was how often noise floor levels varied across individuals. An example of these differences can be seen by simply comparing DP-grams across individuals. In Figure 15, participant 031_SSDP (panel D) showed noise floor levels that were reliably low across frequency which was in contrast to the high, low frequency noise floor levels in participant 007_SSDP (panel A) and the variable noise floor levels in participant 012_SSDP (panel B).

2.3.3. Calculating optimal primary frequency ratio

Figure 17 summarizes our approach for specifying the best or optimal primary frequency ratios for recording DPOAEs from normal-hearing ears. When determining the optimal frequency ratio, we wanted to be sure that emphasis was placed not on the absolute DPOAE level, but instead the frequency ratio that produced the largest DPOAE response relative to the other responses within an individual. To do this across individuals, we undertook a multi-step analysis approach. First, each participant's DPOAE data was filtered such that only DPOAEs that passed a 6 dB SNR criteria were allowed for further processing. Then, at any given f_2

frequency, the remaining participant-specific data was transformed by taking the measured DPOAE levels and assigning a rank to the data sorted from largest to smallest. Take participant 012_SSDP in Figure 15B for example. At 10 kHz, the frequency ratio 1.16 produced the largest DPOAE response, giving it the top ranking for this f_2 frequency, followed by 1.12, 1.14, 1.18, 1.10, 1.20, 1.08, and 1.24 (all other frequency ratios did not meet the 6 dB SNR criteria). These listed rankings were compared across all participants in order to find the stimulus frequency ratios that most commonly produced the largest DPOAEs in a frequency- and level-specific manner.

Results across participants reveal the optimal stimulus frequency ratio at the lowest frequencies to be relatively wide. This optimal ratio systematically decreased or narrowed with increasing test frequency. In contrast, at a given f_2 frequency, as the level of the stimuli increased, the maximum emission amplitude was elicited when primaries were farther apart in frequency. These stimulus level-specific protocols could be used in the future as a guideline for accurately measuring the largest DPOAE responses in normal-hearing, human ears.

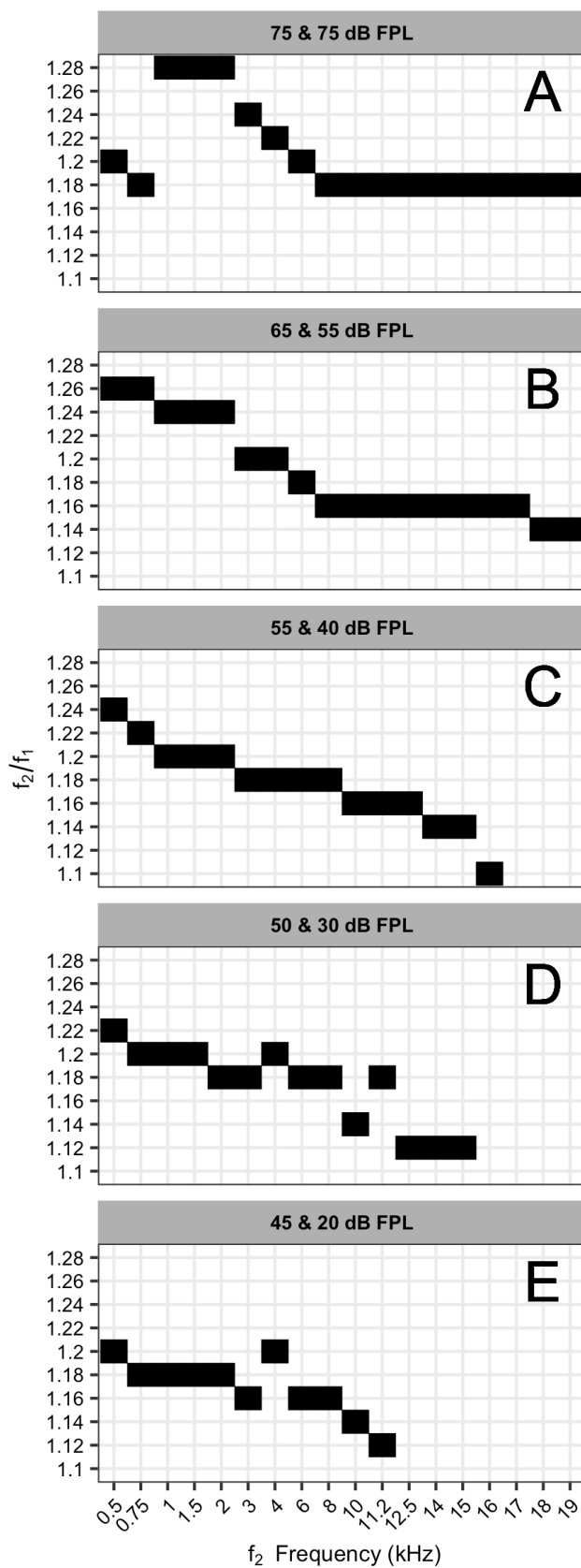


Figure 17. Optimal DPOAE stimulus frequency ratios for normal-hearing ears

Optimal frequency ratio as a function of f_2 frequency for five different stimulus level combinations (A: 75 & 75 dB FPL, B: 65 & 55 dB FPL, C: 55 & 40 dB FPL, D: 50 & 30 dB FPL, and E: 45 & 20 dB FPL). For any given stimulus level and f_2 frequency, f_2/f_1 conditions were rank ordered from largest to smallest based on DPOAE level in order to identify the f_2/f_1 that most commonly was ranked highest across participants. These primary stimulus level-specific protocols could be used as a guideline for accurately measuring the largest DPOAE levels in normal-hearing, human ears.

2.4. Discussion

The behavior of the DPOAE as a function of stimulus condition has been of interest in hearing science research for decades. This interest has been driven by a desire to better understand the mechanisms of normal DPOAE generation and exploit this behavior in order to find and use the best test conditions to avoid underrepresenting cochlear function. The results presented here summarize a broad exploration of the DPOAE parametric space in humans, suggesting that it is possible to record larger DPOAE levels in normal-hearing ears if the f_2/f_1 relationship is allowed to vary with test frequency and stimulus presentation level. These results confirm and strengthen various aspects of our current understanding of normal cochlear function and expand our understanding by extending our observation to previously unexamined higher frequencies.

2.4.1 Previous investigations of the DPOAE stimulus space

Although there have been previous investigations into the DPOAE stimulus parametric space, this is the first investigation to explore such a wide range of f_2/f_1 , L_1 & L_2 , and f_2 parameters in a large sample. The exploration of a large stimulus parameter set was procedurally cumbersome and time consuming in the past. This investigation was undertaken utilizing procedures that allowed for faster evaluations while providing finer frequency resolution (Long et al., 2008; Kalluri & Shera, 2013; Abdala et al., 2015). By measuring DPOAEs using concurrently presented, frequency sweeps, we were able to investigate 90 different stimulus

frequency ratio and level conditions that encompassed wide range of stimulus parameters that produce DPOAEs in normal-hearing individuals.

Johnson et al. (2006) performed DPOAE measurements over an extensive set of stimulus frequency ratios and level combinations. However, even then, DPOAE responses were performed at a select number of frequencies $f_2 = 1, 2, 4,$ and 8 kHz in normal hearing individuals. The optimal L_1 & L_2 and f_2/f_1 conditions that produced maximum DPOAEs from 20 participants were then used to compute frequency-specific, best fit functions. This function was then extrapolated out to frequencies > 8 kHz in order to “oblivate the need for comprehensive evaluations of stimulus conditions in individual subjects” at higher frequencies. Although, a fit like this was a desirable way to summarize the findings at low frequencies and infer to test frequencies beyond the measured data, it also assumed that the fit would translate to other frequencies and samples. The accuracy of this fit across frequency can be compared to data from other groups that have explored the effect of stimulus frequency ratio on DPOAE level (Figure 7). The Johnson et al. (2006) model made to predict optimal ratio does not accurately reflect actual test performance from other groups, including Dreisbach & Siegel (2001) who reported results at f_2 frequencies > 8 kHz (see Figure 7). The differences between the model prediction and reported data could be related to the limited sample size used or inaccurate assumptions of systematic changes in the cochlear properties which influenced the data reported at high frequencies by Dreisbach & Siegel (2001).

Since then, advancements have been made to in-ear emission probe calibration allowing for more accurate stimulus level presentation and emission level recording. The manner in which the stimulus level is calibrated will have an influence on the optimal stimulus parameters for recording DPOAEs. It has been shown that differences in SPL exist in a sealed ear canal when

stimuli are calibrated at the location of the probe compared to the eardrum (Siegel, 1994). These differences are pronounced at the frequencies of a standing wave null which, in humans, usually occurs at frequencies exceeding 2-3 kHz. These differences and their effect on DPOAE recordings across varying stimulus frequency ratios were described first by Dreisbach & Siegel (2001). They found the frequency ratio yielding the largest DPOAE level from a probe tube calibration to decrease with increasing f_2 , whereas a nonmonotonic function with a local peak in the 5- to 8-kHz region was seen when the emission probe microphone was used for in-ear calibration. This discrepancy between probe tube and emission probe calibration was likely from a lack of control over eardrum stimulus levels when the emission probe microphone is the reference for calibration, resulting in increased eardrum stimulus levels in this frequency region. In the present study, calibration techniques were utilized that correct for the differences in SPL when calibrated at the plane of the probe as opposed to the eardrum. A further benefit of calculating FPL and EPL corrections during in-ear calibration is that the exact standing wave effects can be assessed across tests. This was a critical advancement in the work as ear canals can vary dramatically across individuals and probe insertion depth can vary within an individual from test to test.

Overall, we found DPOAEs generated using FPL-corrected stimuli and EPL-corrected emissions, measured at fine frequency resolution, up to the highest frequencies of human hearing, allowed for the recording of large DPOAE levels that accurately reflect cochlear function. Using these techniques for DPOAE measurement, an investigation into the optimal stimulus conditions was undertaken with confidence.

2.4.2. DPOAE measurement reliability

A reliable measure needs to be consistent over time within an individual. This consistency is the foundation that allows for identification of true pathology, progression of disease, and evaluation of treatment outcomes so that pathology can be confidently segregated from normal fluctuation. Therefore, before any measurement instrument or assessment tool can be used for research or clinical applications, their reliability must be established. To establish the reliability of our DPOAE measurement method, we repeated measurements using the same stimulus condition at each of the five test sessions made for a given participant. The median test-retest difference across test sessions was calculated for each participant followed by calculating the average difference across participants (Figure 11). The average test-retest difference was excellent as across f_2 frequency differences remained within 0.5 dB with minimal variation, as indicated by the standard deviation not exceeding 4.5 dB.

Reliability of DPOAE levels was further demonstrated using statistical methods. Excellent ICCs were seen for f_2 between 0.75 and 16 kHz (Table 1), suggesting a high correlation between tests with a range of variation inside the confidence limits. The ICC provided an index that reflected both degree of correlation and agreement between measurements made over the five test sessions. The Bland-Altman analysis (Figure 12) was used to compare measurements made between the first and last test sessions, showing that both test sessions produced similar data and there was an absence of proportional/systematic bias. These findings are in agreement with previous reports where no significant differences were found over two test sessions separated by several days (de Boer & Thornton, 2008; Mishra & Lutman, 2013; Stuart & Cobb, 2015) or weeks (Graham & Hazell, 1994). Although, it is important to note that the previous reports did not use FPL or EPL corrections.

2.4.3. Interactions between primary frequencies and levels

The primary motivation of this study was to better understand DPOAE generation in order to exploit this knowledge to record the largest possible DPOAE levels in normal-hearing ears. The results presented here confirm various aspects of our current understanding of DPOAE generation and strengthen them by extending observations to previously unexamined higher frequencies. Examination of DPOAE behavior across stimulus frequency ratios reveals a shared pattern: the ratio yielding the largest DPOAE level changes as a function of frequency (Figure 13 & Figure 16). At low frequencies, near the cochlear apex, wider primary frequency ratios produced the largest DPOAEs. As assessments were made closer to the cochlear base, narrower ratios produced the largest emission levels at high frequencies. This is consistent with the idea that excitation patterns for the eliciting two primaries are more spatially separated at high frequencies than at low frequencies, requiring a decrease in the frequency ratio or an increase in the stimulus levels in order to create an optimized overlap for generating distortion. These findings were predicted based on what is known about the shared anatomy and physiology across mammals.

The physical characteristics and the active mechanical properties change gradually across the cochlear length. The changing physical properties of the cells and tissues of the cochlear partition are important in determining gross tuning characteristics. These passive properties include mass, which increases from base to apex, and stiffness, which decreases from base to apex. The peak of the traveling wave varies according to the tonotopic map defined by these basal-to-apical gradients. Additionally, as a consequence of the changing active mechanical properties of the cochlear partition from apex to base, mechanical tuning becomes sharper as a function of increasing frequency and decreasing stimulus level (Robles & Ruggero, 2001). It is

these passive and active local cochlear mechanics that determine the spatial properties of the traveling wave. DPOAE generation is then maximized with ideal overlap between the mechanical disturbances of the traveling waves of the two stimulus tones. Therefore, it was expected that stimulus frequency ratio would need to be adjusted as a function of frequency and level in order to generate maximum distortion amplitude. Modifying DPOAE stimulus frequency ratios could be suiting known cochlear partition vibration patterns, allowing for the optimal interaction between the stimulus tones thereby yielding the largest emission response at a given cochlear place.

DPOAE levels exhibited a bandpass shape when plotted as a function of f_2/f_1 (Figure 13). This bandpass shape was found to narrow as f_2 frequency increased and primary levels decreased, both of which are consistent with the sharpening of mechanical tuning of the cochlea. This is consistent with finding from Harris et al. (1989) and Abdala (1996) who also reported that slopes at both narrow and wide stimulus frequency ratios around the peak were steeper for higher frequencies. The general decrease in DPOAE level at narrow frequency ratios can be modeled to be a consequence of two-tone suppression (Shera et al., 2007) or phase interference between multiple distortion generators (Sisto et al., 2018). In contrast, the decrease in level at wider primary frequency ratios likely reflects the consequence of greater physical separation between the mechanical activity patterns of the overlapping f_1 and f_2 stimulus tones, creating a smaller overlap region for distortion generation. The bandpass shape could also suggest that interference phenomena play a crucial role in determining the behavior of the DPOAE across frequency ratio. This behavior could be attributed to a compromise between the positive effect of increasing the extent of the overlap region and the negative interference among distortion product wavelets of different phases within the generation region. These observations further

suggest that the shape of the DPOAE level when plotted as a function of f_2/f_1 is heavily determined by the mechanical tuning of the cochlear partition.

2.4.4. Optimal DPOAE stimulus parameters

A secondary goal of this project was to describe a set of stimulus conditions that vary by frequency and are likely to yield the maximum DPOAE level over the range of frequencies evaluated. By having a protocol such as this, future DPOAE work evaluating young, normal-hearing ears can now have a reference for setting stimulus parameters that have been found to, generally, reflect the peak in cochlear function. Rank ordering stimulus frequency ratios at each test frequency within individual participants and then collating the ratios most likely to yield the largest DPOAE levels across participants allowed the compilation of the best stimulus frequency ratio at each f_2 frequency while accommodating variability in DPOAE level within individuals (Figure 15).

The stimulus conditions ranked as most commonly producing the largest DPOAE levels (Figure 17) are consistent with hypothesized interactions among stimulus frequency ratios and level combinations. Frequency tuning is known to be sharper for high frequencies compared to low frequencies and a spatially extended vibration pattern is expected as stimulus level is increased. This was reflected in the optimal DPOAE measurement protocol which showed narrower frequency ratios to be optimal for maximizing DPOAE levels as either f_2 increased or stimulus level decreased.

2.4.5. Future Directions

In most healthy ears, the use of the standard $f_2/f_1 = 1.22$ may not be problematic for tasks such as screening for hearing loss in lower f_2 frequency regions as DPOAEs can be unequivocally detected. However, in cases with low response amplitude, poor SNR, or

borderline normal hearing, it will likely be most critical to utilize these optimal stimulus frequency ratios to accurately assess DPOAE amplitude and enhance response identification. Although this investigation sheds light on the best frequency ratios to use for a given stimulus level combination to evaluate normal cochlear function, this does not inform the exact stimulus conditions that are sensitive to identifying hearing loss. As a next step, we predict that frequency-specific stimulus parameters are also efficient in identifying cochlear dysfunction. Specifically, we are interested in identifying the exact stimulus frequency ratio and level parameters that improve upon existing clinical assessments. In this case, the most widely used clinical function of DPOAEs is screening for hearing loss. For this to happen, place-specific parameters would need to be sensitive to normal hearing and also cochlear damage that results in hearing loss.

In the present investigation, the composite DPOAE, at the frequency $2f_1-f_2$, was recorded in the ear canal. This composite level is recognized to be a vector sum of two major mechanisms, the distortion component and the reflection component, which are generated at different cochlear regions (Shera et al. 1999; Talmadge et al., 1999). Nonlinearities in stereociliary transduction of OHCs produce distortion in the region of overlap between the mechanical excitation of the two stimulus tones used to evoke DPOAEs (Verpy et al., 2008). From this overlap region, distortion energy is produced at $2f_1-f_2$ and a portion of this energy returns to the ear canal as the distortion component. Portions of this distortion energy also propagate apically to the $2f_1-f_2$ tonotopic place (CF_{dp}), where it is coherently reflected by irregularities in the mechanical properties of the cochlea, and returned to the ear canal as the reflection component (Kim 1980; Shera & Guinan 1999; Talmadge et al. 1999; Knight & Kemp, 2000; Dhar et al. 2005). The composite DPOAE in the ear canal is typically dominated by the distortion component for moderate- and high-level

stimuli (Brown et al., 1996). However, a secondary contribution of the reflection component can be detected at lower stimulus levels (Talmadge et al., 1999; Knight & Kemp, 2000; Dhar et al., 2005). For this investigation, we were interested in first establishing the composite DPOAE behavior across these many stimulus conditions. Since the relative magnitudes of the DPOAE components in the ear-canal varies with stimulus levels (Dhar et al., 2005), future work, will investigate the relative contributions of the two DPOAE components. Furthermore, distortion energy is produced at other combinations of the stimulus tones. Future work will also investigate the influence of stimulus frequency ratio and level on other intermodulation DPOAEs at the same stimulus parameters.

Lastly, a commonly explored research question has centered on determining how accurately or reliably hearing thresholds can be predicted from DPOAEs. Currently, the emphasis of DPOAE clinical protocols is to generally assess cochlear function for the presence or absence of hearing loss. This is done at the f_2 place using the total ear canal DPOAE and not the individual DPOAE components. While the global assessment of total ear canal DPOAEs is sufficient for detecting a significant loss of function, as in a hearing screener, more place-specific measurements can be made by separating the DPOAE generator components. With more precise knowledge about DPOAE distortion and reflection component behavior, a clinical protocol could be designed to bias the ear canal signal towards one of the components thereby mitigating the problem of uncontrolled component mixing. Using these separated components, along with optimized DPOAE stimulus parameters, could provide for DPOAE measurements that more accurately reflect cochlear function at that place in order to predict behavioral hearing threshold.

2.4.6. Conclusions

As the mechanics of the cochlear partition change across its length so should stimulus conditions used to evaluate specific portions of the cochlea. Audiometric tests need to evolve and change as our knowledge of auditory function expands so that we are most accurately assessing cochlear function. Using advanced calibration and measurement techniques, findings from this study are consistent with known cochlear mechanics. Collectively, these data provide confidence that stimulus frequency ratio settings need to be f_2 frequency- and level-specific, which is in opposition to what is done in most settings using a stimulus frequency ratio of 1.22 regardless of the stimulus level or f_2 frequency being tested. Therefore, using an optimized protocol, as presented here, could improve the accuracy for evaluating normal cochlear function and other investigations of cochlear function using DPOAE measurements.

CHAPTER 3

Utilizing Cochlear Place-Specific Properties in Distortion Product Otoacoustic Emission Stimuli for the Identification of Hearing Loss

3.1. Introduction

Hearing loss is a major healthcare issue because of the sheer number of people afflicted (Lin et al., 2011). The consequences of hearing loss go well beyond the primary communication difficulties and may include cognitive, emotional, social, behavioral, and socioeconomic consequences (Bess et al., 1989; Mulrow et al., 1990; LaForge et al., 1992; Carabellese et al., 1993; Appollonio et al., 1996; Heine & Browning, 2002; Cruickshanks et al., 2003; Dalton et al., 2003; Gates & Mills, 2005; Chia et al., 2007; Kochkin, 2010). Effective treatment of hearing loss and the mitigation of its negative sequelae is critically dependent on early diagnosis. Therefore, a sensitive and accessible tool for early and accurate identification of the most common forms of hearing loss is a critical national healthcare need. Utilizing DPOAEs for this purpose are ideal because they provide a unique window into OHC functional integrity as they are a by-product of the active and nonlinear cochlear amplification process (Davis, 1983; Dallos, 1992; Cho, 2000; Zheng et al., 2000; Dallos et al., 2008). The ability of DPOAE measures to provide a non-invasive window into cochlear function has made it a popular clinical tool, particularly for screening for the presence of hearing loss.

The most common forms of adult-onset hearing loss (i.e., ARHL and noise-induced hearing loss) originate in the cochlear base, where high frequency information is encoded, and affects cochlear OHC function (Probst et al., 1991; Ueberfuhr et al., 2016). The OHCs play a

pivotal role in shaping the sharp frequency selectivity, wide dynamic range, and acute sensitivity that are characteristics of a normal auditory system. Thus, OHC dysfunction disrupts some of the most salient features of human hearing. However, current clinical practice is not designed to identify the earliest signs of OHC dysfunction, especially at the highest audible frequencies where such dysfunction starts. Identifying cochlear pathologies using DPOAEs holds promise as they are objective, noninvasive, and directly evaluate the vulnerable OHCs. Furthermore, DPOAEs are already a well-established tool in both clinical and research settings (Dalton et al., 2003). However, timely and accurate detection of cochlear pathology remains suboptimal as current protocols: 1) do not assess up to the highest frequencies of human hearing and 2) do not consider local cochlear mechanical properties when setting DPOAE stimulus parameters. Until the recent past, technical complexities associated with delivering and recording accurately calibrated test signals at these high frequencies was a challenge. However, recent advances in calibration techniques and hardware have allowed for delivery (Probst et al., 1991; Scheperle et al., 2008) and recording (Lee et al., 2012) of accurate emission levels up to the highest frequencies of human hearing. What remains is a need to understand the stimulus parameters that best exploit cochlear function across the cochlear length.

The mechanical properties of the cochlea, driven by a combination of passive (e.g., mass and stiffness) and active (e.g., OHC-driven amplification) properties, vary systematically across its length (Robles & Ruggero, 2001). As a result of the passive mechanical gradient, gross tuning results in displacement at specific positions along the cochlear length. The active cochlear process amplifies the traveling wave at its peak, creating sharper tuning at that CF place. This active cochlear tuning becomes sharper from apex to the base.

It is hypothesized that DPOAE generation is maximized when the mechanical interaction between the two stimulus tones is optimal with minimal mutual suppression between them. Because the spatial properties of the traveling wave are determined by local cochlear mechanics, the frequency relation between the stimulus tones need to be adjusted as a function of frequency to maintain optimal interaction between them. Since there is a sharpening of mechanical tuning with increasing frequency, a narrowing of f_2/f_1 will be required in order to maintain optimal mechanical overlap between the vibration patterns caused by the stimulus tones. This optimal frequency ratio will also be dependent on the levels of the stimulus tones, requiring a widening of f_2/f_1 with increasing stimulus level.

The optimal stimulus frequency ratio for generating high DPOAE levels in normal-hearing ears has been reported to vary as a function of frequency (e.g., Harris et al., 1989; Johnson et al., 2006). In Chapter 2, we demonstrated a systematic decrease in the optimal stimulus frequency ratio across f_2 frequencies in young, normal-hearing ears. Narrower stimulus frequency ratios (f_2/f_1 approaching 1) generated larger DPOAE levels as stimulus frequency increased. A simple interpretation of these findings centers around the sharpening of mechanical tuning with increasing frequency, thereby requiring a narrowing of f_2/f_1 to maintain the optimal mechanical overlap between the vibration patterns caused by the two stimulus tones. Although this work identified the best frequency ratios to use for a given stimulus level combination in order to generate large DPOAEs in normal cochleae, it does not automatically guarantee that these same ratios would also be best suited to segregate normally functioning cochleae from those with dysfunction.

As the next logical step to the work described in Chapter 2, the goal here was to evaluate the clinical efficacy of various stimulus combinations in segregating normal-hearing ears from

those with demonstrated hearing loss. Such screening for hearing loss is already a popular application of DPOAEs but is typically conducted over a limited range of frequencies with variable degrees of success. The optimized stimulus conditions that generated large DPOAEs in normal ears would only be clinically useful if they remained sensitive to cochlear dysfunction. That is, a stimulus combination may generate large DPOAEs in normal-hearing ears but is not clinically useful if ears with hearing loss also yield large DPOAEs when that stimulus combination is used.

The purpose of this study was to develop a DPOAE screening protocol in adults, guided by cochlear mechanical properties, to derive physiologically motivated and locally appropriate stimulus parameters. We investigated the DPOAE stimulus parametric space in humans in order to identify the most appropriate stimulus frequency ratio and level combinations for accurate screening for hearing loss up to 16 kHz. DPOAEs were recorded using a pre-selected set of f_2/f_1 ratios and L_1 & L_2 levels known to produce large emission levels and SNRs in audiometrically normal hearing, young adults (Chapter 2). Participants with normal audiometric hearing and with a variety of degrees and configurations of SNHL were evaluated. Receiver operating characteristic (ROC) curves were used to identify stimulus combinations particularly sensitive to screening for hearing loss. Overall, the best stimulus combinations were found to be frequency-dependent and consistent with known mechanical properties of the cochlea.

3.2. Materials and Methods

3.2.1. Participants

Data are reported from a randomly selected ear of 31 normal hearing adults (17 female) between the ages of 18 and 30 years (mean 21 years) and 24 adult ears with SNHL (10 female) between the ages of 18 to 56 years (mean 37 years). Participants reported no history of ear

surgery, fluctuating hearing loss, Meniere's disease, labyrinthitis, auditory neuropathy, brain injury, ototoxic medications, dementia, or extensive noise exposure. All participants had normal outer ear and middle ear function as determined using otoscopy and tympanometry. The racial and ethnic distribution of participants was proportional to the population of Evanston, Illinois. Participants provided written, informed consent and were compensated monetarily. All procedures were conducted in accordance with the guidelines of the Institutional Review Board at Northwestern University.

3.2.2. Instrumentation, Calibration & Signal Processing

Signals were generated and recorded using custom software written in MATLAB (2015R) (The MathWorks Inc., Natick, MA), running on an Apple Macintosh computer. DPOAE measurements, Thévenin calibration of the probe, ear canal acoustic impedance and reflectance, and forward pressure calculations from the pressure response measured in individual ear canal were performed using custom-designed software (ARLas, Shawn Goodman). Behavioral threshold tracking used custom-designed software which automatically controlled stimulus levels delivered (Lee et al., 2012). Signal generation and recording were done using an input/output RME device (Fireface400) for analog-to-digital (96 kHz sample rate, 24-bit) and digital-to-analog conversion. Generated signals were sent through an Etymotic Research ER10X probe (Etymotic Research, Inc., Elk Grove Village, IL). During DPOAE measurements, signals from the test ear were recorded using the ER10X microphone and preamplifier combination, digitized and stored on disk for analysis. All testing was conducted in a sound treated audiometric booth that met the ambient noise standard (ANSI S3.1–1999).

Stimuli were calibrated using a procedure that allowed the derivation of acoustic quantities that were not affected by standing waves in the ear canal (described in Souza et al.

2014). Thévenin source pressure and impedance calibration of the probe was performed prior to each participant's arrival. In-situ or load calibration was performed prior to data collection with the probe placed in the participant's ear canal. The same wideband chirp stimulus as was used for source and load calibration. Recorded DPOAEs were corrected to EPL and stored along with the associated SPL recordings. EPL corrected DPOAEs are equivalent to the DPOAE measured in an anechoic ear canal, resulting in no standing wave effects for the DPOAE traveling through the ear canal (Charaziak & Shera, 2016).

The presence of an air leak was suspected when absorbance at low frequencies (A_{low}) was 0.2 (-7 dB) or higher based on criteria recommended by Groon et al. (2015). A_{low} was calculated by averaging the absorbance over a range of 0.1 to 0.2 kHz. The recording and analysis software alerted the experimenter when a leak was detected prompting the experimenter to remove and reseat the probe in the participant's ear canal.

Stimulus generation and DPOAE acquisition were controlled using an algorithm that swept the tone upward at a rate of 1 octave/second (each stimulus tone was played through a separate speaker). Using stimulus tones swept in frequency allows rapid OAE measurements with high frequency resolution (e.g., Long et al., 2008; Kalluri and Shera, 2013). In a single swept-tone protocol, the full range of tested frequencies were presented over ~ 5.6 seconds having f_2 {start, stop} frequencies of {0.48, 20.78} kHz. Whenever possible, to expedite data collection, three separate frequency sweeps were presented concurrently (Abdala et al., 2015), each lasting ~1.88 seconds. During concurrent swept-tone measurements, the full range of tested frequencies was divided into three overlapping segments having f_2 {start, stop} frequencies of {0.48, 1.776}, {1.646, 6.075}, and {5.63, 20.78} kHz, respectively, resulting in ~0.1 octave overlap between the sweeps. In pilot experiments, we found no significant differences between

DPOAE levels measured using three concurrent primary sweeps, a single sweep covering the entire frequency range at the same rate, or discrete primary tones. This expedited protocol allowed the recording of DPOAEs from a multitude of stimulus combinations from each participant. Data collection was stopped after 32 repetitions and averaged. Three phase-rotation averaging was employed to cancel out the f_1 and f_2 primaries from the measured response (Whitehead et al., 1996). This was accomplished using three stimulus segments with different primary-tone starting phases interleaved such that the f_1 and f_2 tones cancel when the responses are averaged leaving only the DPOAE at $2f_1-f_2$ remaining.

3.2.3. Protocol

A detailed case history was taken and tympanometry was conducted using a GSI Tymstar Middle Ear Analyzer (Grason-Stadler Inc., Eden Prairie, MN) on the first visit. Before, in-ear calibration, otoscopy was performed to ensure clear ear canals and a visibly intact eardrum. Within a test session, the experimental procedures were administered over a ~2 hour period. In order to complete the multitude of DPOAE test conditions, on average, a participant came in for two visits total.

Pure-tone thresholds were measured using an automated, adaptive task for 19 standard audiometric frequencies from 0.5 and 20 kHz using a modified Békésy audiometry technique. Signals were pulsed tones, 250 ms in duration with 25 ms rise and fall times, presented twice per second. In the first reversal, the participant would press a button when the pulsed tone was heard and release when it was not heard. The second reversal followed when the button was pressed while the presentation level was increasing. A step size of 6 dB was used for the first two reversals followed by a step size of 2 dB for the remainder of the threshold estimation process. Midpoints between reversals were calculated for each ascending run (going from below to above

audibility). After six ascending runs, the tracking procedure would converge on the threshold once the standard error of the mean was less than or equal to 1. Further description of the adaptive threshold task can be found in Lee et al. (2012). Threshold estimation started at 1 kHz, proceeding to the highest frequency, repeating the measurement at 1 kHz, and then proceeding downward to the lowest test frequency. Further description of the adaptive threshold task can be found in Lee et al. (2012). Figure 18 shows behavioral hearing threshold plotted as a function of frequency for each individual participant. The gray shading indicates the normative threshold range, established using data from Lee et al. (2012). For normal-hearing participants, all individual measured thresholds fell within the normative range. For the SNHL participants, thresholds for at least two test frequencies needed to fall above the normative range.

DPOAEs were elicited by pairs of primary tones (f_1 and f_2) and recorded at the frequency of the cubic distortion ($2f_1-f_2$). Recordings from 32 total stimulus conditions (Table 2) were obtained that have previously been shown to reliably produce large DPOAE levels in normal-hearing ears (Chapter 2). DPOAE noise floor levels were estimated on-band at the f_2 frequency.

Table 2. DPOAE stimulus conditions evaluated

In this study, 32 stimulus conditions were tested in total. At each of the listed stimulus level (L_1 & L_2) combinations, the associated frequency ratios are indicated in the same row.

L_1 & L_2 (dB FPL)	f_2/f_1 (in 0.02 steps)
75 & 75	1.1 - 1.28
65 & 55	1.12 - 1.28
55 & 40	1.12 - 1.24
50 & 30	1.12 - 1.22

Before commencing the study, coupler measurements revealed harmonic distortion that influenced DPOAE recordings when concurrent stimulus pairs were presented at 75 & 75 dB FPL. To circumvent this measurement artifact, DPOAE measurements made at 75 & 75 dB FPL

were obtained using the single sweep procedure. Further coupler measurements revealed stimulus contamination when measuring at f_2 frequencies above 16 kHz using frequency ratios of 1.06, 1.08, and 1.10. Therefore, measurements made using these conditions at f_2 frequencies > 16 kHz were removed from further analysis.

3.2.4. Analysis

Composite DPOAE level and phase were estimated using an LSF procedure described by Long & Talmadge (1997). Then, DPOAE level and corresponding noise floors were averaged into one-third-octave frequency bands using a center frequency totaling 15 octave and inter-octave audiometric test frequencies (from 0.5 and 16 kHz).

The influence of stimulus condition on the accuracy with which DPOAEs identified hearing loss was assessed using clinical decision theory (Swets & Pickett, 1982; Swets, 1988). Clinical decision theory is well-suited to assessing the accuracy with which a diagnostic test makes a dichotomous decision – such as normal versus impaired hearing – and has been used previously to evaluate the test performance of DPOAEs (e.g., Gorga et al., 1993, 1997, 1999, 2000, 2005; Kim et al., 1996; Stover et al., 1996; Dorn et al., 1999; Johnson et al., 2007, 2010). Pure-tone behavioral thresholds served as the gold standard to which DPOAEs were compared. Behavioral thresholds above the cut-off of the normative range (Lee et al., 2012) were defined as hearing impaired while thresholds within the normative range were defined as normal hearing. The classification of normal versus impaired was made on a frequency-by-frequency basis.

A description of DPOAE test performance was obtained by computing true positive percentage (TPP) (i.e., sensitivity or hit rate), which is the proportion of ears with hearing loss that were correctly identified as hearing impaired, and corresponding false positive percentage (FPP) (i.e., 1- specificity or false alarm rate), which is the proportion of normal hearing ears

incorrectly identified as hearing impaired. These analyses were performed for DPOAE level and SNR at each f_2 , f_2/f_1 , and L_1 & L_2 . ROC curves (plots of sensitivity versus $1 - \text{specificity}$) were constructed for each test condition and area under the ROC curve (A_{ROC}) was computed. A_{ROC} provides a single estimate of test accuracy and ranges in value from 0.5, where hit and false-alarm rates are equal (chance performance), to 1.0 (perfect performance), where the hit rate is 100% for all false-alarm rates.

3.3. Results

Participants with normal hearing (Figure 18A) or SNHL (Figure 18B) were recruited for this investigation. The participants with SNHL had a wide variety of audiometric configurations and a range of hearing loss magnitude. This variety made it ideal for evaluating the sensitivity and specificity of a DPOAE screener across multiple frequencies and a realistic clinical situation where no control can be exerted over the type, degree, and configuration of hearing loss encountered. The level of the $2f_1-f_2$ DPOAE was measured as stimulus tones were swept continuously in frequency. However, data will be reported after averaging over one-third-octave bands centered around each f_2 frequency of interest. Data are reported for 32 conditions in total over a set of stimulus frequency ratios and level combinations. Across participants, DPOAE level and SNR varied as a function of stimulus frequency ratio, stimulus level, and f_2 frequency.

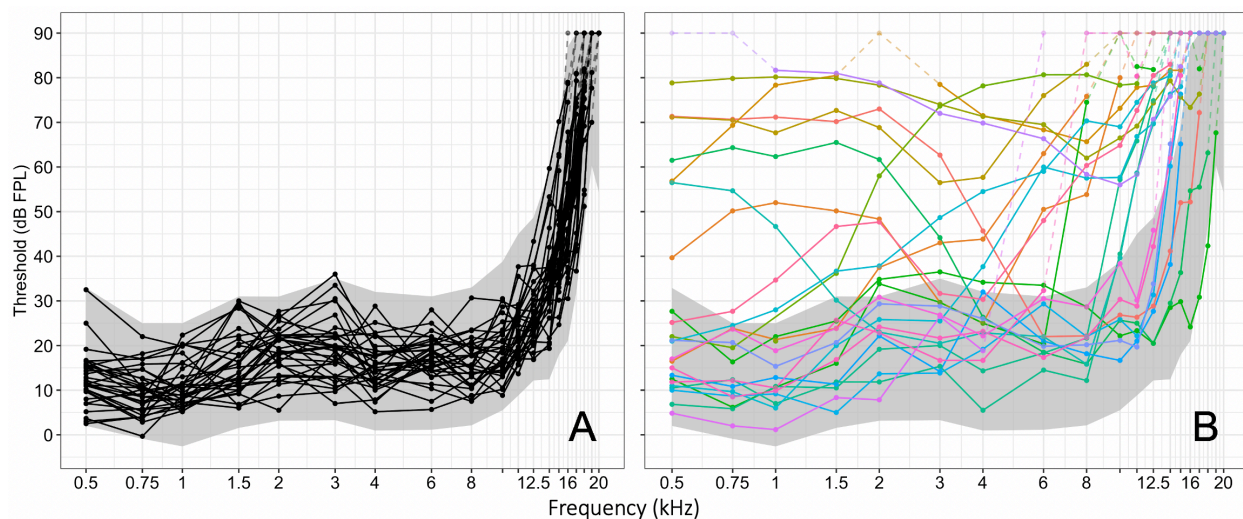


Figure 18. Behavioral hearing thresholds for normal-hearing (A) and hearing-impaired (B) groups

Behavioral hearing thresholds were estimated using a modified Békésy tracking technique. Each line represents the thresholds for a single individual. Thresholds for individuals with normal hearing (A) fell within the normative range (gray shading) which indicates the 5th to 95th percentile range of thresholds for young, audiometrically normal-hearing ears between 17 and 21 years of age (Lee et al., 2012). Participants with SNHL (B) had at least two test frequencies where a threshold fell above the normative range. Thresholds of each individual participant with SNHL are shown in various colors in panel B.

DPOAEs, presented at 75 & 75 dB FPL, and associated behavioral thresholds (inset) for one normal-hearing and three hearing-impaired ears can be compared in Figure 19. The participant with normal hearing (Figure 19A) showed large DPOAE responses that were well above the noise floor which was consistent with hearing thresholds that fell within the normative range. DP-grams and audiograms for three participants with varying degrees and configurations of SNHL (Figure 19C-D) demonstrate the gross relationship between DPOAE responses and behavioral thresholds. The frequency regions of elevated hearing thresholds (that fell outside of the normative range) are marked with red shading on the DP-gram. DPOAE responses were consistently in or near the noise floor in frequency regions where hearing thresholds were elevated.

Line colors in Figure 19 demarcate different stimulus frequency ratios which dramatically affect the DPOAE response. In a given ear, DPOAE levels at a specific frequency

are found to vary over a range of 25 dB with changing stimulus frequency ratios. Comparing the influence of stimulus frequency ratio across these four ears demonstrates the influence of hearing loss (arguably due to cochlear dysfunction) on the optimal ratios that produce the largest DPOAE levels at any given frequency. While the results from the normal hearing ear are consistent with those observed in Chapter 2, those from the ears with SNHL exhibit slight deviations from these trends. In the normal-hearing ear, the frequency ratio that gave the largest DPOAE response was widest in the low frequencies and narrowest in the high frequencies. Although this f_2/f_1 pattern of behavior was similar across the SNHL participants, there were differences in the exact f_2/f_1 that gave the largest DPOAE at a given frequency. In particular, the f_2/f_1 conditions that produced the largest DPOAE response in the hearing-impaired ears were usually wider compared to the normal-hearing ear. Additionally, differences between participants can be seen in the absolute level of the DPOAE or noise floor at a given frequency, even when behavioral thresholds were normal within that frequency region (i.e., no red shading on the DP-gram in Figure 19).

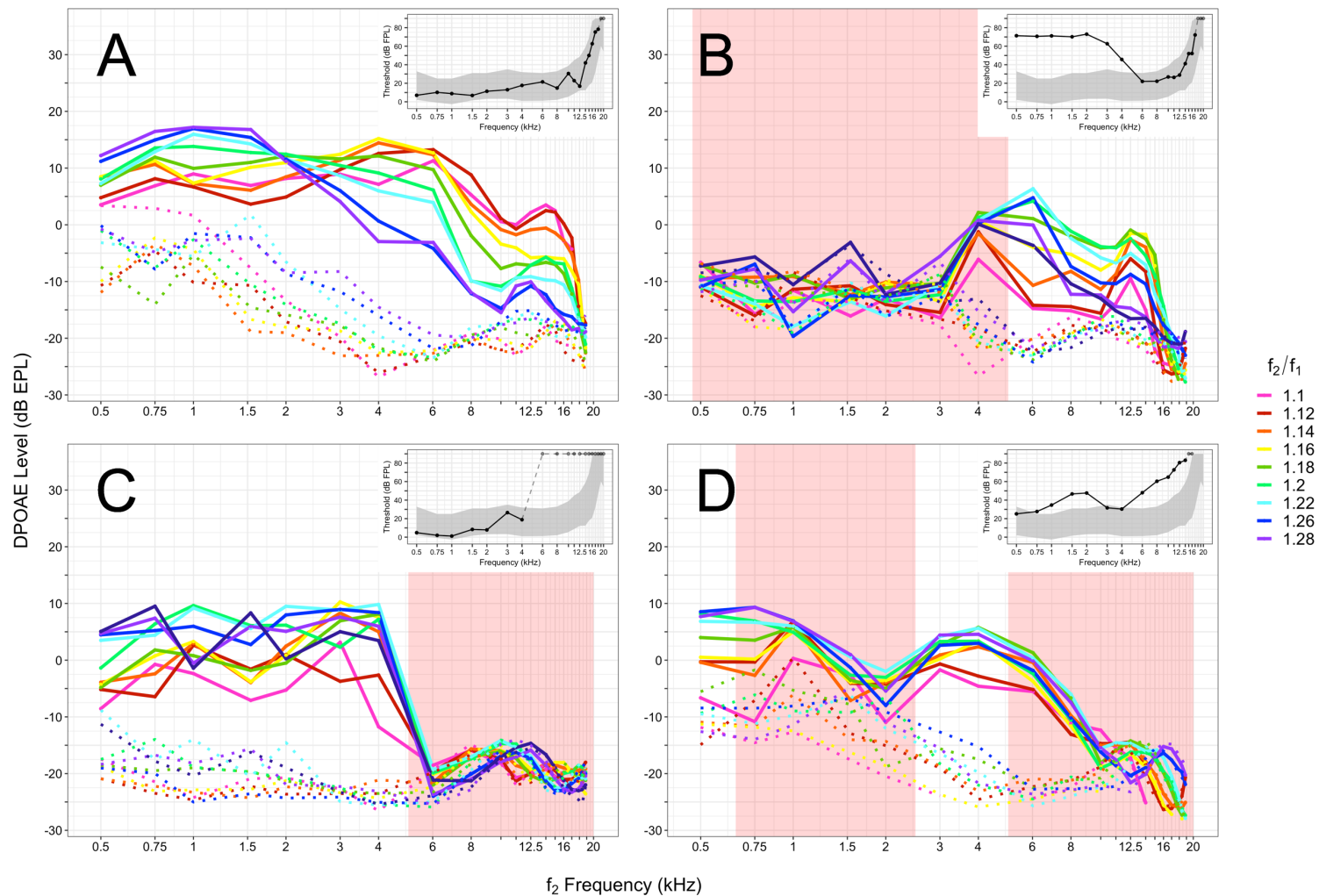


Figure 19. DP-grams for one participant with normal-hearing (A) and three with SNHL (B-D)

DPOAE levels averaged over third-octave frequency bands from four individual participants when stimulus primaries were presented at 75 & 75 dB FPL (A: participant 017_SSDP, B: participant 041_SSDP, C: participant 062_SSDP, and D: participant 070_SSDP). DPOAEs are represented by solid lines and noise floors are represented by dotted lines. Each f_2/f_1 ratio condition is indicated by line color. Inset plots show the associated behavioral hearing thresholds for the participant. Red shaded regions correspond with the frequencies that indicated hearing loss using behavioral tracking thresholds.

3.3.1. Receiver operating characteristic curves

DPOAE data were used to dichotomously determine if hearing was normal or impaired at individual audiometric frequencies. To do this, clinical decision theory was used to illustrate the diagnostic ability of a DPOAE test by constructing ROC curves at each of the 32 stimulus conditions (Table 2) at each f_2 frequency from 0.5 to 16 kHz. First, audiometric thresholds were used as the gold standard for classifying an ear at a given frequency as either normal hearing or impaired. Then, DPOAE level or SNR served as the experimental metric used to classify these ears.

The ROC curve is created by plotting the TPP (or sensitivity) against the FPP (or false alarm rate) at various threshold settings of a diagnostic test. The different points on the curve correspond to the different cut-points used to determine whether the test results are accurate. A perfect test would be represented by a ROC curve that rose vertically to the upper left corner of the graph, where true positive rate is nears 100% and false positive rate nears 0%. In contrast, a test performing at chance would be characterized by equal TPP and FPP, resulting in a curve that would diagonally bisect the plot. The accuracy of a DPOAE screener depends on how well the test separates the participants into one of two groups – either with or without hearing loss. A_{ROC} is customarily used as a global measure of overall diagnostic accuracy. A_{ROC} values range from 0.5 (no diagnostic ability) to 1.0 (perfect diagnostic ability).

ROC curves for a mid (2 kHz) and high (12.5 kHz) f_2 frequency stimulus condition are presented in Figure 20 and Figure 21, respectively. Each panel displays data from a different stimulus level combination while each curve is specific to a stimulus frequency ratio. Movement of the ROC curve towards the upper left corner of the panel signifies an increase in A_{ROC} . The separation of the lines within and across the stimulus levels demonstrates that the choice of

stimulus parameter influences the diagnostic ability of the DPOAE measured. The A_{ROC} for each ROC is listed in the figure legend of both Figure 20 and Figure 21 to make it easier for the reader to identify stimulus conditions that performed well. A_{ROC} values at 2 kHz were greater than 0.5 for all stimulus frequency ratio and level conditions with the greatest A_{ROC} values generally occurring for the 65 & 55 dB FPL level condition. The ROC curve with the largest A_{ROC} occurred at 65 & 55 dB FPL for a stimulus frequency ratio of 1.2. At 12.5 kHz, the ROC curve with the largest A_{ROC} occurred at 75 & 75 dB FPL with a stimulus frequency ratio of 1.16. At this relatively high frequency of 12.5 kHz, A_{ROC} was near 0.5 for all stimulus frequency ratios for the stimulus level combination of 50 & 30 dB FPL.

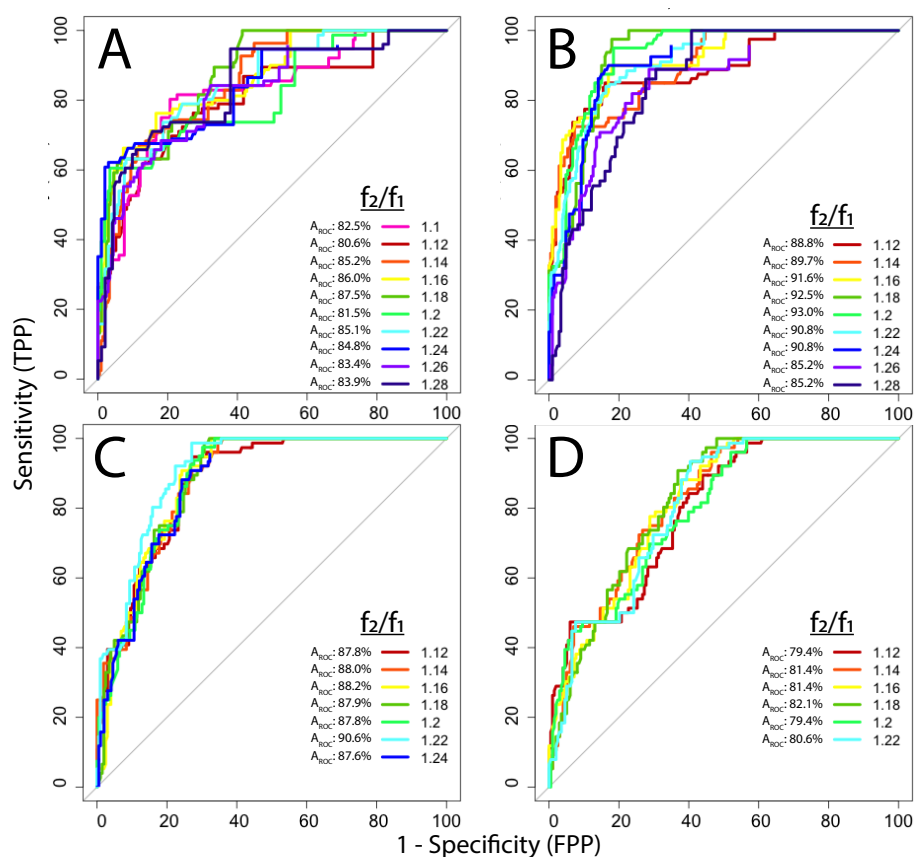


Figure 20. Receiver operating characteristic curves at 2 kHz.

ROC curves showing test performance of DPOAE SNR at 2 kHz. Panels indicate separate stimulus presentation levels (A: 75 & 75 dB FPL, B: 65 & 55 dB FPL, C: 55 & 40 dB FPL, and D: 50 & 30 dB FPL).

While it is clear how the A_{ROC} can be related to the overall ability of a test to correctly identify normal versus impaired hearing, it is not so obvious how one interprets the absolute area itself. When comparing A_{ROC} values, a guide for classifying the accuracy of a diagnostic test based on the A_{ROC} generally describes an A_{ROC} greater than 0.9 as outstanding, 0.8-0.9 as excellent, and 0.7-0.8 as acceptable (Hosmer & Lemeshow, 2000). Therefore, maximum A_{ROC} values in Figure 20 and Figure 21, which were greater than 0.9, indicate outstanding accuracy of the diagnostic test at those stimulus parameters.

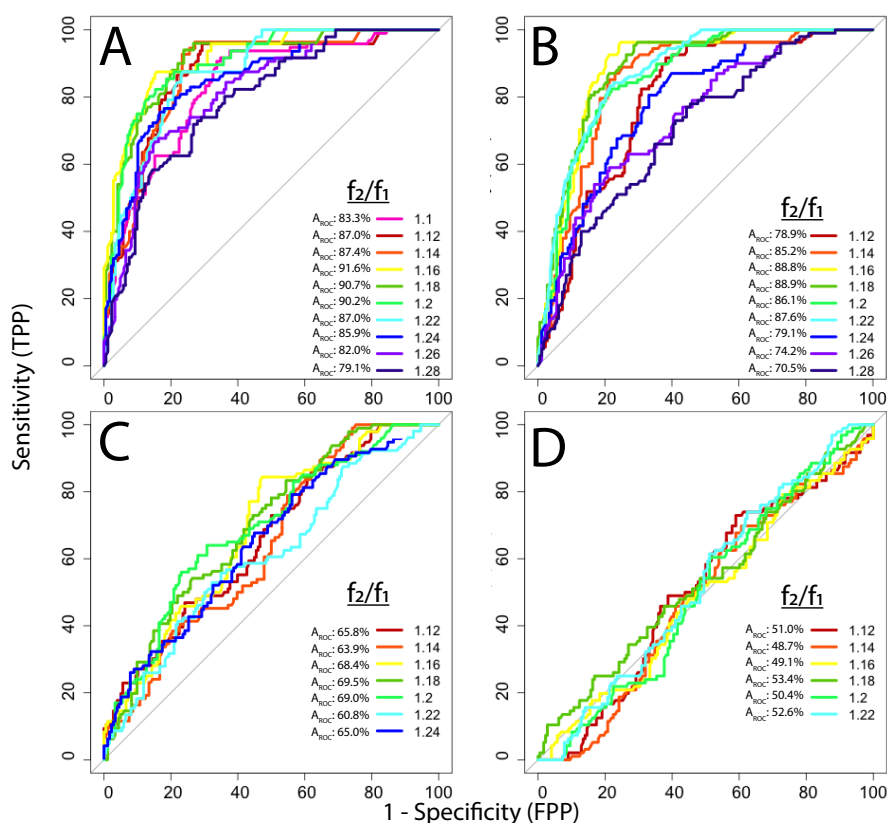


Figure 21. Receiver operating characteristic curves at 12.5 kHz

ROC curves showing test performance of DPOAE level at 12.5 kHz. Panels indicate the separate stimulus presentation levels (A: 75 & 75 dB FPL, B: 65 & 55 dB FPL, C: 55 & 40 dB FPL, and D: 50 & 30 dB FPL).

Figure 22 is a summary plot of A_{ROC} values as a function of f_2/f_1 for each stimulus level combination at each f_2 frequency. Data from each f_2 frequency are presented in separate panels and results from different stimulus level combinations are represented by different symbols in different colors. Such a display allows for the selection of the best stimulus condition at each f_2 frequency by simply visually selecting the symbol with the highest y-axis value. Some of the largest A_{ROC} values were observed in the 4 to 8 kHz frequency range with comparable performance at all stimulus level conditions. More variation in A_{ROC} values can be observed at f_2 frequencies above and below this range by comparing across stimulus frequency ratio and level combinations. Under such circumstances, it becomes easier to find the specific stimulus condition that was most successful for screening for the presence or absence of hearing loss (i.e., the optimal stimulus condition). The symbols that shared the same shape in the frequency panels are arranged over a rather narrow vertical range at the low and mid frequencies, indicating relatively similar test performance irrespective of stimulus frequency ratio chosen. Stimulus level was easier to differentiate at these frequencies. Greater separation in test performance for stimulus frequency ratio and level was observed at the higher frequencies with higher level stimuli (75 & 75 dB FPL) performing better and performance peaking at progressively narrower ratios with increasing frequency. For f_2 frequencies > 12 kHz, the highest stimulus presentation levels yielded the best performance regardless of the f_2/f_1 , with the exception of 16 kHz at a 1.28 frequency ratio (Figure 22). This finding actually argues against the need for careful adjustment of f_2/f_1 at frequencies where tuning is sharpest. This result is probably due to the fact that the stimulus interaction region is constricted by the basal end of the cochlea, so increasing stimulus level does not broaden the generation region appreciably.

In order to determine the stimulus parameter that had the best diagnostic ability, the DPOAE measure that produced the greatest A_{ROC} was used and, thus, considered the optimal stimulus parameter. Test performance was similar for DPOAE level and SNR, although there was a slight tendency for SNR to result in higher estimates of A_{ROC} at low frequencies. The slightly poorer performance of DPOAE amplitude measurements is likely a consequence of those cases in which no response was evident while the signal measured in the ear canal was characterized by high levels of noise. Since noise floors were more likely to be elevated at low frequencies (Gorga et al., 1993), it was not surprising that DPOAE SNR resulted in larger ROC curve areas for f_2 frequencies ≤ 3 kHz. Still, it is important to note that any performance advantage of SNR over level was small. In fact, at frequencies above 3 kHz, DPOAE level resulted in similar but larger A_{ROC} values at these higher frequencies, where noise floor levels were seen to be reliably low across participants.



Figure 22. Area under the ROC curve (A_{ROC}) as a function of f_2/f_1

Area under the ROC curve (A_{ROC}) values as a function of f_2/f_1 across f_2 frequencies (kHz). The parameter within each panel is the presentation level (L_1 & L_2). Panels show separate the f_2 frequencies (label in the upper right corner).

3.3.2. Creating a DPOAE screening protocol

Collectively, these frequency-specific, optimal stimulus conditions make up a novel DPOAE screening protocol. An optimal DPOAE screening protocol can be compiled by selecting the stimulus frequency ratio and level combination that resulted in the largest A_{ROC} at a given test frequency. The compilation of these optimal stimulus conditions reveals a protocol involving dynamically changing frequency ratio and level combinations (Table 3 and Figure 23).

The optimal stimulus frequency ratio decreases systematically as test frequency increases. The highest stimulus level combinations perform best at the frequency extremes with the optimal stimulus level combinations gradually decreasing towards the mid frequencies. It should be noted that the DPOAE noise floors were lowest at the mid frequencies, often rising at the lowest and highest test frequencies due to physiological and instrumentation noise. This noise floor behavior may be at least partially responsible for the observed test performance of different stimulus levels. Additionally, the decline of hearing sensitivity at the highest test frequencies, even in these young individuals, requires the use of high stimulus levels.

Table 3. Optimized DPOAE test protocol for screening for hearing loss

Table listing the DPOAE test protocol that gives the optimal stimulus frequency ratio (f_2/f_1) and level condition (L_1 & L_2) as a function of f_2 frequency. This protocol is based on the stimulus conditions that produced A_{ROC} values that were the largest for a given f_2 frequency. Test performance was similar for DPOAE level and SNR, although there was a tendency for SNR to result in higher estimates of A_{ROC} at f_2 frequencies < 4 kHz.

f_2 (kHz)	L_1 & L_2 (dB FPL)	f_2/f_1	outcome	A_{ROC}
0.5	75/75 dB FPL	1.24	DPOAE SNR	0.728
0.75	65/55 dB FPL	1.22	DPOAE SNR	0.831
1	65/55 dB FPL	1.22	DPOAE SNR	0.929
1.5	65/55 dB FPL	1.18	DPOAE SNR	0.917
2	65/55 dB FPL	1.2	DPOAE SNR	0.930
3	65/55 dB FPL	1.2	DPOAE SNR	0.898
4	55/40 dB FPL	1.18	DPOAE level	0.943
6	55/40 dB FPL	1.18	DPOAE level	0.969
8	65/55 dB FPL	1.18	DPOAE level	0.967
10	65/55 dB FPL	1.16	DPOAE level	0.895
11.2	65/55 dB FPL	1.16	DPOAE level	0.911
12.5	75/75 dB FPL	1.16	DPOAE level	0.916
14	75/75 dB FPL	1.14	DPOAE level	0.899
15	75/75 dB FPL	1.14	DPOAE level	0.916
16	75/75 dB FPL	1.14	DPOAE level	0.890

Overall, screening performance of DPOAEs can be improved by using frequency-specific stimulus conditions that are optimized for the cochlear place of stimulation. Strikingly, the universally used stimulus setting of a frequency ratio of 1.22 and level combination of 65 & 55 dB was found to be optimal only at two test frequencies. Thus, these data provide strong evidence that the current use of DPOAEs for screening can be improved significantly by evaluating high frequencies and adopting stimulus parameters that are dynamic in both stimulus frequency ratio and level combination.

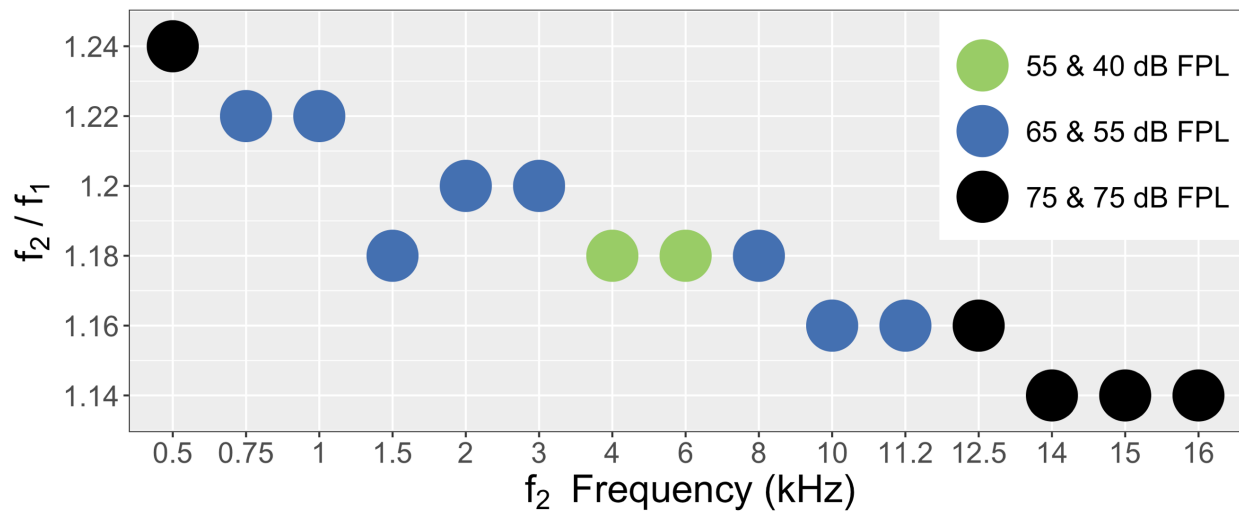


Figure 23. Optimized DPOAE measurement protocol for screening for hearing loss

This DPOAE measurement protocol gives the optimal stimulus frequency ratio (f_2/f_1) and level condition (L_1 & L_2) as a function of f_2 frequency. This protocol is based on the stimulus conditions that produced A_{ROC} values that were the largest for a given f_2 frequency.

3.4. Discussion

3.4.1. Place-specific stimulus parameters are best for screening for hearing loss

The purpose of this study was to develop a DPOAE screening protocol in adults, guided by cochlear mechanical properties, to derive physiologically-motivated, locally appropriate, stimulus parameters. The results described here summarize a broad exploration of the DPOAE stimulus parametric space in order to identify the most appropriate stimulus frequency ratio and level combinations for accurate screening for hearing loss up to 16kHz. DPOAE amplitudes and SNRs for 32 DPOAE stimulus parameter conditions (Table 2) were evaluated in ears with audiometrically normal hearing or with varying magnitudes and configurations of SNHL. By utilizing improved calibration, behavioral threshold, and DPOAE measurement methods, findings from this study describe how frequency-specific stimulus parameters more accurately identify hearing status compared to the traditional, fixed stimulus parameters.

This investigation is the first to evaluate sensitivity and specificity across a multitude of stimulus frequency ratio and level conditions in order to identify the exact parameters for an optimized DPOAE screening protocol in adults. Others have reported on test performance of a DPOAE screener for frequencies up to 8 kHz using clinical decision theory (e.g., Gorga et al., 1997; Johnson et al., 2010). Gorga et al. (1997) were the first to report DPOAE test performance as a hearing screener for a single stimulus condition (L_1 & $L_2 = 65$ & 55 dB SPL, $f_2/f_1 = 1.22$). The outcome of this work established a DPOAE protocol that remains the standard method for hearing screening used in clinical and research settings today. Later, Neely et al. (2005) and Johnson et al. (2006) created a function for frequency-specific stimulus parameters from data that had been shown to produce large DPOAE levels in a group of normal-hearing individuals. However, stimulus conditions that generate large DPOAEs in normal ears can only be clinically useful if they also remain sensitive to cochlear dysfunction. That is, a stimulus combination may generate large DPOAEs in normal-hearing ears but is not clinically useful if ears with hearing loss also yield large DPOAEs. In a later study designed to validate this frequency-specific function, Johnson et al. (2010) reported no difference in diagnostic performance between these new stimuli and the traditional stimuli (L_1 & $L_2 = 65$ & 55 dB SPL, $f_2/f_1 = 1.22$). It is likely this lack of improved performance resulted from the optimal stimulus parameters not being established using both normal-hearing and hearing-impaired ears. Therefore, the purpose of this report was to describe the diagnostic ability of multiple stimulus frequency ratio and level combinations, up to 16 kHz, in order to create an optimized DPOAE screening protocol.

Clinical decision theory was used to determine test performance across a multitude of stimulus conditions in order to identify frequency-specific stimulus parameters for improving DPOAE measurements. To do this, a ROC curve for each of the 32 stimulus conditions (Table 2)

was constructed at each of the 15 octave and inter-octave frequencies. From each curve, the area under the ROC curve was used to qualify the diagnostic accuracy of that particular stimulus condition (Figure 22). In order to determine the stimulus condition that had the best diagnostic ability, the DPOAE outcome variable that produced the greatest A_{ROC} was deemed the optimal stimulus parameter most accurate at differentiating between ears with normal hearing and hearing loss.

The traditional stimulus protocol that has a fixed frequency and level relationship across test frequency (L_1 & $L_2 = 65$ & 55 dB; $f_2/f_1 = 1.22$) did not produce the greatest A_{ROC} across f_2 frequencies, except at 0.75 and 1 kHz (Figure 23). The optimal stimulus frequency ratio changed with frequency, similar to findings from Chapter 2 and previous reports that investigated optimal stimulus parameters in normal-hearing adults (Harris et al., 1989; Gaskill & Brown, 1990). Specifically, as the f_2 frequency increased, the optimal stimulus frequency ratio decreased from the widest at 0.5 kHz ($f_2/f_1 = 1.24$) to the narrowest at 16 kHz ($f_2/f_1 = 1.14$).

Findings here are consistent with the hypothesized interaction between stimulus parameters and cochlear mechanics. The largest A_{ROC} was seen when (1) f_2/f_1 decreased as f_2 increased, and (2) L_1 & L_2 increased as f_2 increased. This is consistent with the understanding that, at high frequencies, (1) excitation patterns for the two eliciting stimulus tones are more spatially separated, and (2) excitation patterns are more sharply tuned. Therefore, high frequencies more than low frequencies required a narrowing in the stimulus frequency ratio in order to create an optimized overlap for generating distortion.

The best test performance (i.e., greatest A_{ROC} values) occurred at mid and high f_2 frequencies (Figure 23). At 4 and 6 kHz, low stimulus levels presented at 55 & 40 dB FPL most accurately identified normal hearing. At these frequencies, the human cochlea is highly sensitive

leading to some of the lowest behavioral thresholds while noise floor levels are at their lowest, allowing for a greater dynamic range of DPOAE responses to be measurable above the noise floor. At the highest frequencies, where sensitivity declines in normal hearing individuals, higher stimulus levels are needed to evoke measurable responses of normal cochlear function.

Establishing optimal stimulus conditions at these high frequencies is especially important when creating a DPOAE screening protocol for adult populations. Stimulus parameters that best exploit responses in the high frequencies will aid in the early identification of ARHL (Poling et al., 2014; Stiepan et al., 2019), opening the door for this accurate and efficient hearing screener to become more accessible to adults if expanded to healthcare settings such as primary care clinics.

Poorer test performance was seen at lower frequencies (i.e., 0.5 and 0.75 kHz) compared to mid and high frequencies. This, at least in part, is due to reduced SNRs as a result of high noise floor levels in low frequency regions. DPOAE noise floor measurements are an independent estimate of noise from many sources including physiological, environmental, and instrumental sources. Common sources of physiological noise, as recorded in the ear canal, are related to circulation, respiration, and general muscle activity (Shaw, 1974). At low frequencies, noise floor levels rise due to physiological noise and, thus, become more confounding to DPOAE measurements. This compels a need for high stimulus levels in order to reliably distinguish the DPOAE above the noise floor (i.e., to improve the SNR). This is why, at frequencies below 1 kHz, ROC curves were more likely to perform near chance (i.e., have A_{ROC} values that were near 0.5) at low stimulus levels (Figure 22). Not surprisingly, there was a tendency for DPOAE SNR, rather than level, to result in higher estimates of A_{ROC} at low frequencies. This is consistent with findings from Gorga et al. (1997) at similar low frequencies. Although higher estimates were

seen at low frequencies for DPOAE SNR, the performance advantage was small compared to DPOAE level.

Methods to circumvent the problem of higher noise floors have been proposed in the literature. For example, Gorga et al. (2000) attempted the simultaneous use of the DPOAEs at $2f_1-f_2$ and $2f_2-f_1$ in order to improve test performance by measuring a distortion product at a lower frequency where a more favorable SNR should exist. The gains reported were minimal, perhaps partly due to the limited frequency range explored. Differences in middle ear energy transfer could be another factor influencing test performance at lower frequencies. That is, energy may be transmitted less efficiently by the middle ear in the forward (stimuli) and reverse (DPOAE generated) directions at low frequencies, resulting in reduced DPOAE amplitudes relative to higher frequencies.

3.4.2. Clinical Implications

The DPOAE protocol described in Figure 23 is optimized for the screening of hearing loss in adults. This protocol is an ideal first step towards making hearing healthcare more accessible to adult populations. Increasing hearing healthcare access with an accurate, comprehensive, and automated DPOAE hearing screener has major implications in monitoring for the onset and progression of hearing loss. Since the most common forms of adult-onset hearing loss (e.g., ARHL, noise-induced hearing loss, and ototoxicity) are associated with OHC dysfunction or damage occurring first at the cochlear base (Ueberfuhr et al., 2016), DPOAEs make for an ideal monitoring tool for the early identification of dysfunction. Early identification can then lead to appropriate counseling and follow-up recommendations which would facilitate early treatment, effectively reducing the burden of the hearing loss.

Hearing loss, particularly in adults, remains under-detected as current diagnostic tests ignore high frequency regions that are first affected by aging. Auditory aging is reflected in both behavioral hearing thresholds and DPOAEs (Lee et al., 2012; Poling et al., 2014; Stiepan et al., 2019), indicating a relationship between hearing decline and OHC degradation at high frequencies. OHC function is crucial to normal peripheral auditory processing as it provides sharp frequency selectivity, wide dynamic range, and acute sensitivity (Stavroulaki et al., 1999). Notably, these are often the first functions to be compromised due to aging. Therefore, it is fundamental that an assessment for detecting age-related auditory decline early and accurately evaluates OHC function at high frequencies. An assessment of DPOAEs is the ideal choice as this tool could provide an objective, efficient, and noninvasive measure of OHC function. However, in their current clinical state, DPOAE measurements are limited to evaluating frequencies below 8 kHz (Lonsbury-Martin & Martin, 2003). Previously, the adoption of routine tests of auditory function, including DPOAEs, at frequencies above 8 kHz (International Organization for Standardization (ISO), 1997) had remained elusive due to equipment and calibration limitations. Now, new calibration techniques enable accurate signal delivery (Sheperle et al., 2008; Souza et al., 2014) and OAE recordings (Charaziak & Shera, 2016) at frequencies up to 20 kHz. Therefore, the work accomplished here, utilizing these advanced calibration techniques while establishing optimizations to DPOAE measurements, is a logical first step towards making this a popular clinical tool for identifying and monitoring for early signs of adult-onset hearing loss, particularly ARHL.

Early identification and monitoring can aid in the prevention of known negative cognitive, emotional, social, behavioral, and socioeconomic consequences of hearing impairment (Bess et al., 1989; Mulrow et al., 1990; LaForge et al., 1992; Carabellese et al., 1993; Appollonio

et al., 1996; Heine & Browning, 2002; Cruickshanks et al., 2003; Dalton et al., 2003; Gates & Mills, 2005; Kochkin, 2010). Benefits of early intervention, following early identification, have been reported in hearing aid users as better physical, emotional, mental, and social well-being compared to matched controls that did not use hearing aids (Cruickshanks et al., 2010; Kochkin, 2010).

Yet, even in light of these reported positive outcomes of treatment, there exists a critically underserved population that the field of audiology and hearing science needs to address. Before seeking treatment, the average adult will go on living with untreated hearing loss for 6 to 9 years (Kochkin, 2010; Simpson et al., 2019). Fortunately, a solution to the dire need to close the 6- to 9-year gap could come from healthcare settings adopting screening tools that identify hearing loss as early as possible. Findings from the present study support the use of optimized DPOAEs measurements for such a tool. By having a DPOAE screening tool that assesses up to the highest frequencies of human hearing, trained healthcare workers could identify a patient's hearing loss even before the patient has recognized its effects in daily life. It is to the patient's advantage to be informed of early signs of hearing loss. Early identification gives the patient time to recognize and accept his or her hearing loss while the hearing loss is relatively mild and contained to frequency regions where current hearing aid technology cannot amplify. The added bonus of having the screener measure DPOAEs is the fast test times, making this an efficient tool for healthcare settings.

While this gap between identification and treatment is certainly deleterious to the effectiveness of today's treatments (such as amplification), it will be even more critical in the future when molecular and genetic treatments for hearing loss become available. Early detection and effective monitoring of hearing status would also have major implications for hearing

conservation purposes, allowing the patient to make lifestyle changes that are known to reduce the risk and progression of hearing loss (Cruickshanks et al., 2010; Zhan et al., 2011). Thus, an accurate and comprehensive probe of function is expected to become even more important in the future as innovative options for prevention and treatment of hearing loss become available.

While the explicit goal of this work was to identify the earliest signs of cochlear aging, we are hamstrung by the use of hearing thresholds as the gold standard. That is, if changes in hearing thresholds are not the first signs of age-related decline, our choice of test parameters may not be optimized to detect the earliest changes. Unfortunately, better alternatives that demonstrate cochlear dysfunction are not available today. One possibility of overcoming this limitation may be to use longitudinal DPOAE data from large samples to establish a new standard of reference using DPOAE levels to mark the initiation of aging.

3.4.3. Other applications of place-specific stimulus parameters

Here we have demonstrated that frequency-specific stimulus parameters provide an improvement in DPOAE test performance; however, this does not provide all information necessary for use in a clinical setting. In order to use any measurement in the clinic, one must select criteria that will serve as guidelines for interpretation. In clinical settings especially, a normative range for DPOAE level and/or SNR is necessary in order to report if measurements are normal, present but abnormal, or absent. In the early stages of evaluating a new diagnostic test, the property of a ROC curve most useful for summarizing the overall diagnostic performance is the A_{ROC} . In our case, comparing the A_{ROC} values across multiple stimulus conditions allowed us to construct frequency-specific recommendations for a screening protocol. Now that the diagnostic ability of a DPOAE screening protocol is established, a validation study can follow. In future work, we will compare this optimized DPOAE protocol (Figure 23) to the

traditional fixed protocol (L_1 & $L_2 = 65$ & 55 dB, $f_2/f_1 = 1.22$) while also creating a normative range of DPOAE responses in a larger sample of ears with and without age-related decline.

The use of appropriate stimulus frequency ratio and level combinations has been shown here to enhance DPOAE amplitudes at high frequencies and to improve detection of hearing loss in adults. However, DPOAEs are used predominantly in clinical settings to screen cochlear function in neonates and children and are occasionally included in pediatric hearing assessment batteries. DPOAEs that are optimized to more sensitively detect auditory dysfunction in pediatric populations would be a huge advancement for the field. In general, researchers and clinicians have used the stimulus and recording parameters defined from studies of adult populations when evaluating neonates and children. Previous work investigating the optimal stimulus parameters for neonatal populations showed average optimal primary frequencies and levels were comparable to adults (Abdala, 1996). However, this work was limited to evaluating optimal stimulus parameters at only 1.5 and 6 kHz. Furthermore, DPOAE calibration and measurement techniques have long since advanced, allowing for even more accurate DPOAE recordings.

3.4.4. Conclusions

The timely and accurate detection of cochlear pathology using DPOAEs remains suboptimal as current protocols: 1) do not assess cochlear function up to the highest frequencies of human hearing, and 2) do not consider local cochlear mechanical properties when setting DPOAE stimulus parameters. Using advanced calibration and measurement techniques, DPOAEs were evaluated in normal hearing ears as well as from ears with SNHL of various degrees and configurations. ROC curves were used to identify stimulus settings that most accurately differentiated between normal-hearing and hearing-impaired ears. Overall, findings from this study support how optimal DPOAE stimulus frequency ratios and levels change

systematically with known local cochlear mechanics. These results support a dramatic shift in current adult DPOAE screening protocols from stimulus parameters that are agnostic to the test frequency to a combination of stimulus conditions that accommodates known properties of the cochlea and leads to significantly improved test performance.

CHAPTER 4

Discussion

4.1. Overview

With an increasing understanding of the early onset of age-related SNHL, its common prevalence, and the quality-of-life consequences associated with it, the demand for developing objective and accurate tools for assessing hearing status is undeniable. These tools would need to provide a deep understanding of normal function as well as impaired function in order for individualized intervention strategies to be realized. Therefore, the accurate assessment of specific auditory function should aid in intervention strategies such as the prevention of loss of function or establishing treatment recommendations. Furthermore, early and accurate assessment of cochlear dysfunction will become even more important in the future when regeneration of tissue or function becomes a reality for human subjects. Taken together, the early and accurate diagnosis of SNHL followed by appropriate intervention would allow for improved patient quality of life in the acoustically complex listening environments of the world.

However, a currently utilized tool that directly assess cochlear function, DPOAEs, is not optimized to accurately quantify function up to the highest frequencies where ARHL and other common forms of adult-onset SNHLs first manifest. With the advent of advancements in calibration and measurement techniques signals can now be delivered and recorded for more accurate DPOAE assessments in the high frequencies (Scheperle et al., 2008; Lee et al., 2012; Souza et al., 2014; Charaziak & Shera, 2016). Yet, even with these advancements, DPOAE measurements still remain suboptimal as fixed stimulus parameters are used across test

frequencies. We contend that the varying passive and active mechanical properties along the cochlear partition are not accounted for in current DPOAE test protocols where stimulus properties remain invariant with frequency. Therefore, this dissertation tackled a remaining important step: developing a DPOAE measurement protocol guided by local cochlear mechanical properties and evaluating its test performance.

The studies undertaken in this dissertation explored and characterized DPOAE responses across a wide frequency range in young and middle-aged adults with either audiometrically normal hearing or various degrees and configurations of SNHL. We hypothesized that DPOAE stimulus parameters optimized for the cochlear place of stimulation would evoke emissions that accurately quantify cochlear health and, therefore, would also be closely aligned with identifying the presence or absence of hearing loss. DPOAE responses were also used to explore more complex ideas and theoretical frameworks regarding human DPOAE generation and propagation.

The global aim of this research was to directly explore the efficacy of DPOAEs as a screener for hearing loss, setting the groundwork for developing a new and objective test of auditory function for use in both clinical and laboratory settings. A secondary motivation of this work was to better understand the potential utility of DPOAE measurements up to the highest frequencies of human hearing.

The results from the two studies presented in Chapters 2 and 3 yield insight into improved protocols for quantifying normal and impaired cochlear function by utilizing optimized measurement methods when recording DPOAEs. Overall, stimulus frequency ratio and level combinations that are adjusted in a frequency-specific manner maximized DPOAE generation to improve test performance for both measuring DPOAEs in normal ears and screening for hearing

loss. We predict DPOAE measurement protocols that adopt these optimal stimuli will improve the accuracy with which DPOAEs are used to assess cochlear function in adult populations, significantly positioning DPOAEs as an important tool for early detection of auditory dysfunction in adults.

4.2. Chapter summaries

4.2.1. Chapter 2

The primary motivation of the first study, described in Chapter 2, was to better understand the mechanisms of normal DPOAE generation in order to exploit this behavior for the purpose of characterizing cochlear function in young, normally functioning ears. To do this, a broad exploration of the DPOAE parametric space was undertaken in a large group of audiometrically normal-hearing humans. Using this experimental approach, results revealed how more accurate DPOAE measurements are acquired when the stimulus parameters are tuned to known local cochlear mechanicals.

Examination of DPOAE responses across stimulus frequency ratios showed a distinct pattern: the frequency ratio yielding the largest DPOAE level changed as a function of frequency and stimulus level (Figure 13 & Figure 16). Specifically, at a constant L_1 & L_2 combination, the f_2/f_1 producing the largest DPOAE level was decreased with increasing frequency. Similarly, at a given f_2 frequency, the f_2/f_1 producing the largest DPOAE level was wider as L_1 & L_2 increased. This is consistent with the idea that excitation patterns for the eliciting two primaries are more spatially separated at high frequencies than at low frequencies, requiring a decrease in the stimulus frequency ratio or an increase in the stimulus level combination in order to create an optimized overlap for generating distortion. These results confirm and strengthen various aspects

of our current understanding of normal cochlear function and expand our understanding by extending our observation to previously unexamined higher frequencies.

Collectively, these data provide confidence that stimulus frequency ratio settings need to be frequency- and level-specific, which is in opposition to current practice of using a frequency ratio of 1.22 regardless of the stimulus level being presented or the f_2 frequency being evaluated. After finding that stimulus optimizations (Figure 17) result in higher DPOAE levels, we then predicted frequency-specific stimulus parameters would also provide a clinical advantage to screening protocols.

4.2.2. Chapter 3

The investigation undertaken in Chapter 3 is the first to establish DPOAE stimulus conditions that most accurately identify the presence of hearing loss up to the highest frequencies of human hearing. Others have reported stimulus frequency ratios and levels that elicit the largest DPOAE responses in human adults (Harris et al., 1989; Gaskill & Brown, 1990; Johnson et al., 2006). However, these studies are limited in the limited number of stimulus conditions, the number of participants, and the calibration techniques used. Furthermore, measurements were limited to f_2 frequencies at and below 8 kHz. This report is the first to describe the overall diagnostic accuracy across a multitude of stimulus conditions in both normal-hearing and hearing-impaired participants in order to identify an optimized DPOAE screening protocol up to 16 kHz.

Chapter 3 describes a broad exploration of the DPOAE stimulus parametric space in order to identify the stimulus frequency ratios and levels best for screening at individual f_2 frequencies. DPOAE amplitudes and SNRs for 32 DPOAE stimulus parameter conditions were evaluated in ears with audiometrically normal hearing or with SNHL. For the DPOAEs evaluated

in the present set of measurements, the screener performed well at separating ears into normal or impaired categories when normal hearing was defined from a normative range established for FPL calibrated stimuli (Lee et al., 2012). It was likely a combination of the advanced calibration methods, behavioral threshold estimation procedure, and DPOAE measurement procedures that made findings from this study more accurate at identifying hearing loss than the traditional, fixed stimulus parameter setting (65 & 55 dB FPL, $f_2/f_1 = 1.22$).

DPOAE test performance was established using clinical decision theory. First, ROC curves for each of the 32 stimulus conditions were constructed at each of the 15 octave and inter-octave f_2 frequencies from 0.5 to 16 kHz. From an individual curve, the area under the ROC curve represented the diagnostic accuracy of DPOAE recordings for that particular stimulus condition. Using the A_{ROC} values obtained across stimulus conditions, the exact frequency ratio and level condition most accurate at differentiating between normal hearing and hearing loss had the greatest A_{ROC} and, thus, was the optimal stimulus condition at that f_2 frequency. This was done on a frequency-by-frequency basis in order to collectively organize the optimal stimuli into a novel DPOAE screening protocol (Figure 23).

As predicted, the stimulus frequency ratio and level condition that produced the best test performance (or diagnostic accuracy) was found to be frequency specific. Optimal stimulus frequency ratio decreased with increasing frequency in a pattern similar to that observed when optimizing stimulus parameters to yield high DPOAE levels in normal-hearing adults (Chapter 2). The overall best test performance was seen for mid and high frequencies. At 4 and 6 kHz, low stimulus levels presented at 55 & 40 dB FPL were best at identifying normal hearing or hearing loss. This is likely due to the fact that, for normal hearing individuals at these frequencies, hearing and cochlear function is highly sensitive while noise floor levels are often low. At the

highest audible frequencies, where sensitivity declines in normal hearing individuals, higher stimulus levels were needed to be able to measure normal cochlear function. This is a key finding of this work as we predict that using stimulus parameters that best exploit DPOAE responses in the high frequencies will aid in the early identification of ARHL. Poorer test performance was seen at low frequencies which was likely due to reduced SNRs. At low frequencies, noise floor levels rise due to physiological noise levels of the human body and, thus, become more confounding, requiring high stimulus levels in order to reliably distinguish the DPOAE above the noise floor. Not surprisingly, better diagnostic performance was seen at low frequencies when DPOAE SNR was used as the outcome measure. This is consistent with findings reported from Gorga et al. (1997), the investigation that launched what became the gold standard DPOAE screening criteria (i.e., traditional stimulus parameter setting of L_1 & $L_2 = 65$ & 55 dB FPL, $f_2/f_1 = 1.22$) that is used clinically to this day.

4.3. Implications

4.3.1. Aligning DPOAE measurements with cochlear mechanics

4.3.1.1. Local cochlear mechanical properties need to be considered when setting DPOAE stimulus parameters

In clinical and research settings today, DPOAE measurements are obtained under suboptimal conditions as fixed stimulus parameters used across test frequency are not consistent with dynamically changing local cochlear mechanical properties. This is in the face of previous studies reporting that cochlear mechanics in the low-frequency, apical regions are different than in the high-frequency, basal regions (Robles & Ruggero, 2001; Warren et al. 2016; Recio-Spinoso et al., 2017; Dong et al. 2018). The use of suboptimal stimuli that do not consider local cochlear mechanics could compromise the vulnerability of responses to cochlear function or

could point to unexplained variability in DPOAE characteristics seen both within and across human ears (Scheperle et al., 2008; Lee et al., 2012).

The passive and active mechanical properties of the mammalian cochlea change gradually across the cochlear length. As a result of this mechanical gradient, stimulus tones of different frequencies cause maximal displacement at specific positions along the cochlear partition. The changing physical properties of the cochlear partition are important in determining gross tuning characteristics. These passive properties include mass, which increases from base to apex, stiffness, which decreases from base to apex, and damping which controls the shape of the resonance. The peak of the traveling wave varies according to the tonotopic map defined by these basal-to-apical gradients.

Passive mechanical models of the cochlea alone cannot reproduce the low-threshold, sharply tuned component of the traveling wave. This active process of the cochlear amplifier renders the cochlea with enhanced sensitivity, dynamic range, and frequency selectivity which has been observed in mammalian ears (Robles & Ruggero, 2001). The amplifier, provided by the OHCs, detects the movement of the cochlear partition and feeds mechanical energy back into the traveling wave. Responses in the low-frequency region exhibit a smaller degree of nonlinearity and broader tuning compared to higher frequency regions (Cooper & Dong, 2003; Cooper & Rhode, 1997, 1995; Dong & Cooper, 2006; Zinn et al, 2000). As a consequence of the changing active mechanical properties of the cochlear partition from apex to base, mechanical tuning becomes sharper as a function of increasing frequency and decreasing stimulus level (Robles & Ruggero, 2001).

Together, these passive and active local cochlear mechanics determine the spatial properties of the traveling wave. DPOAE measurements become particularly valuable when

assessing cochlear function in human ears, as they noninvasively provide quantitative information about the range and operational characteristics of the cochlear amplifier (i.e., sensitivity, compression, and frequency selectivity).

4.3.1.2. Mechanisms of DPOAE generation

When a two-tone complex is presented to a healthy cochlea, intermodulation distortion products arise in the cochlea at expected frequencies. The frequencies of this distortion energy occur at arithmetic frequencies of the f_1 and f_2 stimulus tones. The cubic distortion product ($f_{dp} = 2f_1 - f_2$), is the largest and most widely measured distortion product and, thus, was the focus of this dissertation.

Models and experimental findings suggest that the DPOAE arises from two distinct cochlear sources: one located at the region of overlap of the stimulus tone traveling waves and the other located at the characteristic frequency place of $2f_1 - f_2$ (CF_{dp}) (Figure 2). During DPOAE stimulation, nonlinear distortion predominates in the f_1 and f_2 overlap region where the emission energy is first produced. Specifically, it is the nonlinearities in stereociliary transduction of OHCs that produce distortion in the region of overlap between the mechanical excitation of the two stimulus tones (Verpy et al., 2008). A portion of this energy returns to the ear canal as the distortion component while another portion of this distortion energy propagates apically to the CF_{dp} . The CF_{dp} region is hypothesized to be dominated by a component originating from coherent reflections, due to irregularities in the mechanical properties of the cochlea, returning a reflection component to the ear canal (Dhar et al. 2005; Kim 1980; Knight et al. 2000; Shera and Guinan 1999; Talmadge et al. 1999). In the ear canal, energy from the CF_{dp} region combines with energy from the overlap region creating the composite wave that is recorded as the DPOAE.

Therefore, the DPOAE measured in the ear canal is a vector sum of two underlying components, coming from different cochlear locations via different mechanisms of generation. The relative amplitudes and phases of these two components are determined, in part, by stimulus conditions and by subject-related factors. When there is little energy from the CF_{dp} region, the nonlinear distortion energy from the overlap region is predominantly responsible for the level of the emission recorded. In fact, the DPOAE in the ear canal is typically dominated by the distortion component for moderate- and high-level stimuli (Brown et al., 1996). This is why DPOAE amplitude is commonly plotted as a function of f_2 , which approximates the frequency of the overlap region, as it is likely to reflect OHC responses at the f_2 location. Although it is not common, when there is a significant reflection component from the CF_{dp} region, the DPOAE measured in the ear canal will contain OHC responses from both cochlear locations.

4.3.1.3. Maximizing DPOAE generation

DPOAE generation is maximized with ideal overlap between the mechanical disturbances of the traveling waves of the two stimulus tones. This ideal overlap is created when the mechanical interaction between two stimulus tones is optimal with minimal mutual suppression and minimal phase interference between them. Therefore, it can be expected that stimulus frequency ratio would need to be adjusted as a function of frequency and presentation level to generate the maximum distortion amplitude. By modifying DPOAE stimulus frequency ratio to suit known cochlear partition vibration patterns, we allow for the interaction that gives the largest emission response to be determined at a given cochlear place.

In this dissertation, peak or best performance was identifiable when DPOAE levels were plotted as a function of f_2/f_1 , demonstrating the typical bandpass shape that has been reported previously in the literature (Harris et al., 1989; Brown & Gaskill, 1990). The peak of the

bandpass shape represents the f_2/f_1 condition that produced the largest DPOAE level measured at a particular f_2 frequency when presented at a specified stimulus level combination. Around the peak, the general decrease in DPOAE level at narrow stimulus frequency ratios can be modeled to be a consequence of two-tone suppression (Shera et al., 2007) or phase interference between multiple distortion generators (Sisto et al., 2018). In contrast, the decrease in level at wider stimulus frequency ratios is a consequence of greater physical separation between the mechanical activity patterns of the f_1 and f_2 primaries, creating a smaller overlap region for distortion generation (Figure 24).

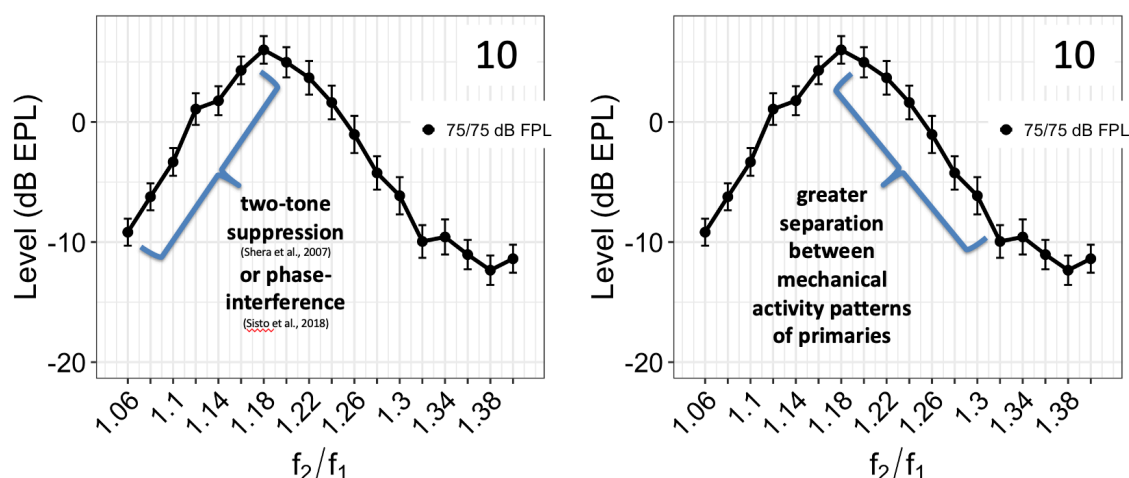


Figure 24. Bandpass shape seen when DPOAE levels are plotted as a function of stimulus frequency ratio

Bandpass shape showing peak performance when DPOAE levels are plotted as a function of stimulus frequency ratio. The peak represents the f_2/f_1 condition that produced the largest DPOAE level measured at 10 kHz when presented at 75 & 75 dB FPL. Around the peak, the general decrease in DPOAE level at narrow stimulus frequency ratios can be modeled to be a consequence of two-tone suppression (Shera et al., 2007) or phase interference between multiple distortion generators (Sisto et al., 2018). The decrease in level at wider stimulus frequency ratios is a consequence of greater physical separation between the mechanical activity patterns of the f_1 and f_2 stimulus tones.

Median DPOAE level as a function of stimulus frequency ratio at an f_2 of 10 kHz when stimulus pairs are presented at 75 & 75 dB FPL. Around the peak, the general decrease in DPOAE level at narrow stimulus frequency ratios can be modeled as a consequence of two-tone suppression (Shera et al., 2007) or phase interference between multiple distortion generators (Sisto et al., 2018). The decrease in level at wider stimulus frequency ratios is a consequence of greater physical separation between the mechanical activity patterns of the f_1 and f_2 tones.

A number of theoretical studies have traced the bandpass behavior of the DPOAE across stimulus frequency ratio to interference effects within the distributed source region (Talmadge et al., 1998; Shera, 2003; Shera et al., 2007). This behavior could be mostly attributed to a compromise between the positive effect of increasing the width of the overlap region and the negative interference among DP wavelets of different phases within the generation region. These observations further suggest that this bandpass shape depends on a single parameter, i.e., the mechanical tuning of the cochlear partition.

Fahey et al. (2006) provided experimental evidence suggesting that the decrease in DPOAE amplitude as the frequency ratio approaches 1 arises primarily from vector cancellation among multiple sources. In addition, measurements of the relative amplitudes of the distortion and reflection components of DPOAEs (e.g., Knight & Kemp, 2000) provide additional experimental evidence for changes in distortion source “directionality” as a function of f_2/f_1 .

4.3.2. Importance of evaluating high frequencies

Common forms of adult-onset hearing loss include those related to aging and ototoxicity. ARHL is a complex condition of auditory degradation representing the end stage sequela of intrinsic (genetic predisposition) and extrinsic (environmental) factors acting in concert over the lifetime of an individual (Schuknecht, 1955). With more people living to older ages, the burden of hearing impairment in society is only expected to increase due to this growth in the older population (Kochkin, 2005a). Ototoxicity is regarded as anything that has a toxic effect on the ear. It commonly is caused by agents such as ototoxic medications, chemotherapies, and excessive noise exposure. SNHL loss due to aging or ototoxic damage, starts by developing in the basal end of the cochlea and progresses towards the apex. Therefore, in the case of identifying ARHL or monitoring for ototoxicity, understanding auditory function at the basal end

of the cochlea, where high frequency information is encoded, is essential for the early detection of progressive or cumulative forms of hearing loss.

Since the damage or dysfunction related to adult-onset hearing losses often progresses from base to apex, evaluating high frequency function would allow for the earliest detection of declining auditory status due to cochlear pathology. Therefore, hearing loss in adults remains under detected as current clinical assessments ignore frequency regions that are affected first in the majority of adult-onset hearing losses. Furthermore, since most forms of adult-onset hearing losses initially effect OHC function in these basal regions, it is essential that a test detects age-related auditory decline early using a tool that accurately and efficiently evaluates OHC function at high frequencies. DPOAEs have the potential to be that tool as they provide an objective and noninvasive measure of OHC function and are popular in both clinical and research settings (Gates & Mills, 2005). However, currently utilized DPOAE measurements methods in clinical settings are limited to measuring at frequencies below 8 kHz (Lonsbury-Martin & Martin, 2003).

The work established here optimizes a popular clinical tool for effective utilization at frequencies where adult-onset auditory dysfunction is first evident. Previously, the adoption of routine tests of auditory function, including DPOAEs, at frequencies above 8kHz remained elusive due to equipment and calibration limitations (International Standards Organization, 1998). With other groups, our lab has developed, validated, and adopted calibration techniques enabling accurate signal delivery (Souza et al., 2014) and OAE recordings (Charaziak & Shera, 2016) up to 20 kHz (Scheperle et al., 2008; Lee et al., 2012). By leveraging these modern techniques of signal delivery and recording, we created a new clinical standard that can be utilized in DPOAE applications for all age groups. In particular, this clinical standard would be most relevant for the most commonly used application of DPOAEs – screening for hearing loss.

4.3.3. Changing the way we screen for hearing loss

There is a principal question that any applied research endeavor should ask before its undertaking: “How can this work inform and improve clinical practice?” Therefore, for this dissertation, we were interested in taking the knowledge gained on how to accurately assess function across the cochlear length in order to improve upon existing clinical assessments. In this case, the most widely used clinical function of DPOAEs – screening for hearing loss. However, this is most often a test only utilized for pediatric populations. Hearing loss is a disorder that constitutes a substantial burden on the adult population in the United States, yet, screening for hearing loss is not routine (Chou et al., 2011). This is perplexing given that hearing loss in adults is encountered in all medical settings and frequently influences medical encounters.

4.3.3.1. Hearing screenings in adults are underutilized

In the United States there are no readily accessible, low-cost hearing screening programs for adults implemented in primary healthcare settings. Instead, the first step to identifying hearing impairment is most often seen in an audiology clinic where the exact magnitude of hearing loss is evaluated using behavioral measures such as pure-tone audiometry and speech recognition. The process for an individual seeking treatment from an audiologist involves (1) self-motivation, (2) often an inquiry with a primary care physician about his or her hearing ability (which is often times done without the healthcare provider asking about it), and (3) an awareness of how to navigate the hearing healthcare environment. All of these factors can be seen as barriers to an individual entering into hearing healthcare which can be detrimental considering the consequences associated with hearing loss.

The importance of early identification becomes clear once the plethora of consequences associated with hearing loss are understood. Hearing loss can impede our ability to respond to

safety warnings, hear and understand healthcare providers, and communicate effectively in our daily life. Hearing loss has been associated with increase in the risk of falls, hospitalization, cognitive decline, and poor self-reported health (Berkman et al., 2000; Lin et al., 2011; Lin et al., 2013; Wallhagen et al., 2008). There are societal costs to communication difficulties due to hearing loss including increased likelihood of social isolation, stigmas, and other healthcare-related associations (e.g., co-occurring or new onset conditions). Financial burdens can result from lost earnings, low productivity, the inability to secure and maintain employment, the need for premature retirement, and disability costs associated with hearing loss (Hong et al., 2013; Kochkin, 2005b; Jung & Bhattacharyya, 2012; WHO, 2017). Interestingly, the financial burden of hearing loss is likely underestimated – mainly because screening for hearing loss is underutilized resulting in an undetermined number of people affected.

Although these negative health- and financial-related associations of undetected and, thus, untreated hearing loss are expected to be significant, hearing screening is still not a routine component of primary care. The United States Preventative Services Task Force acknowledges the importance of identification and treatment of hearing loss for older adults but has stated that there is inadequate evidence to determine the balance of benefit and harm of screening for hearing loss in asymptomatic individuals (Chou et al., 2011). Despite this, the Department of Health and Human Services, American Speech-Language-Hearing Association, National Academies of Sciences, Engineering and Medicine, and systematic reviews recommend older adults be screened for hearing loss (Yueh et al., 2003; American Speech-Language Hearing Association, 2011; National Academies of Sciences, Engineering, and Medicine, 2016).

4.4.3.2. Benefits of early identification

Early identification and intervention for hearing loss can prevent the known negative cognitive, emotional, social, behavioral, and socioeconomic consequences of hearing impairment (Bess et al, 1989; Mulrow et al, 1990; LaForge et al., 1992; Carabellese et al., 1993; Appollonio et al., 1996; Heine et al., 2002; Dalton et al; 2003; Gates et al., 2005; Kochkin, 2010). For many losses, hearing aids or assistive listening devices may be an ideal option for intervention.

Benefits of early intervention have been reported in hearing aid users as better physical, emotional, mental, and social well-being compared to matched controls that did not use hearing aids (Kochkin, 2010, Cruickshanks et al., 2010). In a study by Simpson et al. (2016), the burden of hearing loss among adults was found to be mitigated with appropriate care. They found that negative health-related effects of hearing loss may manifest earlier than is generally recognized and may affect use of healthcare across the continuum of care. Even in middle-aged individuals, hearing loss can become costly for large numbers of adults unless early, appropriate intervention is undertaken, which may then prevent future hearing-related disabilities and decreased quality of life.

Another advantage to hearing screening comes from the opportunity to close the gap between identification of dysfunction and acceptance of treatment. Studies have found that the average adult will wait 6 to 9 years after the identification of hearing loss before seeking treatment (Kochkin, 2010; Simpson et al., 2019). While this gap between disease and treatment onset is certainly deleterious to the effectiveness of today's treatments (e.g., amplification), closing this gap will be even more critical in the future when molecular and genetic treatments for hearing loss become available. Additionally, early detection and effective monitoring of hearing status would have major implications for hearing conservation purposes, allowing the

patient to make lifestyle changes that have been shown to reduce the risk and progression of hearing loss (Cruickshanks et al., 2010; Zhan et al., 2011). Thus, the importance of an accurate and effective probe of function at the cochlear base is expected to only increase with time as other, medically advanced options for prevention and treatment of hearing loss become available.

4.4.3.3. Improving outcomes by increasing the access and accuracy of hearing screenings

In an ideal situation where hearing screenings are implemented into primary care, those who fail a screening could then be appropriately informed by a healthcare provider on how to navigate his/her hearing healthcare needs. Depending on the screening results, either continued or more frequent screenings might be recommended or referral for diagnostic testing may be given. If the patient does not have hearing concerns and the screening results indicate decline solely in the extended high frequencies, then monitoring the rate of decline could be essential to following exactly when the hearing loss becomes severe enough to warrant intervention. Alternatively, if the failed screening is more widespread, an immediate referral can be given to undergo diagnostic testing by an audiologist to confirm, characterize, and quantify the hearing loss and develop a plan for accommodations or treatment.

Employing DPOAEs for early identification of hearing loss makes sense as they are objective, noninvasive, and directly evaluate the vulnerable OHCs. The main question of this dissertation asked: Is our current standard for DPOAE hearing screenings good enough? We contested that the current clinical test performance is far from ideal. First, the use of non-optimized test stimuli was likely one factor contributing to this malperformance. Second, the lack of extended high frequency evaluation, where the most common forms of adult-onset hearing loss begin, is unacceptable. While there have been attempts to utilize optimized, frequency-specific DPOAE stimuli for the purposes of hearing screening (Johnson et al., 2010),

this is the first to show improved performance of frequency-specific stimuli while also incorporating a frequency range beyond 8 kHz. Establishing a protocol for accurate high frequency evaluation was an especially important portion of the dissertation as the cochlear base is most sensitive to dysfunction related to aging and ototoxicity and, thus, a critical region to be monitoring for onset and progression SNHL in adults.

Although this dissertation was not designed to answer on the feasibility of implementing adult hearing screenings in health care settings, it is hard not to see the benefits that can come from utilizing optimized DPOAE methods for this purpose. DPOAEs can be tested in a way that is automated, allowing for testers without advanced degrees to be able to execute the measurements, while having a non-behavioral response requirement, allowing for evaluation of difficult to test populations (such as children, those with low-cognitive ability or dementia, malingerers, etc.). Taken together, these benefits make it desirable to fully exploit DPOAE responses, so they can assess auditory status while being an ideal tool for widespread use. Lastly, using the optimal hearing screening protocol established in Chapter 3 (Figure 23), there is potential for the accuracy of hearing screenings to be improved while evaluating up to the highest frequencies of human hearing. These innovations are especially important as accurate and extensive measurements using DPOAEs would allow for a fully realized progression of care for the individual.

4.4. Limitations

The primary limitation of the present work was the inclusion of a relatively small and homogeneous study population. This restricted the age and gender-related conclusions that could be drawn. Although it is important to note that this project was not designed with the intention of characterizing age or gender differences. In fact, limiting the age range of participants was

desired in order to reduce the number of variables influencing the measurements. In the future, inclusion of a larger study population in a validation study would aid in defining the variability in the responses and identify outlying individuals. Unfortunately, the demanding and time-consuming nature of the current experiments necessarily limited the number of participants involved.

On a related note, this work was also limited in the inclusion of varying degrees and configurations of SNHL. The importance of this restriction can be understood in light of the ROC analysis conducted in Chapter 3 in order to identify the stimulus parameters most accurate at identifying hearing loss. Limiting the SNHL participants into a specific age range was intentional in order to closely age-match the normal-hearing participants. However, doing this made it difficult to recruit a large sample of participants that had varying configurations of hearing loss so that enough mild degrees of hearing loss could be represented across test frequencies.

A technical limitation of this work came from the span of stimulus parameters that were investigated. During project development, we knew that it would not be feasible to evaluate every possible stimulus frequency ratio and level combination that could produce cochlear distortion products. Instead, we made the strategic decision to reduce the number of stimulus conditions while also evaluating across a wide span of frequency ratio and level conditions that have been shown previously to produce DPOAE responses in normal hearing ears. Because of these gaps in the data collected, it is possible that the exact stimulus condition that produced the true peak performance was missed. However, since there was a small stimulus frequency ratio step size (of 0.02), if the true peak performance was missed, it would have only been missed by 0.01. However, one could argue that the precise f_2/f_1 is not critical given the broad tuning of the

operating curves see in Figure 22. The step size for the stimulus presentation levels were slightly bigger (10 dB L1 step size). In order to combat this, future work will focus on performing DPOAE input/output functions that use a level swept measurement paradigm in order to obtain a finer resolution of presentation levels.

Lastly, some could argue that the lack of DPOAE source component separation was a limitation of this work. However, the intention of this project was to be a first step in a line of investigation into place specific DPOAE measurements. This dissertation was geared towards finding methodological improvements that could be translated first and quickly into real-world applications, which currently measure the composite DPOAE. Furthermore, clinical settings that utilize DPOAE measurements will predominantly see patients that are less likely to have a strong reflection component. Ears with strong distortion and reflection components are typically only seen in pristine human ears (i.e., young and normal hearing). In those rare individuals, the strong reflection component would increase the fine structure, thus, creating the potential for a DPOAE measurement to be made at a deep amplitude minimum. However, when even a small degree of wear-and-tear happens to the human ear (e.g., from aging or noise exposure), the reflection component has been seen to nearly disappear leaving, essentially, the distortion component from the overlap region to be measured (Poling et al., 2014). Lastly, for this project, DPOAE sweeps were third-octave band averaged in order to avoid inaccurate cochlear assessments due to constructive or destructive interference from the interaction of source components.

4.5. Future work

4.5.1 Generalizability

If the results of a study are broadly applicable to many different types of people or situations, the study is said to have good generalizability. Hearing loss is the most common form

of sensory impairment in humans, affecting 360 million worldwide (Besser et al., 2018). The main causes of SNHL are associated with aging, noise exposure, exposure to therapeutic drugs that have ototoxic side effects, genetic mutations, and chronic conditions. Many of these degenerative forms of hearing losses can be first identified with the implementation of an accurate DPOAE hearing screening protocol in primary care or other healthcare settings. By gathering the information from these hearing screenings of the general population that is seeking hearing healthcare, our understanding of the impact of SNHL will increase exponentially. This could be a ground-breaking step towards establishing a baseline understanding of cochlear function by accurately quantifying DPOAE responses in a much wider sample of the general population.

4.5.1.1 Aging

Hearing ability decreases with age. In fact, age is the strongest predictor of hearing loss among adults aged 20-69, with men being almost twice as likely as women to have hearing loss (Hoffman et al., 2016). ARHL or presbycusis is an important public health concern as it is one of the most common chronic conditions and the most common sensory deficit affecting aging adults (Bowl & Dawson, 2018). Disabling hearing loss has been reported in about 2 percent of adults aged 45 to 54, 8.5 percent aged 55 to 64, 25 percent aged 65 to 74, and 50 percent of those 75 and older. Because of the increasing aging population in the United States and other developed countries, the burden of hearing impairment in society is expected to increase, making it an increasingly prevalent disability as time goes on (Kochkin, 2005a).

ARHL is a complex condition of auditory degradation representing the end stage sequela of intrinsic (genetic predisposition) and extrinsic (environmental) factors acting in concert over the lifetime of an individual (Schuknecht, 1955). This process begins physiologically as early as

the fourth decade of life and is first manifested as impairments in cochlear function at the highest frequencies of hearing (Lee et al., 2012; Poling et al., 2014). Age-related morphological changes have been shown in the cochlea in the hair cells, auditory nerve, and stria vascularis (Schuknecht & Gacek, 1993). Therefore, the etiology of presbycusis can be complex and multifactorial. Risk factors can be divided into four categories: cochlear aging (due to increasing amounts of free radicals), environment (e.g., noise exposure, ototoxic medications), genetic predisposition (e.g., sex, ethnicity, genetic variants), and medical comorbidities (e.g., hypertension, diabetes, stroke, tobacco use) (Yamasoba et al., 2013).

Declining behavioral hearing thresholds in the high frequencies have historically been the marker of ARHL. As shown in Figure 4A, age-related change from the youngest age group (of 10-21 years) to the oldest age group (of 55-68 years) describes how behavioral hearing threshold declines first in the highest frequencies and then progresses gradually to lower and lower frequencies with age. However, a shift in behavioral hearing threshold is often not the first sign on age-related decline.

DPOAEs provide a means of identifying the first signs of ARHL in the vulnerable OHCs as a result of cochlear dysfunction. Since ARHL is primarily a result of sensory cell damage or dysfunction in the cochlea (Wu et al., 2020), DPOAEs are an ideal alternative to behavioral threshold testing as they are the by-product of the nonlinear sound amplification process in the cochlea and hence can serve as a measure for evaluating cochlear integrity. DPOAE plotted as a function of frequency shows age-related decline in the same high frequencies as behavioral thresholds as well as at lower frequencies (Figure 4B). In fact, even within the limited age range of participants evaluated this dissertation, we observed DPOAEs to be sensitive to age-related

changes in cochlear function (Figure 25). Thus, DPOAEs have great diagnostic potential because they are sensitive to the earliest signs of cochlear aging (Poling et al., 2014; Stiepan et al., 2019).

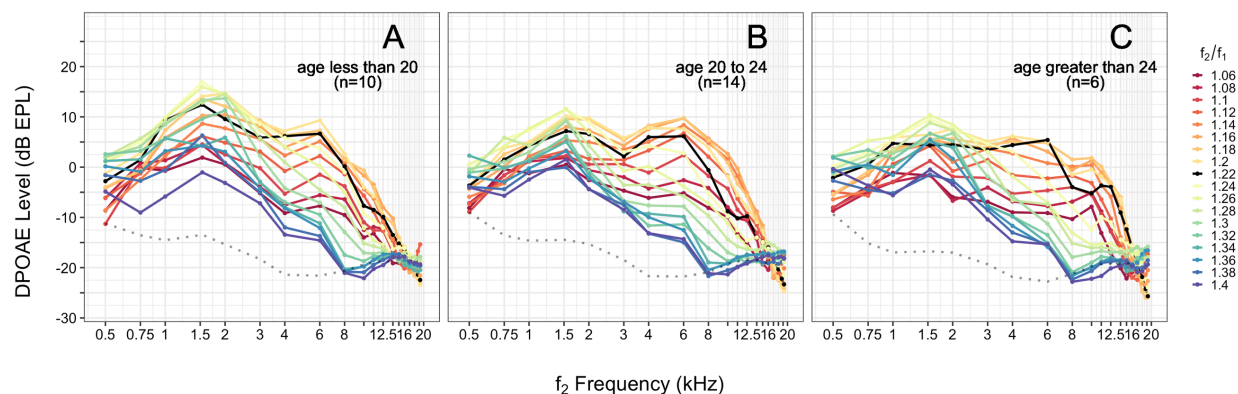


Figure 25. Median DPOAE level as a function of f_2 frequency for three different age groups

Median DPOAE level as a function of f_2 frequency from the audiometrically normal-hearing participants in this dissertation. Participants were separated into three age groups (indicated by panel label in upper right corner) in order to show aging effects.

4.5.1.2 Ototoxic medications

Various chemicals and drugs adversely affect the auditory system. The main ototoxic medications in clinical use are aminoglycoside antibiotics and cisplatin, both of which are toxic to sensory hair cells. There is no question that it is important to try and prevent ototoxicity because the adverse effects of the medications producing irreversible hearing loss. However, many of these ototoxic medications are treatments for life-threatening diseases, particularly the chemotherapeutic ones, and hence cause hearing impairment because of their innate toxicity.

Some of the aminoglycoside class of antibiotics (e.g., gentamicin, streptomycin, or kanamycin) are the most powerful ototoxic drugs in general therapeutic use. Hearing loss develops in approximately 20% of patients receiving aminoglycoside antibiotics (Forge & Schacht, 2000; Duggal & Sarkar, 2007), and the prevalence is as high as 56% among patients with cystic fibrosis (Garinis et al., 2017; Al-Malky et al., 2015), a population exposed to repeated courses of aminoglycoside therapy. Aminoglycosides appear to generate free radicals within the

inner ear which cause subsequent permanent damage to sensory cells and neurons, resulting in permanent hearing loss (Selimoglu, 2007). As aminoglycosides are indispensable agents both in the treatment of infections and Meniere's disease, a great effort has been made to develop strategies to prevent aminoglycoside ototoxicity.

Among adults who have received the antitumor agent cisplatin, clinically significant hearing loss has been shown to develop in approximately 60% of patients with testicular cancer (Frisina et al., 2016) and 65% of patients with head and neck cancer (Theunissen et al., 2014). Certain antitumor agents (e.g., cisplatin or carboplatin) show evidence that the drug blocks the MET process of the OHCs leading to cytotoxicity within the affected OHCs (McAlpine & Johnstone, 1990). The resulting imbalance in the ionic environment of the cell affects the metabolic enzyme system and eventually results in fatal morphological damage to the receptor presenting as permanent hearing loss.

Irreversible injury and/or destruction of crucial structural elements within the cochlea by ototoxins initially occur to the OHCs in the base. The damage systematically progresses along the organ of Corti both apically and laterally to the inner hair cells as dosage and frequency of treatment continues (Wright & Schaefer, 1982). Examination of the ultrastructure of the temporal bones from patients treated with ototoxic drugs confirms the primary site of ototoxicity initially to be the OHCs at the basal turn of the cochlea (Wright & Schaefer, 1982; Strauss et al., 1983). The greater vulnerability of basal OHC may arise because of lower antioxidant defenses in the OHCs (Sha et al., 2001). Further support of oxidative damage comes from studies that have shown antioxidants to provide some protection (for review, see Rybak et al., 2007; Sheth et al., 2017).

A major problem with predicting potential ototoxicity is that it depends on a number of patient-specific factors including the status of renal function, age, length and dose of treatment, and interactions with other medications and treatment modalities. Thus, the only certain method of preventing incapacitating ototoxicity is to detect it as early as possible in the treatment regimen so that medications can be substituted, doses changed, and/or the mode of administration altered. In this manner, the spread of ototoxic effects can be halted before they progress to involve the middle to low frequencies that are especially crucial for effective human communication. The choice between hearing impairment and death is what makes such risky treatments necessary. However, with increasing survival rates, particularly with respect to oncological disease, prevention and early detection of ototoxicity is important for providing effective management options. Therefore, a discerning awareness of the consequent levels of exposure to damaging treatments is necessary to reduce risk, limit actual loss, and facilitate management for the patient whose hearing is adversely affected.

The most effective protocol for identifying the onset of ototoxicity is the monitoring of hearing sensitivity in patients receiving ototoxic medications. For use as an ototoxicity monitor, audiometric testing depends on intra-subject comparisons so that each patient serves as his or her own control at baseline. Thus, to document the ototoxic effects of drug therapy, it is necessary to perform quantitative observations of auditory function systematically during treatment.

Since the essential damage induced by the above-mentioned ototoxic compounds most often concerns the basal regions of critical cochlear components, it is advantageous to use measures of DPOAEs as a monitoring tool to assess pre- and post-treatment effects. DPOAEs, specifically, would be preferable over other emission measures, such as TEOAEs, because DPOAEs provide more accurate high frequency results (Gorga et al., 1993a). Perhaps of most

interest is the greater sensitivity of DPOAEs compared to behavioral hearing thresholds to cochlear damage resulting from ototoxicity (Littman et al., 1998). In this sense, DPOAEs may be predictive, foretelling a substantial threshold shift for a given frequency prior to a measurable sensitivity loss. This “predictive” drop in DPOAE is likely reflecting the progression of cochlear damage or dysfunction. Thus, at the initial stage of ototoxicity, the agents may only damage one or two rows of OHCs, affecting DPOAEs but not threshold sensitivity. Subsequently, as the drugs damage the remaining OHCs in that cochlear region, pure-tone hearing sensitivity is reduced. This further supports the need for more accurate DPOAE measurements that use frequency-specific stimuli as emission levels will, thus, accurately quantify OHC function. Warning of impending hearing loss is incredibly useful for the oncologist, who might have the option of adjusting the treatment to a potentially less ototoxic regimen. Likewise, early indicators of auditory decline would be useful for planning audiologic management and counseling. Therefore, test protocols that use DPOAEs have promise to sensitively detect the onset and progression of such treatment-related hearing loss.

4.5.1.3. Acoustic trauma

Noise exposure is responsible for approximately 10% of hearing loss in adults, most notably affecting military veterans (Gordon et al., 2016). In the mildest cases of acoustic trauma, the stereocilia of OHCs can be slightly splayed and tip links broken, while the rootlets of the stereocilia become less dense in transmission electron micrographs (Liberman & Dodds, 1987; Clark & Pickles, 1996). In more severe cases, leading to permanent damage, the stereocilia kink or fracture at the rootlet and the packed actin filaments, which give stereocilia their rigidity, depolymerize (Liberman & Dodds, 1987). The links between the stereocilia break and the stereocilia separate widely, with loss of tip links and consequent loss of transduction. In other

cases, the stereocilia become fused, bent, splayed apart, or detached. In very severe acoustic trauma, such as blast noise, the whole organ of Corti can be ripped apart mechanically (Patterson & Hamernik, 1997).

Intracellularly, hair cells show changes associated with metabolic stress, including breakdown of internal structures and swelling and disruption of mitochondria, which can be expected to lead to cell death over hours or days (Lim, 1986). As with ototoxicity, oxidative damage may contribute to cell death, since enhanced levels of reactive oxygen species have been identified in hair cells after acoustic overstimulation (for review, see Henderson et al., 2006). The reactive oxygen species are likely to have been produced by impaired oxidation in partially damaged mitochondria.

Decreased DPOAEs can be seen immediately following the acoustic trauma. Although the DPOAEs are found to recover in cases of temporary noise-induced hearing loss, this can signal to the clinician that a decline occurred and could be consistent with other pathologies related to noise exposure (e.g., synaptopathy). By making DPOAE testing more accessible, following either a temporary or permanent noise-induced hearing loss event, individuals can be screened immediately following exposure, especially if hearing screenings become accessible in primary care settings in the future. This could then allow for the serial monitoring of such exposure events in order to chronicle a detailed history of noise-induced hearing loss. In addition to the counseling and preventative measures that can be given to the patient, this could open the door for a mammoth opportunity in research efforts to more accurately characterize noise-induced hearing loss in humans.

4.5.2. DPOAE input/output functions

The objective, automated, and time-conserving nature of DPOAE testing makes this diagnostic tool especially valuable when providing hearing healthcare. Furthermore, these benefits make it desirable to exploit DPOAE responses for other uses such as predicting degree of auditory function. However, DPOAE measurements have been used almost exclusively in a dichotomous decision as to whether hearing is normal or impaired, without regard to the magnitude of the hearing loss (e.g., Gorga et al., 1993b; Gorga et al., 1997, 1999, 2000, 2003, 2005; Dorn et al., 1999; Kim et al., 1996; Stover et al., 1996; Gaskill et al., 1993; Johnson et al., 2007, 2010).

The dynamic range of DPOAE responses can be seen using input/output functions which plot the DPOAE level as a function of stimulus-tone level for a selected f_2 frequency. These functions have the potential to (1) provide a lowest level of DPOAE detection, allowing for an estimate of behavioral threshold, and (2) provide a rate of growth with stimulus level change, allowing for characterization of the compressive nature of the cochlear amplifier. In the case of cochlear hearing loss, DPOAE input/output functions could also be used as a tool to predict loudness growth (i.e., to indicate recruitment) (Neely et al., 2003). When cochlear damage exists that affects OHC function, DPOAE thresholds have been elevated and nonlinear behaviors have been reduced or eliminated (e.g., Dallos et al., 1980). Quantifying auditory threshold and recruitment using DPOAEs are of particular interest as an audiometric tool as they can serve as important indicators of (1) auditory function and (2) input parameters for hearing aid fitting, especially in young children.

Using the data collected from the normal-hearing participants in this dissertation, one can already foresee the potential ramifications of an investigation into the most appropriate stimulus

parameters when evaluating DPOAE input/output functions. Figure 26 shows DPOAE input/output functions across participants and plotted as separate panels for each f_2 frequency in kHz. From these plots, we see how different frequency ratios at varying stimulus levels produce different DPOAE outputs. This shows how the shape of the input/output function could change across stimulus condition thus giving a different interpretation of cochlear amplifier function. Additionally, at the lowest stimulus levels, an optimal frequency ratio will likely produce a DPOAE threshold that will be more accurate at predicting behavioral threshold. These benefits make it desirable to fully exploit DPOAE responses, so they can provide a more comprehensive look into cochlear function using stimulus parameters that best reflect function.

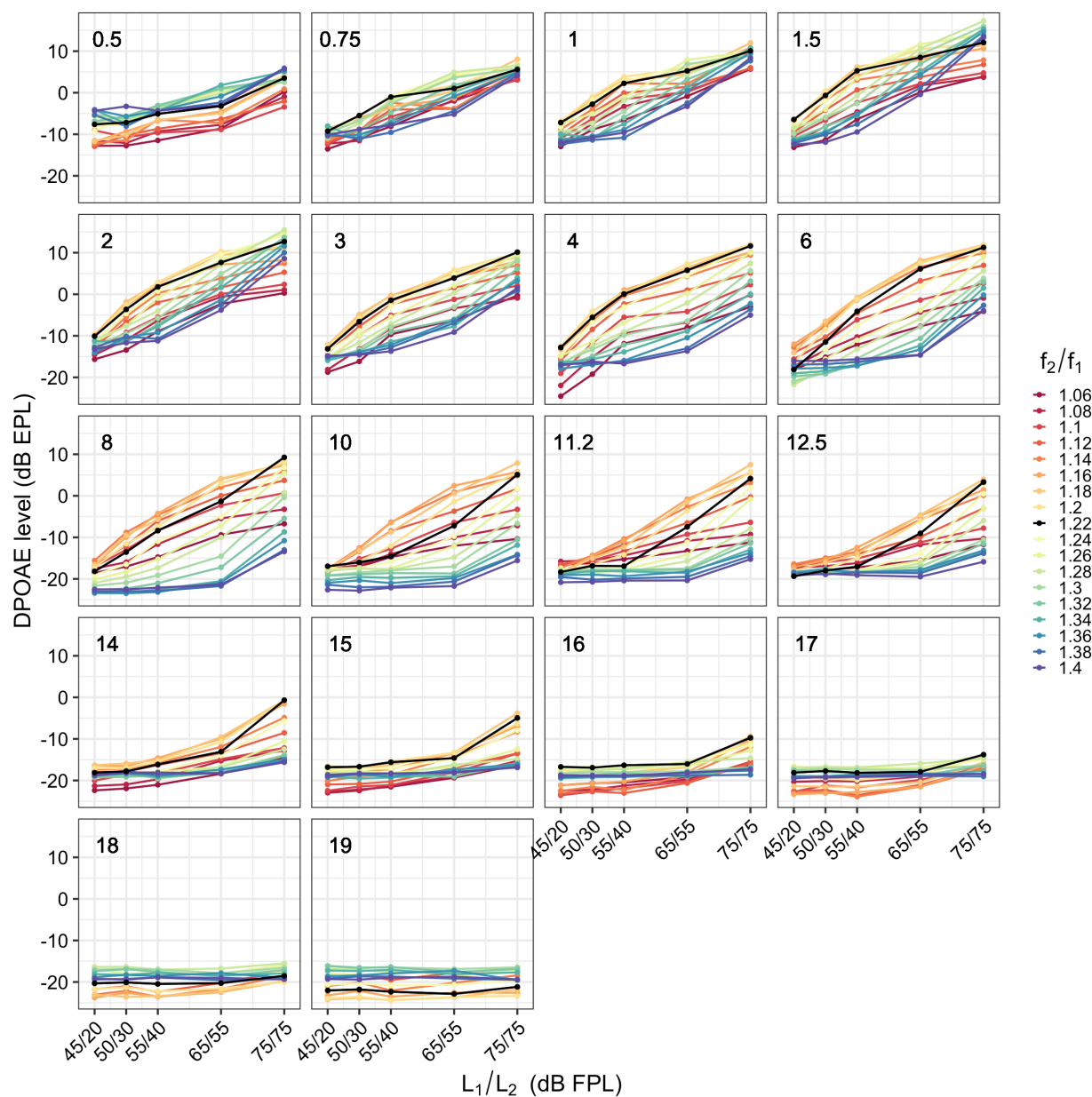


Figure 26. DPOAE input/output functions for 18 different f_2 frequencies

Median DPOAE level from normal-hearing participants plotted as a function of stimulus presentation levels for f_2 frequencies ranging from 0.5 to 19 kHz (f_2 frequency indicated by the label in the upper left of panel). Each f_2/f_1 condition is indicated by line color.

4.5.3. Separating DPOAE source components

When fine frequency resolution measurements are obtained, a pattern of, somewhat, regularly spaced amplitude minima and maxima is revealed known as fine structure. An example of DP-gram showing fine structure from a participant in this project can be seen in Figure 3. This

quasi-periodic amplitude variation can vary by as much as 20 dB peak-to-peak. Fine structure has been observed in fine resolution recordings of all types of evoked OAEs and behavioral thresholds (Talmadge et al., 1998; Poling et al., 2014; Dewy & Dhar, 2017). In the case of DPOAEs, the fine structure arises from the constructive and destructive interference of the components from the overlap and CF_{dp} regions due to the inherently different phase properties. As a result, fine structure is observed in the composite DPOAE signal.

Fine structure has previously been identified as a potential limitation to the diagnostic utility of DPOAEs (Shaffer et al., 2003; Dhar & Shaffer, 2004; Shera, 2004; Shaffer & Dhar, 2006). The argument is that the natural variation in DPOAE level, as a result of the interaction between the two source components, limits the correlation between DPOAE level and hearing thresholds. In this dissertation, one-third-octave band averaging was used which attempts to control the potential effect of this constructive and destructive interference. However, a limitation to this averaging is that the frequency specificity is not as fine as compared to that when a behavioral threshold is found to a presenting pure tone. Instead of performing this averaging, a solution to matching the frequency-specificity of a behavioral threshold with a DPOAE could be attained instead from separating out the DPOAE source components. In separating out the underlying components, the relationship between behavioral hearing threshold and DPOAE distortion component level, rather than composite level, would likely provide an improved estimation of hearing threshold at that place of the overlap region (i.e., near the f_2 frequency place).

Other studies have measured the DPOAE coming from a single generator (at the overlap region) in the hopes that DPOAE amplitude would be more closely correlated with behavioral thresholds. However, using a suppressed and unsuppressed CF location condition, Dhar &

Shaffer (2004) found correlations of behavioral thresholds to the DPOAE generator component to not be improved when compared to correlations observed in an unsuppressed condition of the reflection component. Correlations between hearing thresholds and DPOAE levels did not show an improvement using either the iFFT or a low-pass filtering method when compared to the composite level (Shaffer & Dhar, 2006). However, one critical limitation of these studies was that stimulus parameters used to evoke the DPOAEs were not optimized for the measurement frequency. Future work stemming from this dissertation would utilize DPOAE stimulus frequency ratios that are optimized for the cochlear place of stimulation in order to correlated behavioral hearing threshold with the DPOAE distortion component level.

Another way to exploit the differing OAE generation mechanisms can be for the purpose of differential diagnosis of cochlear pathology. As has been seen with aging, DPOAEs decline with age while SFOAEs appear to be maintained, suggesting that a dual-emission approach may be useful for differential diagnosis of ARHL (Abdala et al., 2018; Ortmann & Abdala, 2016; Hoth et al., 2010; Dorn et al., 2001; Stiepan et al., 2019). As a next step, measuring the DPOAE distortion component using place-specific stimulus parameters would allow for a more detailed look into the similarities and differences between generation mechanisms in the aging ear.

4.5.4. Individualized optimal stimuli for DPOAE recordings

Findings from this this dissertation led to the identification of optimized measurement methods based on the quantification of normal and impaired cochlear function across a sample of human ears. Collectively, these optimizations were found to improve DPOAE measurements in adults when compared to stimulus conditions typically used in clinical and research settings (L_1 & $L_2 = 65$ & 55 dB SPL, $f_2/f_1 = 1.22$). Another important finding came from the analysis of DPOAE recordings – individual variation in optimal stimulus parameters exists (see Figure 15

and Figure 19 for examples). Although the findings from this dissertation shed light on the expected performance in the average individual, the optimal measurement protocols detailed in Chapter 2 for normal hearing ears and in Chapter 3 for hearing screening are not necessarily the exact optimal stimuli for every individual ear.

Why would there be individual variation in stimulus parameters that produce the largest DPOAE response? First, the anatomical and physiological characteristics of passive cochlear mechanics depend on the size and shape of the cochlea itself. Therefore, it stands to reason that individual variation in the physical properties of the cochlea will also be reflected in the stimuli that best exploit DPOAE responses for that cochlea. Second, varying degrees of cochlear function, or dysfunction, influence the stimulus parameters that produce the largest DPOAE responses to accurately reflect cochlear status. In the case of ears with SNHL (as is seen in Figure 19), higher stimulus levels and wider frequency ratios were needed in order to accurately assess cochlear function compared to the normal-hearing ears.

In the future, studies could establish methods for individualized, optimal stimulus parameters to be undertaken before diagnostic testing in order to be certain of an accurate evaluation of cochlear function. Utilizing the concurrent sweep paradigm described in this dissertation, multiple DPOAE sweeps could be presented simultaneously with the goal of performing a quick search for the customized, place-specific frequency ratios for that individual. These measurements for determining individualized optimal stimuli would happen immediately following in-ear calibration and precede diagnostic DPOAE evaluation.

4.6. Conclusions

This dissertation leverages the latest developments in calibration and measurement techniques to develop a DPOAE measurement system that is optimized based on local cochlear

properties. These optimizations in combination are expected to improve DPOAE test performance significantly positioning this new test as an important and accessible tool for early detection of auditory decline in adult populations. The direct clinical implications are significant as we propose to improve a well-accepted clinical tool that can be automated for widespread deployment. Additionally, the need for early and accurate detection of cochlear decline will only become more important as the promise of molecular, stem cell, and gene therapies become a reality.

The sheer reality that a response to two tones could create such a complex, yet vast understanding of the inaccessible human cochlea is endlessly fascinating while also leaving provoking follow-up questions that yearn to be answered. These yet unanswered questions regarding the mechanisms of OAE generation and propagation will continue to fuel a recognizable persistence that drives research: a quest for the complete truth.

REFERENCES

- Al-Malky, G., Dawson, S. J., Sirimanna, T., Bagkeris, E., & Suri, R. (2015). High-frequency audiometry reveals high prevalence of aminoglycoside ototoxicity in children with cystic fibrosis. *Journal of cystic Fibrosis*, *14*(2), 248-254.
- Abdala, C. (1996). Distortion product otoacoustic emission ($2f_1 - f_2$) amplitude as a function of f_2/f_1 frequency ratio and primary tone level separation in human adults and neonates. *The Journal of the Acoustical Society of America*, *100*(6), 3726-3740.
- Abdala, C., Luo, P., & Shera, C. A. (2015). Optimizing swept-tone protocols for recording distortion-product otoacoustic emissions in adults and newborns. *The Journal of the Acoustical Society of America*, *138*(6), 3785-3799.
- Abdala, C., Ortmann, A. J., & Shera, C. A. (2018). Reflection-and distortion-source otoacoustic emissions: Evidence for increased irregularity in the human cochlea during aging. *Journal of the Association for Research in Otolaryngology*, *19*(5), 493-510.
- Agrawal, Y., Platz, E. A., & Niparko, J. K. (2008). Prevalence of hearing loss and differences by demographic characteristics among US adults: data from the National Health and Nutrition Examination Survey, 1999-2004. *Archives of internal medicine*, *168*(14), 1522-1530.
- Ahmed, H. O., Dennis, J. H., Badran, O., Ismail, M., Ballal, S. G., Ashoor, A., & Jerwood, D. (2001). High-frequency (10–18 kHz) hearing thresholds: reliability, and effects of age and occupational noise exposure. *Occupational Medicine*, *51*(4), 245-258.

- American National Standards Institute (ANSI). *Maximum Permissible Ambient Noise Levels for Audiometric Test Rooms: ANSI S3.1-1999*. New York, NY: American National Standards Institute; 1999.
- Appollonio, I., Carabellese, C., Frattola, L., Trabucchi, M. (1996). Effects of sensory aids on the quality of life and mortality of elderly people: a multivariate analysis. *Age Ageing*, 25, 89-96.
- Ashmore, J. (2008). Cochlear outer hair cell motility. *Physiological reviews*, 88(1), 173-210.
- Békésy, G. von (1960). *Experiments in Hearing* (McGraw-Hill Book, New York).
- Bell, A., & Fletcher, N. H. (2004). The cochlear amplifier as a standing wave: "Squirting" waves between rows of outer hair cells?. *The Journal of the Acoustical Society of America*, 116(2), 1016-1024.
- Berkman, L. F., Glass, T., Brissette, I., & Seeman, T. E. (2000). From social integration to health: Durkheim in the new millennium. *Social science & medicine*, 51(6), 843-857.
- Bess, F.J., Lichtenstein, M.J., Logan, S., Burger, M., Nelson, E. (1989) Hearing impairment as a determinant of function in the elderly. *J Am Geriatric Soc*, 37:123-128.
- Besser, J., Stropahl, M., Urry, E., & Launer, S. (2018). Comorbidities of hearing loss and the implications of multimorbidity for audiological care. *Hearing research*, 369, 3-14.
- Bland, J. M., & Altman, D. (1986). Statistical methods for assessing agreement between two methods of clinical measurement. *The lancet*, 327(8476), 307-310.
- Boege, P., & Janssen, T. (2002). Pure-tone threshold estimation from extrapolated distortion product otoacoustic emission I/O-functions in normal and cochlear hearing loss ears. *The Journal of the Acoustical Society of America*, 111(4), 1810-1818.

- Brown, A. M., & Gaskill, S. A. (1990). Measurement of acoustic distortion reveals underlying similarities between human and rodent mechanical responses. *The Journal of the Acoustical Society of America*, 88(2), 840-849.
- Brown, A. M., Gaskill, S. A., & Williams, D. M. (1992). Mechanical filtering of sound in the inner ear. *Proceedings of the Royal Society of London. Series B: Biological Sciences*, 250(1327), 29-34.
- Brown, A. M., Harris, F. P., & Beveridge, H. A. (1996). Two sources of acoustic distortion products from the human cochlea. *The Journal of the Acoustical Society of America*, 100(5), 3260-3267.
- Brown, A. M., McDowell, B., & Forge, A. (1989). Acoustic distortion products can be used to monitor the effects of chronic gentamicin treatment. *Hearing research*, 42(2-3), 143-156.
- Brown, A. M., Sheppard, S. L., & Russell, P. T. (1994). Acoustic distortion products (ADP) from the ears of term infants and young adults using low stimulus levels. *British journal of audiology*, 28(4-5), 273-280.
- Brownell, W. E. (1990). Outer hair cell electromotility and otoacoustic emissions. *Ear and hearing*, 11(2), 82.
- Brownell, W. E., Bader, C. R., Bertrand, D., & De Ribaupierre, Y. (1985). Evoked mechanical responses of isolated cochlear outer hair cells. *Science*, 227(4683), 194-196.
- Brundin, L., Flock, A., & Canlon, B. (1989). Tuned motile responses of isolated cochlear outer hair cells. *Acta Oto-Laryngologica*, 108(sup467), 229-234.
- Brundin, L., & Russell, I. (1994). Tuned phasic and tonic motile responses of isolated outer hair cells to direct mechanical stimulation of the cell body. *Hearing research*, 73(1), 35-45.

- Buus, S., Obeling, L., Florentine, M., Breebart, A. J. M., & Houtsma, A. (2001). Can basilar-membrane compression characteristics be determined from distortion-product otoacoustic-emission input-output functions in humans?. *Physiological and Psychophysical Bases of Auditory Function*, 373-381.
- Carabellese, C., Appollonio, I., Rozzini, R., Bianchetti, A., Frisoni, G.B., Frattola, L., Trabucchi, M. (1993). Sensory impairment and quality of life in a community elderly population. *J Am Geriatr Soc.*,41, 401- 407.
- Charaziak, K., & Shera, C. (2016). Removing effects of ear-canal acoustics from measurements of otoacoustic emissions. *The Journal of the Acoustical Society of America*, 139(4), 2074-2074.
- Charaziak, K. K., & Siegel, J. H. (2015). Tuning of SFOAEs evoked by low-frequency tones is not compatible with localized emission generation. *Journal of the Association for Research in Otolaryngology*, 16(3), 317-329.
- Chen, F., Zha, D., Fridberger, A., Zheng, J., Choudhury, N., Jacques, S. L., ... & Nuttall, A. L. (2011). A differentially amplified motion in the ear for near-threshold sound detection. *Nature neuroscience*, 14(6), 770.
- Christensen, A. T., Ordoñez, R., & Hammershøi, D. (2015). Stimulus ratio dependence of low-frequency distortion-product otoacoustic emissions in humans. *The Journal of the Acoustical Society of America*, 137(2), 679-689.
- Cooper, N. P., & Rhode, W. S. (1992a). Basilar membrane mechanics in the hook region of cat and guinea-pig cochleae: sharp tuning and nonlinearity in the absence of baseline position shifts. *Hearing research*, 63(1-2), 163-190.

- Cooper, N. P., & Rhode, W. S. (1992b). Basilar membrane tonotopicity in the hook region of the cat cochlea. *Hearing research*, 63(1-2), 191-196.
- Cooper, N. P., Vavakou, A., & van der Heijden, M. (2018). Vibration hotspots reveal longitudinal funneling of sound-evoked motion in the mammalian cochlea. *Nature communications*, 9(1), 1-12.
- Cruikshanks, K. J., Nondahl, D. M., Tweed, T. S., Wiley, T. L., Klein, B. E., Klein, R., Chappell, R., Dalton, D.S., Nash, S. D. (2010). Education, occupation, noise exposure history and the 10-yr cumulative incidence of hearing impairment in older adults. *Hearing research*, 264(1), 3-9.
- Cruikshanks, K. J., Tweed, T. S., Wiley, T. L., Klein, B. E., Klein, R., Chappell, R., Nondahl, D.M., Dalton, D. S. (2003). The 5-year incidence and progression of hearing loss: the epidemiology of hearing loss study. *Archives of Otolaryngology-Head & Neck Surgery*, 129(10), 1041-1046.
- Dallos, P. (1980). Two-tone suppression and intermodulation distortion in the cochlea: Effect of outer hair cell lesions. In *Psychophysical, Physiological and Behavioural Studies in Hearing*(pp. 242-249). Delft University Press.
- Dallos, P. (1992). The active cochlea. *Journal of Neuroscience*, 12(12), 4575-4585.
- Dallos, P., & Cheatham, M. A. (1976). Compound action potential (AP) tuning curves. *The Journal of the Acoustical Society of America*, 59(3), 591-597.
- Dallos, P., Wu, X., Cheatham, M. A., Gao, J., Zheng, J., Anderson, C. T., ... & He, D. Z. (2008). Prestin-based outer hair cell motility is necessary for mammalian cochlear amplification. *Neuron*, 58(3), 333-339.

- Dalton, D.S., Cruickshanks, K.J., Klein, B.E., Klein, R., Wiley, T.L., Nondahl, D.M. The impact of hearing loss on quality of life in older adults. *Gerontologist*. 2003;43(5):661–668.
- Davis, H. (1958). Transmission and transduction in the cochlea. *The Laryngoscope*, 68(3), 359-382.
- Davis, H. (1983). An active process in cochlear mechanics. *Hearing Research*, 9(1), 79–90.
- de Boer, J., & Thornton, A. R. D. (2008). Neural correlates of perceptual learning in the auditory brainstem: efferent activity predicts and reflects improvement at a speech-in-noise discrimination task. *Journal of Neuroscience*, 28(19), 4929-4937.
- Dewey, J. B., Applegate, B. E., & Oghalai, J. S. (2019). Amplification and suppression of traveling waves along the mouse organ of Corti: evidence for spatial variation in the longitudinal coupling of outer hair cell-generated forces. *Journal of Neuroscience*, 39(10), 1805-1816.
- Dhar, S., Long, G. R., Talmadge, C. L., & Tubis, A. (2005). The effect of stimulus-frequency ratio on distortion product otoacoustic emission components. *The Journal of the Acoustical Society of America*, 117(6), 3766-3776.
- Dille, M. F., McMillan, G. P., Reavis, K. M., Jacobs, P., Fausti, S. A., & Konrad-Martin, D. (2010). Ototoxicity risk assessment combining distortion product otoacoustic emissions with a cisplatin dose model. *The Journal of the Acoustical Society of America*, 128(3), 1163-1174.
- Dong, W., Xia, A., Raphael, P. D., Puria, S., Applegate, B., & Oghalai, J. S. (2018). Organ of Corti vibration within the intact gerbil cochlea measured by volumetric optical coherence tomography and vibrometry. *Journal of neurophysiology*, 120(6), 2847-2857.

Dorn, P. A., Konrad-Martin, D., Neely, S. T., Keefe, D. H., Cyr, E., & Gorga, M. P. (2001).

Distortion product otoacoustic emission input/output functions in normal-hearing and hearing-impaired human ears. *The Journal of the Acoustical Society of America*, *110*(6), 3119-3131.

Dorn, P. A., Piskorski, P., Gorga, M. P., Neely, S. T., Keefe, D. H. (1999). Predicting audiometric status from distortion product otoacoustic emissions using multivariate analyses. *Ear and Hearing*, *20*(2), 149-163.

Dorn, P. A., Piskorski, P., Keefe, D. H., Neely, S. T., & Gorga, M. P. (1998). On the existence of an age/threshold/frequency interaction in distortion product otoacoustic emissions. *The Journal of the Acoustical Society of America*, *104*(2), 964-971.

Dreschler, W. V., vd Hulst, R. J. A. M., Tange, R. A., & Urbanus, N. A. M. (1985). The role of high-frequency audiometry in early detection of ototoxicity. *Audiology*, *24*(6), 387-395.

Dreisbach, L. E., & Siegel, J. H. (2001). Distortion-product otoacoustic emissions measured at high frequencies in humans. *The Journal of the Acoustical Society of America*, *110*(5), 2456-2469.

Duggal, P., & Sarkar, M. (2007). Audiologic monitoring of multi-drug resistant tuberculosis patients on aminoglycoside treatment with long term follow-up. *BMC Ear, Nose and Throat Disorders*, *7*(1), 5.

Emmett, S. D., Francis, H. W. (2014). The Socioeconomic Impact of Hearing Loss in US Adults. *Otol Neurotol*.

Engdahl, B. O., & Kemp, D. T. (1996). The effect of noise exposure on the details of distortion product otoacoustic emissions in humans. *The Journal of the Acoustical Society of America*, *99*(3), 1573-1587.

- Frank, T. (1990). High-frequency hearing thresholds in young adults using a commercially available audiometer. *Ear and Hearing, 11*(6), 450-454.
- Franklin, D. J., Lonsbury-Martin, B. L., Stagner, B. B., & Martin, G. K. (1991). Altered susceptibility of $2f_1-f_2$ acoustic-distortion products to the effects of repeated noise exposure in rabbits. *Hearing research, 53*(2), 185-208.
- Frisina, R. D., Wheeler, H. E., Fossa, S. D., Kerns, S. L., Fung, C., Sesso, H. D., ... & Beard, C. J. (2016). Comprehensive audiometric analysis of hearing impairment and tinnitus after cisplatin-based chemotherapy in survivors of adult-onset cancer. *Journal of Clinical Oncology, 34*(23), 2712.
- Forge, A., & Schacht, J. (2000). Aminoglycoside antibiotics. *Audiology and Neurotology, 5*(1), 3-22.
- Gao, S. S., Wang, R., Raphael, P. D., Moayed, Y., Groves, A. K., Zuo, J., ... & Oghalai, J. S. (2014). Vibration of the organ of Corti within the cochlear apex in mice. *Journal of neurophysiology, 112*(5), 1192-1204.
- Garinis, A. C., Cross, C. P., Srikanth, P., Carroll, K., Feeney, M. P., Keefe, D. H., ... & Steyger, P. S. (2017). The cumulative effects of intravenous antibiotic treatments on hearing in patients with cystic fibrosis. *Journal of Cystic Fibrosis, 16*(3), 401-409.
- Gaskill, S. A., & Brown, A. M. (1990). The behavior of the acoustic distortion product, $2f_1 - f_2$, from the human ear and its relation to auditory sensitivity. *The Journal of the Acoustical Society of America, 88*(2), 821-839.
- Gaskill, S. A., Brown, A. M. (1993). Comparing the level of the acoustic distortion product $2f_1 - f_2$ with behavioural threshold audiograms from normal-hearing and hearing-impaired ears. *British journal of audiology, 27*(6), 397-407.

- Gates, G.A., Mills, J.H. Presbycusis. *Lancet*. 2005;366(9491):1111–1120.
- Goodman, S. S., Withnell, R. H., & Shera, C. A. (2003). The origin of SFOAE microstructure in the guinea pig. *Hearing research*, 183(1-2), 7-17.
- Gold, T. (1948). Hearing. II. The physical basis of the action of the cochlea. *Proceedings of the Royal Society of London. Series B-Biological Sciences*, 135(881), 492-498.
- Gorga, M. P., Dierking, D. M., Johnson, T. A., Beauchaine, K. L., Garner, C. A., Neely, S. T. (2005). A validation and potential clinical application of multivariate analyses of DPOAE data. *Ear and hearing*, 26(6), 593.
- Gorga, M. P., Neely, S. T., Bergman, B. M., Beauchaine, K. L., Kaminski, J. R., Peters, J., ... & Jesteadt, W. (1993a). A comparison of transient-evoked and distortion product otoacoustic emissions in normal-hearing and hearing-impaired subjects. *The Journal of the Acoustical Society of America*, 94(5), 2639-2648.
- Gorga, M. P., Neely, S. T., Bergman, B., Beauchaine, K. L., Kaminski, J. R., Peters, J., Jesteadt, W. (1993b). Otoacoustic emissions from normal-hearing and hearing-impaired subjects: Distortion product responses. *The Journal of the Acoustical Society of America*, 93(4), 2050-2060.
- Gorga, M. P., Neely, S. T., Dorn, P. A. (1999). Distortion product otoacoustic emission test performance for a priori criteria and for multifrequency audiometric standards. *Ear and Hearing*, 20(4), 345.
- Gorga, M. P., Neely, S. T., Dorn, P. A., Hoover, B. M. (2003). Further efforts to predict pure-tone thresholds from distortion product otoacoustic emission input/output functions. *The Journal of the Acoustical Society of America*, 113(6), 3275-3284.

- Gorga, M. P., Neely, S. T., Ohlrich, B., Hoover, B., Redner, J., & Peters, J. (1997). From laboratory to clinic: A large scale study of distortion product otoacoustic emissions in ears with normal hearing and ears with hearing loss. *Ear and hearing, 18*(6), 440-455.
- Gorga, M. P., Nelson, K., Davis, T., Dorn, P. A., Neely, S. T. (2000). Distortion product otoacoustic emission test performance when both $2 f_1 - f_2$ and $2 f_2 - f_1$ are used to predict auditory status. *The Journal of the Acoustical Society of America, 107*(4), 2128-2135.
- Green, D. M., Kidd Jr, G., & Stevens, K. N. (1987). High-frequency audiometric assessment of a young adult population. *The Journal of the Acoustical Society of America, 81*(2), 485-494.
- Graham, R. L., & Hazell, J. W. P. (1994). Contralateral suppression of transient evoked otoacoustic emissions: intra-individual variability in tinnitus and normal subjects. *British journal of audiology, 28*(4-5), 235-245.
- Groon, K. A., Rasetshwane, D. M., Kopun, J. G., Gorga, M. P., & Neely, S. T. (2015). Air-leak effects on ear-canal acoustic absorbance. *Ear and hearing, 36*(1), 155.
- Guinan Jr, J. J. (2012). How are inner hair cells stimulated? Evidence for multiple mechanical drives. *Hearing research, 292*(1-2), 35-50.
- Guinan Jr, J. J., Salt, A., & Cheatham, M. A. (2012). Progress in cochlear physiology after Békésy. *Hearing research, 293*(1-2), 12-20.
- Hallmo, P., Sundby, A., & Mair, I. W. (1994). Extended high-frequency audiometry: Air-and bone-conduction thresholds, age and gender variations. *Scandinavian audiology, 23*(3), 165-170.

- Harding, G. W., Bohne, B. A., & Ahmad, M. (2002). DPOAE level shifts and ABR threshold shifts compared to detailed analysis of histopathological damage from noise. *Hearing research, 174*(1-2), 158-171.
- Harris, F. P., Lonsbury-Martin, B. L., Stagner, B. B., Coats, A. C., & Martin, G. K. (1989). Acoustic distortion products in humans: Systematic changes in amplitude as a function of f_2/f_1 ratio. *The Journal of the Acoustical Society of America, 85*(1), 220-229.
- Harris, J. D., & Myers, C. K. (1971). Tentative Audiometric Threshold-Level Standards from 8 through 18 kHz. *The Journal of the Acoustical Society of America, 49*(2B), 600-601.
- Hauser, R., & Probst, R. (1991). The influence of systematic primary-tone level variation $L_2 - L_1$ on the acoustic distortion product emission $2f_1 - f_2$ in normal human ears. *The Journal of the Acoustical Society of America, 89*(1), 280-286.
- He, N. J., & Schmiedt, R. A. (1993). Fine structure of the $2f_1 - f_2$ acoustic distortion product: Changes with primary level. *The Journal of the Acoustical Society of America, 94*(5), 2659-2669.
- Heine, C., Browning, C.J. Communication and psychosocial consequences of sensory loss in older adults: overview and rehabilitation directions. *Disabil Rehabil. 2002;24*(15):763–773.
- Hong, O., Kerr, M. J., Poling, G. L., & Dhar, S. (2013). Understanding and preventing noise-induced hearing loss. *Dis Mon, 59*(4), 110-118.
- Hoth, S., Gudmundsdottir, K., & Plinkert, P. (2010). Age dependence of otoacoustic emissions: the loss of amplitude is primarily caused by age-related hearing loss and not by aging alone. *European archives of oto-rhino-laryngology, 267*(5), 679-690.
- Hudspeth, A. J. (1989). How the ear's works work. *Nature, 341*(6241), 397.

- Hudspeth, A. J. (1997). Mechanical amplification of stimuli by hair cells. *Current opinion in neurobiology*, 7(4), 480-486.
- Hudspeth, A. J., & Corey, D. P. (1977). Sensitivity, polarity, and conductance change in the response of vertebrate hair cells to controlled mechanical stimuli. *Proceedings of the National Academy of Sciences*, 74(6), 2407-2411.
- Heitmann, J., Waldmann, B., & Plinkert, P. K. (1996). Limitations in the use of distortion product otoacoustic emissions in objective audiometry as the result of fine structure. *European archives of oto-rhino-laryngology*, 253(3), 167-171.
- International Standards Organization (1998). Acoustics: Reference Zero for the Calibration of Audiometric Equipment. Part 5: Reference Equivalent Threshold Sound Pressure Levels for Pure Tones in the Frequency Range 8 kHz to 16 kHz (ISO 389-5-1998). Geneva, Switzerland: International Standards Organization.
- Jimenez, A. M., Stagner, B. B., Martin, G. K., & Lonsbury-Martin, B. L. (1999). Age-related loss of distortion product otoacoustic emissions in four mouse strains. *Hearing research*, 138(1-2), 91-105.
- Johnson, T. A., Neely, S. T., Garner, C. A., & Gorga, M. P. (2006). Influence of primary-level and primary-frequency ratios on human distortion product otoacoustic emissions. *The Journal of the Acoustical Society of America*, 119(1), 418-428.
- Johnson, T. A., Neely, S. T., Kopun, J. G., Dierking, D. M., Tan, H., Converse, C., Kennedy, E., Gorga, M. P. (2007). Distortion product otoacoustic emissions: Cochlear-source contributions and clinical test performance. *The Journal of the Acoustical Society of America*, 122(6), 3539-3553.

- Jung, D., & Bhattacharyya, N. (2012). Association of hearing loss with decreased employment and income among adults in the United States. *Annals of Otolaryngology, Rhinology & Laryngology*, 121(12), 771-775.
- Kalluri, R., & Shera, C. A. (2013). Measuring stimulus-frequency otoacoustic emissions using swept tones. *The Journal of the Acoustical Society of America*, 134(1), 356-368.
- Katbamna, B., Homnick, D. N., & Marks, J. H. (1999). Effects of chronic tobramycin treatment on distortion product otoacoustic emissions. *Ear and hearing*, 20(5), 393-402.
- Kemp, D. T. (1978). Stimulated acoustic emissions from within the human auditory system. *The Journal of the Acoustical Society of America*, 64(5), 1386-1391.
- Kemp, D. T. (1979). Evidence of mechanical nonlinearity and frequency selective wave amplification in the cochlea. *Archives of oto-rhino-laryngology*, 224(1-2), 37-45.
- Kemp, D. T., Bray, P., Alexander, L., & Brown, A. M. (1986). Acoustic emission cochleography--practical aspects. *Scandinavian audiology. Supplementum*, 25, 71.
- Kennedy, H. J., Crawford, A. C., & Fettiplace, R. (2005). Force generation by mammalian hair bundles supports a role in cochlear amplification. *Nature*, 433(7028), 880-883.
- Kennedy, H. J., Evans, M. G., Crawford, A. C., & Fettiplace, R. (2003). Fast adaptation of mechano-electrical transducer channels in mammalian cochlear hair cells. *Nature neuroscience*, 6(8), 832-836.
- Khanna, S. M., & Leonard, D. G. B. (1986). Relationship between basilar membrane tuning and hair cell condition. *Hearing research*, 23(1), 55-70.
- Kiang, N. Y. S., Sachs, M. B., & Peake, W. T. (1967). Shapes of tuning curves for single auditory-nerve fibers. *The Journal of the Acoustical Society of America*, 42(6), 1341-1342.

- Kim, D. O. (1980). Cochlear mechanics: Implications of electrophysiological and acoustical observations. *Hearing research*, 2(3-4), 297-317.
- Kim, D. O., Molnar, C. E., & Matthews, J. W. (1980). Cochlear mechanics: Nonlinear behavior in two-tone responses as reflected in cochlear-nerve-fiber responses and in ear-canal sound pressure. *The Journal of the Acoustical Society of America*, 67(5), 1704-1721.
- Kim, D. O., Paparello, J., Jung, M. D., Smurzynski, J., Sun, X. (1996). Distortion product otoacoustic emission test of sensorineural hearing loss: Performance regarding sensitivity, specificity and receiver operating characteristics. *Acta otolaryngologica*, 116(1), 3-11.
- Knight, R. D., & Kemp, D. T. (2000). Indications of different distortion product otoacoustic emission mechanisms from a detailed f₁, f₂ area study. *The Journal of the Acoustical Society of America*, 107(1), 457-473.
- Knight, R. D., & Kemp, D. T. (2001). Wave and place fixed DPOAE maps of the human ear. *The Journal of the Acoustical Society of America*, 109(4), 1513-1525.
- Kochkin, S. (2005a). MarkeTrak VII: Hearing loss population tops 31 million people. *Hearing Review*, 12(7), 16-29.
- Kochkin, S. (2005b). The impact of untreated hearing loss on household income. *Better Hearing Institute*, 1-10.
- Kochkin, S. (2010). MarkeTrak VIII: 25-year trends in the hearing health market. *Hearing Review*, 16(11), 12-31.
- Koo, T. K., & Li, M. Y. (2016). A guideline of selecting and reporting intraclass correlation coefficients for reliability research. *Journal of chiropractic medicine*, 15(2), 155-163.

- Kummer, P., Janssen, T., & Arnold, W. (1998). The level and growth behavior of the 2 f₁– f₂ distortion product otoacoustic emission and its relationship to auditory sensitivity in normal hearing and cochlear hearing loss. *The Journal of the Acoustical Society of America*, 103(6), 3431-3444.
- Kummer, P., Janssen, T., Hulin, P., & Arnold, W. (2000). Optimal L₁– L₂ primary tone level separation remains independent of test frequency in humans. *Hearing research*, 146(1-2), 47-56.
- LaForge, R.G., Spector, W.D., Sternberg, J. (1992). The relationship of vision and hearing impairment to one year mortality and functional decline. *J Aging Health*, 4:126-148.
- Lee, J., Dhar, S., Abel, R., Banakis, R., Grolley, E., Lee, J., Zecker, S., and Siegel, J. (2012). “Behavioral hearing thresholds between 0.125 and 20 kHz using depth-compensated ear simulator calibration,” *Ear. Hear.* 33, 315–329.
- Lee, H. Y., Raphael, P. D., Park, J., Ellerbee, A. K., Applegate, B. E., & Oghalai, J. S. (2015). Noninvasive in vivo imaging reveals differences between tectorial membrane and basilar membrane traveling waves in the mouse cochlea. *Proceedings of the National Academy of Sciences*, 112(10), 3128-3133.
- Lee, H. Y., Raphael, P. D., Xia, A., Kim, J., Grillet, N., Applegate, B. E., ... & Oghalai, J. S. (2016). Two-dimensional cochlear micromechanics measured in vivo demonstrate radial tuning within the mouse organ of Corti. *Journal of Neuroscience*, 36(31), 8160-8173.
- Legan, P. K., Lukashkina, V. A., Goodyear, R. J., Kössl, M., Russell, I. J., & Richardson, G. P. (2000). A targeted deletion in α -tectorin reveals that the tectorial membrane is required for the gain and timing of cochlear feedback. *Neuron*, 28(1), 273-285.

- Lewis, J. D., & Goodman, S. S. (2015). Basal contributions to short-latency transient-evoked otoacoustic emission components. *Journal of the Association for Research in Otolaryngology*, *16*(1), 29-45.
- Liberman, M. C., & Dodds, L. W. (1984). Single-neuron labeling and chronic cochlear pathology. III. Stereocilia damage and alterations of threshold tuning curves. *Hearing research*, *16*(1), 55-74.
- Liberman, L. D., & Liberman, M. C. (2019). Cochlear efferent innervation is sparse in humans and decreases with age. *Journal of Neuroscience*, *39*(48), 9560-9569.
- Lin, F. R., Metter, E. J., O'Brien, R. J., Resnick, S. M., Zonderman, A. B., & Ferrucci, L. (2011). Hearing loss and incident dementia. *Archives of neurology*, *68*(2), 214-220.
- Lin, F. R., Yaffe, K., Xia, J., Xue, Q. L., Harris, T. B., Purchase-Helzner, E., ... & Health ABC Study Group, F. (2013). Hearing loss and cognitive decline in older adults. *JAMA internal medicine*, *173*(4), 293-299.
- Long, G. R., & Talmadge, C. L. (1997). Spontaneous otoacoustic emission frequency is modulated by heartbeat. *The Journal of the Acoustical Society of America*, *102*(5), 2831-2848.
- Long, G. R., Talmadge, C. L., & Lee, J. (2008). Measuring distortion product otoacoustic emissions using continuously sweeping primaries. *The Journal of the Acoustical Society of America*, *124*(3), 1613-1626.
- Lonsbury-Martin, B. L., & Martin, G. K. (2003). Otoacoustic emissions. *Current Opinion in Otolaryngology & Head and Neck Surgery*, *11*(5), 361-366.

- Lonsbury-Martin, B. L., Martin, G. K., Probst, R., & Coats, A. C. (1987). Acoustic distortion products in rabbit ear canal. I. Basic features and physiological vulnerability. *Hearing research*, 28(2-3), 173-189.
- Martin, G. K., Jassir, D., Stagner, B. B., & Lonsbury-Martin, B. L. (1998). Effects of loop diuretics on the suppression tuning of distortion-product otoacoustic emissions in rabbits. *The Journal of the Acoustical Society of America*, 104(2), 972-983.
- Martin, G. K., Lonsbury-Martin, B. L., Probst, R., Scheinin, S. A., & Coats, A. C. (1987). Acoustic distortion products in rabbit ear canal. II. Sites of origin revealed by suppression contours and pure-tone exposures. *Hearing research*, 28(2-3), 191-208.
- Martin, G. K., Stagner, B. B., Chung, Y. S., & Lonsbury-Martin, B. L. (2011). Characterizing distortion-product otoacoustic emission components across four species. *The Journal of the Acoustical Society of America*, 129(5), 3090-3103.
- Mauermann, M., & Kollmeier, B. (2004). Distortion product otoacoustic emission (DPOAE) input/output functions and the influence of the second DPOAE source. *The Journal of the Acoustical Society of America*, 116(4), 2199-2212.
- McAlpine, D., & Johnstone, B. M. (1990). The ototoxic mechanism of cisplatin. *Hearing research*, 47(3), 191-203.
- Mills, D. M., & Schmiedt, R. A. (2004). Metabolic presbycusis: differential changes in auditory brainstem and otoacoustic emission responses with chronic furosemide application in the gerbil. *Journal of the Association for Research in Otolaryngology*, 5(1), 1-10. This paper demonstrates the electrophysiologic changes associated with chronic lowering of the endocochlear potential.

- Mishra, S. K., & Lutman, M. E. (2013). Repeatability of click-evoked otoacoustic emission-based medial olivocochlear efferent assay. *Ear and hearing, 34*(6), 789-798.
- Moore, B. C. (1978). Psychophysical tuning curves measured in simultaneous and forward masking. *The Journal of the Acoustical Society of America, 63*(2), 524-532.
- Moore, B. C., Glasberg, B. R., & Roberts, B. (1984). Refining the measurement of psychophysical tuning curves. *The Journal of the Acoustical Society of America, 76*(4), 1057-1066.
- Mulrow, C.D., Aguilar C., Endicott, J.E., Valez, R., Tuley, M.R., Charlip, W.S., Hill, J.A. (1990). Association between hearing impairment and the quality of life of elderly individuals. *J Am Geriatr Soc., 38*:45-50.
- Neely, S. T., Gorga, M. P., & Dorn, P. A. (2003). Cochlear compression estimates from measurements of distortion-product otoacoustic emissions. *The Journal of the Acoustical Society of America, 114*(3), 1499-1507.
- Neely, S. T., Johnson, T. A., & Gorga, M. P. (2005). Distortion-product otoacoustic emission measured with continuously varying stimulus level. *The Journal of the Acoustical Society of America, 117*(3), 1248-1259.
- Neely, S. T., Johnson, T. A., Kopun, J., Dierking, D. M., & Gorga, M. P. (2009). Distortion-product otoacoustic emission input/output characteristics in normal-hearing and hearing-impaired human ears. *The Journal of the Acoustical Society of America, 126*(2), 728-738.
- Narayan, S. S., Temchin, A. N., Recio, A., & Ruggero, M. A. (1998). Frequency tuning of basilar membrane and auditory nerve fibers in the same cochleae. *Science, 282*(5395), 1882-1884.

- Olson, E. S. (2004). Harmonic distortion in intracochlear pressure and its analysis to explore the cochlear amplifier. *The Journal of the Acoustical Society of America*, 115(3), 1230-1241.
- O'Mahoney, C. F., & Kemp, D. T. (1995). Distortion product otoacoustic emission delay measurement in human ears. *The Journal of the Acoustical Society of America*, 97(6), 3721-3735.
- Ortmann, A. J., & Abdala, C. (2016). Changes in the compressive nonlinearity of the cochlea during early aging: estimates from distortion OAE input/output functions. *Ear and hearing*, 37(5), 603.
- Osterhammel, D., & Osterhammel, P. (1979). Age and sex variations for the normal stapedial reflex thresholds and tympanometric compliance values. *Scandinavian Audiology*, 8(3), 153-158.
- Patuzzi, R. (1996). Cochlear micromechanics and macromechanics. In *The cochlea* (pp. 186-257). Springer, New York, NY.
- Pickles JO (2012) An introduction to the physiology of hearing, 4th Edition. Bingley, UK: Emerald.
- Poling, G. L., Siegel, J. H., Lee, J., Lee, J., & Dhar, S. (2014). Characteristics of the 2f1-f2 distortion product otoacoustic emission in a normal hearing population. *The Journal of the Acoustical Society of America*, 135(1), 287-299.
- Preyer, S., Hemmert, W., Pfister, M., Zenner, H. P., & Gummer, A. W. (1994). Frequency response of mature guinea-pig outer hair cells to stereociliary displacement. *Hearing research*, 77(1-2), 116-124.
- Probst, R., & Hauser, R. (1990). Distortion product otoacoustic emissions in normal and hearing-impaired ears. *American journal of otolaryngology*, 11(4), 236-243.

- Probst, R., Lonsbury-Martin, B. L., & Martin, G. K. (1991). A review of otoacoustic emissions. *The Journal of the Acoustical Society of America*, *89*(5), 2027-2067.
- Ramamoorthy, S., Zha, D., Chen, F., Jacques, S. L., Wang, R., Choudhury, N., ... & Fridberger, A. (2014). Filtering of acoustic signals within the hearing organ. *Journal of Neuroscience*, *34*(27), 9051-9058.
- Reavis, K. M., McMillan, G., Austin, D., Gallun, F., Fausti, S. A., Gordon, J. S., ... & Konrad-Martin, D. (2011). Distortion-product otoacoustic emission test performance for ototoxicity monitoring. *Ear and hearing*, *32*(1), 61.
- Reavis, K. M., Phillips, D. S., Fausti, S. A., Gordon, J. S., Helt, W. J., Wilmington, D., ... & Konrad-Martin, D. (2008). Factors affecting sensitivity of distortion-product otoacoustic emissions to ototoxic hearing loss. *Ear and hearing*, *29*(6), 875-893.
- Recio-Spinoso, A., & Oghalai, J. S. (2017). Mechanical tuning and amplification within the apex of the guinea pig cochlea. *The Journal of physiology*, *595*(13), 4549-4561.
- Ren, T., He, W., & Kemp, D. (2016). Reticular lamina and basilar membrane vibrations in living mouse cochleae. *Proceedings of the National Academy of Sciences*, *113*(35), 9910-9915.
- Ress, B.D., Sridhar, K.S., Balkany, T.J., Waxman, G.M., Stagner, B.B., Lonsbury-Martin B.L. Effects of cis-platinum chemotherapy on otoacoustic emissions: The development of an objective screening protocol. *Otolaryngol Head Neck Surg* *121*(6), 693–701.
- Rhode, W. S. (1971). Observations of the vibration of the basilar membrane in squirrel monkeys using the Mössbauer technique. *The Journal of the Acoustical Society of America*, *49*(4B), 1218-1231.
- Robles, L., & Ruggero, M. A. (2001). Mechanics of the mammalian cochlea. *Physiological reviews*, *81*(3), 1305-1352.

- Roland, P. S., & Rutka, J. A. (2004). *Ototoxicity*. PMPH-USA.
- Ruggero, M. A., & Rich, N. C. (1991). Furosemide alters organ of corti mechanics: evidence for feedback of outer hair cells upon the basilar membrane. *Journal of Neuroscience*, *11*(4), 1057-1067.
- Ruggero, M. A., Rich, N. C., Robles, L., & Shivapuja, B. G. (1990). Middle-ear response in the chinchilla and its relationship to mechanics at the base of the cochlea. *The Journal of the Acoustical Society of America*, *87*(4), 1612-1629.
- Ruggero, M. A., Robles, L., Rich, N. C., & Recio, A. (1992). Basilar membrane responses to two-tone and broadband stimuli. *Philosophical transactions of the Royal Society of London. Series B: Biological sciences*, *336*(1278), 307-315.
- Rybak, L. P., Whitworth, C. A., Mukherjea, D., & Ramkumar, V. (2007). Mechanisms of cisplatin-induced ototoxicity and prevention. *Hearing research*, *226*(1-2), 157-167.
- Sakamoto, M., Sugasawa, M., Kaga, K., & Kamio, T. (1998). Average thresholds in the 8 to 20 kHz range in young adults. *Scandinavian audiology*, *27*(3), 169-172.
- Schmiedt, R. A. (1986). Acoustic distortion in the ear canal. I. Cubic difference tones: effects of acute noise injury. *The Journal of the Acoustical Society of America*, *79*(5), 1481-1490.
- Schuknecht, H. F. (1955). Presbycusis. *The Laryngoscope*, *65*(6), 402-419.
- Schuknecht, H. F., & Gacek, M. R. (1993). Cochlear pathology in presbycusis. *Annals of Otolaryngology, Rhinology & Laryngology*, *102*(1_suppl), 1-16.
- Selimoglu, E. (2007). Aminoglycoside-induced ototoxicity. *Current pharmaceutical design*, *13*(1), 119-126.

- Sellick, P. M., Patuzzi, R., & Johnstone, B. M. (1983). Comparison between the tuning properties of inner hair cells and basilar membrane motion. *Hearing research, 10*(1), 93-100.
- Sha, S. H., Taylor, R., Forge, A., & Schacht, J. (2001). Differential vulnerability of basal and apical hair cells is based on intrinsic susceptibility to free radicals. *Hearing research, 155*(1-2), 1-8.
- Shaw, E. A. (1974). The external ear. In *Auditory system* (pp. 455-490). Springer, Berlin, Heidelberg.
- Shera, C. A., & Guinan Jr, J. J. (1999). Evoked otoacoustic emissions arise by two fundamentally different mechanisms: a taxonomy for mammalian OAEs. *The Journal of the Acoustical Society of America, 105*(2), 782-798.
- Shera, C. A. (2003). Wave interference in the generation of reflection-and distortion-source emissions. In *Biophysics of the cochlea: from molecules to models* (pp. 439-453).
- Shera, C. A., Tubis, A., Talmadge, C. L., de Boer, E., Fahey, P. F., & Guinan Jr, J. J. (2007). Allen–Fahey and related experiments support the predominance of cochlear slow-wave otoacoustic emissions. *The Journal of the Acoustical Society of America, 121*(3), 1564-1575.
- Sheth, S., Mukherjea, D., Rybak, L. P., & Ramkumar, V. (2017). Mechanisms of cisplatin-induced ototoxicity and otoprotection. *Frontiers in cellular neuroscience, 11*, 338.
- Siegel, J. H. (1994). Ear-canal standing waves and high-frequency sound calibration using otoacoustic emission probes. *The Journal of the Acoustical Society of America, 95*(5), 2589-2597.

- Simpson, A. N., Matthews, L. J., Cassarly, C., & Dubno, J. R. (2019). Time From Hearing-aid Candidacy to Hearing-aid Adoption: a Longitudinal Cohort Study. *Ear and hearing, 40*(3), 468.
- Simpson, A. N., Simpson, K. N., & Dubno, J. R. (2016). Higher health care costs in middle-aged US adults with hearing loss. *JAMA Otolaryngology–Head & Neck Surgery, 142*(6), 607-609.
- Sisto, R., Wilson, U. S., Dhar, S., & Moleti, A. (2018, May). Cochlear tuning and DPOAE dependence on the primary tone frequency ratio. In *AIP Conference Proceedings* (Vol. 1965, No. 1, p. 170002). AIP Publishing LLC.
- Souza, N. N., Dhar, S., Neely, S. T., & Siegel, J. H. (2014). Comparison of nine methods to estimate ear-canal stimulus levels. *The Journal of the Acoustical Society of America, 136*(4), 1768-1787.
- Stankovic, K. M., & Guinan Jr, J. J. (1999). Medial efferent effects on auditory-nerve responses to tail-frequency tones. I. Rate reduction. *The Journal of the Acoustical Society of America, 106*(2), 857-869.
- Stankovic, K. M., & Guinan Jr, J. J. (2000). Medial efferent effects on auditory-nerve responses to tail-frequency tones II: alteration of phase. *The Journal of the Acoustical Society of America, 108*(2), 664-678.
- Stelmachowicz, P. G., Beauchaine, K. A., Kalberer, A., & Jesteadt, W. (1989). Normative thresholds in the 8-to 20-kHz range as a function of age. *The Journal of the Acoustical Society of America, 86*(4), 1384-1391.

- Stiepan, S., Siegel, J., Lee, J., Souza, P., & Dhar, S. (2020). The Association Between Physiological Noise Levels and Speech Understanding in Noise. *Ear and hearing, 41*(2), 461-464.
- Stover, L. J., Neely, S. T., & Gorga, M. P. (1999). Cochlear generation of intermodulation distortion revealed by DPOAE frequency functions in normal and impaired ears. *The Journal of the Acoustical Society of America, 106*(5), 2669-2678.
- Stover, L., Gorga, M. P., Neely, S. T., Montoya, D. (1996). Toward optimizing the clinical utility of distortion product otoacoustic emission measurements. *The Journal of the Acoustical Society of America, 100*(2), 956-967.
- Strauss, M., Towfighi, J., Lord, S., Lipton, A., Harvey, H. A., & Brown, B. (1983). Cis-platinum ototoxicity: Clinical experience and temporal bone histopathology. *The Laryngoscope, 93*(12), 1554-1559.
- Stuart, A., & Cobb, K. M. (2015). Reliability of measures of transient evoked otoacoustic emissions with contralateral suppression. *Journal of Communication Disorders, 58*, 35-42.
- Sutton, L. A., Lonsbury-Martin, B. L., Martin, G. K., & Whitehead, M. L. (1994). Sensitivity of distortion-product otoacoustic emissions in humans to tonal over-exposure: time course of recovery and effects of lowering L2. *Hearing research, 75*(1-2), 161-174.
- Talmadge, C. L., Long, G. R., Tubis, A., & Dhar, S. (1999). Experimental confirmation of the two-source interference model for the fine structure of distortion product otoacoustic emissions. *The Journal of the Acoustical Society of America, 105*(1), 275-292.

- Talmadge, C. L., Tubis, A., Long, G. R., & Piskorski, P. (1998). Modeling otoacoustic emission and hearing threshold fine structures. *The Journal of the Acoustical Society of America*, *104*(3), 1517-1543.
- Talmadge, C. L., Tubis, A., Long, G. R., & Tong, C. (2000). Modeling the combined effects of basilar membrane nonlinearity and roughness on stimulus frequency otoacoustic emission fine structure. *The Journal of the Acoustical Society of America*, *108*(6), 2911-2932.
- Theunissen, E. A., Zuur, C. L., Bosma, S. C., Lopez-Yurda, M., Hauptmann, M., van der Baan, S., ... & Balm, A. J. (2014). Long-term hearing loss after chemoradiation in patients with head and neck cancer. *The Laryngoscope*, *124*(12), 2720-2725.
- Ueberfuhr, M. A., Fehlberg, H., Goodman, S. S., & Withnell, R. H. (2016). A DPOAE assessment of outer hair cell integrity in ears with age-related hearing loss. *Hearing Research*, *332*, 137-150.
- Vázquez, A. E., Jimenez, A. M., Martin, G. K., Luebke, A. E., & Lonsbury-Martin, B. L. (2004). Evaluating cochlear function and the effects of noise exposure in the B6. CAST+ Ahl mouse with distortion product otoacoustic emissions. *Hearing research*, *194*(1-2), 87-96.
- Verpy, E., Weil, D., Leibovici, M., Goodyear, R. J., Hamard, G., Houdon, C., ... & Petit, C. (2008). Stereocilin-deficient mice reveal the origin of cochlear waveform distortions. *Nature*, *456*(7219), 255-258.
- Wallhagen, M. I., Strawbridge, W. J., & Shema, S. J. (2008). The relationship between hearing impairment and cognitive function: a 5-year longitudinal study. *Research in Gerontological Nursing*, *1*(2), 80-86.

- Warren, R. L., Ramamoorthy, S., Ciganović, N., Zhang, Y., Wilson, T. M., Petrie, T., ... & Fridberger, A. (2016). Minimal basilar membrane motion in low-frequency hearing. *Proceedings of the National Academy of Sciences*, *113*(30), E4304-E4310.
- Whitehead, M. L., Lonsbury-Martin, B. L., & Martin, G. K. (1990). Actively and passively generated acoustic distortion at $2f_1 - f_2$ in rabbits. In *The Mechanics and Biophysics of Hearing* (pp. 243-250). Springer, New York, NY.
- Whitehead, M. L., Lonsbury-Martin, B. L., & Martin, G. K. (1992). Evidence for two discrete sources of $2f_1 - f_2$ distortion-product otoacoustic emission in rabbit: I. Differential dependence on stimulus parameters. *The Journal of the Acoustical Society of America*, *91*(3), 1587-1607.
- Whitehead, M. L., McCoy, M. J., Lonsbury-Martin, B. L., & Martin, G. K. (1995a). Dependence of distortion-product otoacoustic emissions on primary levels in normal and impaired ears. I. Effects of decreasing L₂ below L₁. *The Journal of the Acoustical Society of America*, *97*(4), 2346-2358.
- Whitehead, M. L., Stagner, B. B., Martin, G. K., & Lonsbury-Martin, B. L. (1996). Visualization of the onset of distortion-product otoacoustic emissions, and measurement of their latency. *The Journal of the Acoustical Society of America*, *100*(3), 1663-1679.
- Whitehead, M. L., Stagner, B. B., McCoy, M. J., Lonsbury-Martin, B. L., & Martin, G. K. (1995b). Dependence of distortion-product otoacoustic emissions on primary levels in normal and impaired ears. II. Asymmetry in L₁, L₂ space. *The Journal of the Acoustical Society of America*, *97*(4), 2359-2377.

- Whitehead, M. L., Stagner, B. B., Lonsbury-Martin, B. L., & Martin, G. K. (1995c). Effects of ear-canal standing waves on measurements of distortion-product otoacoustic emissions. *The Journal of the Acoustical Society of America*, 98(6), 3200-3214.
- Wiener, F. M., & Ross, D. A. (1946). The pressure distribution in the auditory canal in a progressive sound field. *The Journal of the Acoustical Society of America*, 18(2), 401-408.
- Wiederhold, M. L., Mahoney, J. W., & Kellogg, D. L. (1986). Acoustic overstimulation reduces 2f1-f2 cochlear emissions at all levels in the cat. In *Peripheral auditory mechanisms* (pp. 322-329). Springer, Berlin, Heidelberg.
- Wilson, J. P. (1980). The combination tone, 2f1– f2, in psychophysics and ear-canal recording. In *Psychophysical, physiological and behavioral studies in hearing* (pp. 43-50). Delft University Press Delft, The Netherlands.
- Withnell, R. H., Hazlewood, C., & Knowlton, A. (2008). Reconciling the origin of the transient evoked ototacoustic emission in humans. *The Journal of the Acoustical Society of America*, 123(1), 212-221.
- Withnell, R. H., Yates, G. K., & Kirk, D. L. (2000). Changes to low-frequency components of the TEOAE following acoustic trauma to the base of the cochlea. *Hearing research*, 139(1-2), 1-12.
- World Health Organization. (2017). *Global costs of unaddressed hearing loss and cost-effectiveness of interventions: a WHO report, 2017*. World Health Organization.
- Wright, C. G., & Schaefer, S. D. (1982). Inner ear histopathology in patients treated with Cis-Platinum. *The Laryngoscope*, 92(12), 1408-1413.

- Wu, P. Z., O'Malley, J. T., de Gruttola, V., & Liberman, M. C. (2020). Age-related hearing loss is dominated by damage to inner ear sensory cells, not the cellular battery that powers them. *Journal of Neuroscience*, *40*(33), 6357-6366.
- Yates, G. K., Johnstone, B. M., Patuzzi, R. B., & Robertson, D. (1992). Mechanical preprocessing in the mammalian cochlea. *Trends in neurosciences*, *15*(2), 57-61.
- Yates, G. K., & Withnell, R. H. (1999). The role of intermodulation distortion in transient-evoked otoacoustic emissions. *Hearing research*, *136*(1-2), 49-64.
- Zhan, W., Cruickshanks, K. J., Klein, B. E., Klein, R., Huang, G. H., Pankow, J. S., Gangnon, R.E., Tweed, T. S. (2011). Modifiable determinants of hearing impairment in adults. *Preventive medicine*, *53*(4), 338-342.
- Zheng, J., Shen, W., He, D. Z., Long, K. B., Madison, L. D., & Dallos, P. (2000). Prestin is the motor protein of cochlear outer hair cells. *Nature*, *405*(6783), 149-155.
- Zweig, G., & Shera, C. A. (1995). The origin of periodicity in the spectrum of evoked otoacoustic emissions. *The Journal of the Acoustical Society of America*, *98*(4), 2018-2047.
- Zwicker, E. (1981). Dependence of level and phase of the $(2f_1 - f_2)$ -cancellation tone on frequency range, frequency difference, level of primaries, and subject. *The Journal of the Acoustical Society of America*, *70*(5), 1277-1288.